Electronic Supplementary Information

L- and *rac*-lactide polymerisation using scandium and aluminium permethylindenyl complexes

Nichabhat Diteepeng, Isobel A. P. Wilson, Jean-Charles Buffet, Zoë R. Turner and Dermot O'Hare*

Chemistry Research Laboratory, Department of Chemistry, University of Oxford, 12 Mansfield Road, OX1 3TA Oxford, UK.
E-mail: dermot.ohare@chem.ox.ac.uk

Table of Contents

General experimental techniques and physical methods

General details

All air- and moisture-sensitive compounds were manipulated under an inert atmosphere of nitrogen using Schlenk line techniques[1] on a dual manifold vacuum/nitrogen line or in an MBraun Labmaster 100 glovebox. Tetrahydrofuran (THF) was distilled from sodium/benzophenone, stored over pre-activated 4 Å molecular sieves, and degassed under partial vacuum before use. Pentane, hexane, toluene and benzene were dried using an MBraun SPS 800 solvent purification system, stored over pre-activated 4 Å molecular sieves, and degassed under partial vacuum before use.
Deuterated solvents were dried over potassium metal (benzene-d_6) or CaH_2 (pyridine-d_5) at 80 °C, distilled under static vacuum, freeze-pump-thaw degassed and stored over pre-activated 4 Å molecular sieves. Chloroform-*d* was used as received.

Solution NMR spectroscopy

Air-sensitive NMR samples were prepared in a MBraun Labmaster 100 glove box under an inert atmosphere of nitrogen, using dried deuterated solvents and sealed in 5 mm Wilmad 507-PP tubes fitted with J. Young Teflon valves. ^{1}H and ^{1}H{^{1}H} NMR spectra were recorded on a Bruker Avance III HD NanoBay NMR (9.4 T, 400.2 MHz), and ^{13}C{^{1}H} NMR spectra were recorded on a Bruker Avance NMR (11.75 T, 500.3 MHz) with a ^{13}C-detect cryoprobe. Spectra were recorded at 298 K unless otherwise stated and referenced internally to the residual *protio* solvent resonance. Chemical shifts, δ, are reported in parts per million (ppm) relative to tetramethylsilane (δ = 0 ppm) and coupling constants, *J*, in Hz. Assignments were confirmed using two dimensional ^{1}H-^{1}H (COSY), ^{13}C-^{1}H (HSQC and HMBC) correlation experiments.

Single-crystal X-ray diffraction

Crystallographic data and parameters for the single-crystal determinations of compounds presented in this work are included in the additional crystallographic data. Data collection and structure determination were performed by Dr Zoë Turner (University of Oxford). Crystals were mounted on MiTeGen Micromounts using perfluoropolyether oil and rapidly transferred to a goniometer head on a diffractometer fitted with an Oxford Cryosystems Cryostream open-flow nitrogen cooling device.[2] Data collections were carried out at 150 K using an Oxford Diffraction Supernova diffractometer using mirror-monochromated Cu *Kα* radiation (λ = 1.54178 Å) and data was processed using CryAlisPro.[3] The structures were solved using direct methods (SIR-92)[4] or a charge flipping algorithm (SUPERFLIP)[5] and refined by full-matrix least squares procedures using the Win-GX software suite.[6]

Gel permeation chromatography (GPC)

Polymer molecular weights (M_n, M_w and M_w/M_n) were determined by GPC using an Agilent 1260 Infinity II GPC/SEC instrument equipped with an Agilent PLgel Mixed-D column (300 mm length, 7.5 mm diameter) and a refractive index (RI) detector. THF (Sigma-Aldrich, HPLC grade containing 250 ppm BHT as inhibitor) was used as an eluent at 35 °C with a flow rate of 1.0 mL min^{-1}. Samples were dissolved in THF at a concentration of 1.0 mg

mL^{-1} and filtered before injection. Linear polystyrenes were used as primary calibration standards and the appropriate Mark-Houwink corrections were applied to calculate the experimental molecular weights.[7]

Polymer Tacticity Determination

The tacticity of PLA was analysed by $^1H\{^1H\}$ NMR spectroscopy performed with a Bruker Avance III 400 spectrometer at ambient temperature. P_r values were calculated from integration obtained from $^1H\{^1H\}$ NMR spectra. Alternatively, peak deconvolution, using the Mnova software package, was used to improve accuracy in the determination.[8] The probability of a particular tetrad can be calculated using Bernoullian statistics.[9] Samples were prepared by dissolving PLA (10 mg) in chloroform-*d* (0.6 mL) and transferring the solution to a NMR tube.

Elemental Analysis

Samples were prepared in a MBraun Labmaster 100 glovebox and sealed inside glass vials under a nitrogen atmosphere. Elemental analysis was carried out by Mr Stephen Boyer (London Metropolitan University).

Literature preparations and commercially supplied materials

Hexamethylindene ($C_9Me_6H_2$, Ind#H) was supplied by SCG Chemicals Co., Ltd. (Thailand) and used as received. ^{n}BuLi (1.6 M in hexane) was supplied by ACROS Organics and used as received. Benzyl alcohol was supplied by Sigma Aldrich and stored over 4 Å molecular sieves. $ScCl_3$·3THF was synthesised by a modified literature procedure,[10] in which trimethylsilyl chloride (Me_3SiCl) in THF was used as an alternative to thionyl chloride ($SOCl_2$) to react with $ScCl_3$·$(H_2O)_6$. $AlCl_3$·THF was prepared by dissolving sublimed $AlCl_3$ in THF at room temperature, pentane was added into the solution. $AlCl_3$·THF precipitated as white powder was filtered and then the volatiles were removed *in vacuo*. Purac® *L*-lactide (*L*-LA) and *rac*-lactide (*rac*-LA) were provided courtesy of Corbion and used without further purification. *Tert*-butylamine (^{t}BuNH$_2$), isopropylamine (^{i}PrNH$_2$), *n*-butylamine (^{n}BuNH$_2$) and aniline (PhNH$_2$) were supplied by Alfa Aesar and stored over 4 Å molecular sieves. Reaction of Ind#H (10 g, 50 mmol) and 1.1 eq. ^{n}BuLi (35 mL, 55 mmol) afforded (Ind#)Li.[11] The resultant (Ind#)Li was reacted *in situ* with 3 equivalents of Me_2SiCl_2 (18.1 mL, 150 mmol) yielding Ind*SiMe$_2$Cl in 83% yield (11.9 g, 40.6 mmol)[12]. To synthesise (^{t}BuNH)Li, ^{t}BuNH$_2$ (8 mL, 76.0 mmol) was dissolved in hexane (15 mL), and ^{n}BuLi (43 mL, 69.0 mmol) was added drop-wise at 5 °C. The reaction mixture was stirred at room temperature for 1 h and was dried under vacuum. (^{t}BuNH)Li was obtained as a white solid in quantitative yield (5.5 g). (^{i}PrNH)Li, (^{n}BuNH)Li and (PhNH)Li were prepared using this procedure and obtained as a white solid in 92% yield, a yellow solid in quantitative yield and as a white solid in 90% yield, respectively. Proligands ^{Me2}Si(^{R}N,I*)H$_2$ and dilithium salts ^{Me2}Si(^{R}N,I*)Li$_2$(THF)$_x$ (R = ^{t}Bu, ^{n}Bu, ^{i}Pr and Ph) were synthesised using a literature procedure.[13] Ind*SiMe$_2$Cl (2.0 g, 6.8 mmol) and (^{R}NH)Li (7.2 mmol) were added into a Schlenk flask. The mixture was cooled down to 5 °C and THF (20 mL) was added. The reaction mixture was warmed up to room temperature and stirred for 2 h. The volatiles were removed *in vacuo*, and extraction using pentane (3 × 10 mL) yielded the proligand as a brown oil. The proligand was then dissolved in THF (20 mL) and cooled down to 5 °C. 2.2 equivalents of ^{n}BuLi (9.4 mL, 15.0 mmol) were added drop-wise and the mixture was stirred at room temperature for 30 minutes. The volatiles were removed *in vacuo*. The dilithium salt was washed with pentane (3 × 20 mL) and dried under

vacuum, affording a yellow powder. The value of *x* represents the amount of THF molecules measured in $^{Me}_2$Si(^{R}N,I*)Li$_2$(THF)$_x$, which can be calculated from their ^{1}H NMR spectra in pyridine-d_5.

Synthesis of proligands and dilithium salts

Ind*SiMe$_2$Cl, proligands $^{Me}_2$SB(^{R}N,I*)H$_2$ and dilithium salts $^{Me}_2$SB(^{R}N,I*)Li$_2$ (R = ^{i}Pr, ^{t}Bu, ^{n}Bu and Ph) were synthesised according to a literature procedure.[13] Ind*SiMe$_2$Cl reacted with ^{R}NHLi in a 1:1 molar ratio in THF to give a yellow oil product of $^{Me}_2$SB(^{R}N,I*)H$_2$ (Equation S1). $^{Me}_2$SB(^{R}N,I*)Li$_2$ was generated *in situ* from drop-wise addition of 2.2 equivalents of ^{n}BuLi into the solution of $^{Me}_2$SB(^{R}N,I*)H$_2$ in THF at 5 °C, affording a yellow solid of $^{Me}_2$SB(^{R}N,I*)Li$_2$(THF)$_x$ after purification in a good yield (70, 54, 50 and 90% for those with R = ^{i}Pr, ^{t}Bu, ^{n}Bu and Ph, respectively) (Equation S2). We note the value of *x* representing the amount of THF molecules measured in $^{Me}_2$SB(^{R}N,I*)Li$_2$(THF)$_x$ which can be calculated from the ^{1}H NMR spectra of $^{Me}_2$SB(^{R}N,I*)Li$_2$(THF)$_x$ (Fig. S1–S4).

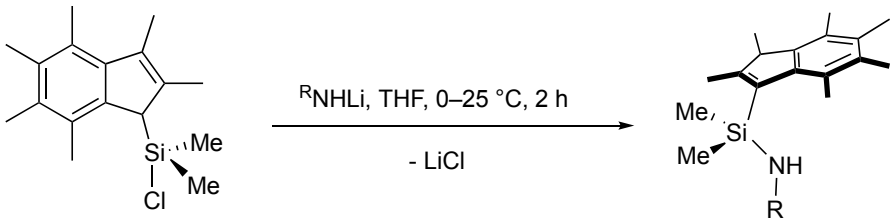

Equation S1 Synthesis of $^{Me}_2$SB(^{R}N,I*)H$_2$ (R = ^{i}Pr, ^{t}Bu, ^{n}Bu and Ph).

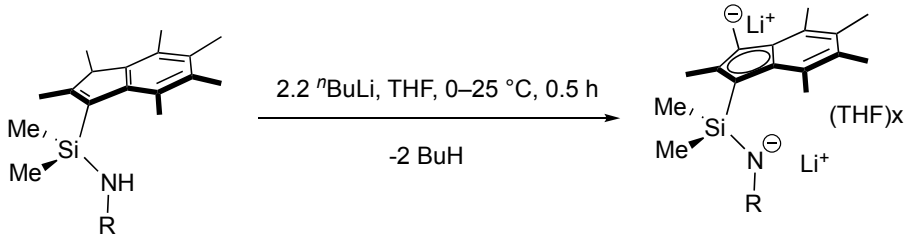

Equation S2 Synthesis of $^{Me}_2$SB(^{R}N,I*)Li$_2$(THF)$_x$ (R = ^{i}Pr, ^{t}Bu, ^{n}Bu and Ph).

Synthesis of $^{Me}_2$SB(^{iPr}N,I*)Sc(Cl)(THF) (1)

To a mixture of $^{Me}_2$SB(^{iPr}N,I*)Li$_2$(THF)$_{0.17}$ (0.50 g, 1.47 mmol) and ScCl$_3$·3THF (0.54 g, 1.47 mmol) was added benzene (20 mL). The reaction mixture was stirred at room temperature for 18 h and then the volatiles were removed *in vacuo*. The product was extracted with benzene (2 × 15 mL) and evaporation of the solution afforded an orange solid which was then cooled to 0 °C and washed with pentane (2 × 15 mL) to afford $^{Me}_2$SB(^{iPr}N,I*)Sc(Cl)(THF) (**1**) as a pale orange powder (0.23 g, 35%).

^{1}H NMR (C$_6$D$_6$, 400.2 MHz, 298 K): 3.33 (1H, sept, $^3J_{H\text{-}H}$ = 6.30 Hz, NC**H**Me$_2$), 3.07 (4H, m, OC**H$_2$**CH$_2$), 2.82, 2.59, 2.57, 2.50 (3H each, s, Ind***Me**), 1.96 (6H, s, Ind***Me**), 1.30 (3H, d, $^3J_{H\text{-}H}$ = 6.31 Hz, NCH**Me$_2$**), 1.23 (3H, d, $^3J_{H\text{-}H}$ = 6.31 Hz, NCH**Me$_2$**), 0.86 (3H, overlapping s, Si**Me**), 0.85 (4H, overlapping m, OCH$_2$C**H$_2$**), 0.64 (3H, s, Si**Me**) ppm.

^{13}C{^{1}H} NMR (C$_6$D$_6$, 125.8 MHz, 298 K): 141.64, 136.42, 129.30, 127.12, 120.90 (**Ind***), 95.30 (Si-**C**Ind*), 72.80 (O**C**H$_2$CH$_2$), 49.70 (N**C**HMe$_2$), 29.14, 28.88 (NCH**Me$_2$**), 25.09 (OCH$_2$**C**H$_2$), 21.82, 17.17, 16.88, 16.11, 15.67, 15.60 (Ind***Me**), 7.41, 7.09 (Si**Me**) ppm.

Anal. Calcd for C$_{25}$H$_{41}$ClNOScSi: C, 62.54; H, 8.61; N, 2.92. Found: C, 61.53; H, 8.25; N, 2.73.

Synthesis of ^{Me_2}SB(^{nBu}N,I*)Sc(Cl)(THF) (2)

To a mixture of ^{Me_2}SB(^{nBu}N,I*)$Li_2(THF)_{0.18}$ (0.50 g, 1.41 mmol) and $ScCl_3$·3THF (0.52 g, 1.41 mmol) was added benzene (20 mL). The reaction mixture was stirred at room temperature for 18 h and then the volatiles were removed *in vacuo*. The product was extracted into benzene (2 × 15 mL) and evaporation of the solution afforded an orange solid which was then cooled to 0 °C and washed with pentane (2 × 15 mL) to afford ^{Me_2}SB(^{nBu}N,I*)Sc(Cl)(THF) (**3**) as a pale orange powder (0.04 g, 6%). Colourless crystals suitable for an X-ray diffraction study were obtained from a saturated benzene-d_6 solution at 5 °C.

^{1}H NMR (C_6D_6, 500.3 MHz, 298 K): 3.17 (2H, overlapping m, N-C_α**H**$_2$), 3.14 (4H, overlapping m, OC**H**$_2$CH$_2$), 2.81, 2.60, 2.58, 2.52 (3H each, s, Ind***Me**), 1.97 (6H, s, Ind***Me**), 1.68 (2H, m, N-C_β**H**$_2$), 1.45 (2H, m, N-C_γ**H**$_2$), 1.01 (3H, t, $^3J_{H\text{-}H}$ = 7.28 Hz, N-C_δ**H**$_3$), 0.93 (4H, overlapping m, OCH$_2$C**H**$_2$), 0.86, 0.65 (3H each, s, Si**Me**) ppm.

^{13}C{^{1}H} NMR (C_6D_6, 125.8 MHz, 298 K): 141.63, 136.35, 129.36, 129.16, 128.59, 127.02, 119.87 (**Ind***), 94.95 (Si-**C**Ind*), 72.13 (O**C**H$_2$CH$_2$), 48.84 (N-**C**$_\alpha$), 38.69 (N-**C**$_\beta$), 25.09 (OCH$_2$**C**H$_2$), 21.86 (Ind***Me**), 21.28 (N-**C**$_\gamma$), 17.17, 16.89, 16.13, 15.63, 15.58 (Ind***Me**), 14.51 (N-**C**$_\delta$), 6.40, 6.20 (Si**Me**) ppm.

Synthesis of ^{Me_2}SB(^{Ph}N,I*)Sc(Cl)(THF) (3)

To a mixture of ^{Me_2}SB(^{Ph}N,I*)$Li_2(THF)_{0.90}$ (0.50 g, 1.17 mmol) and $ScCl_3$·3THF (0.43 g, 1.17 mmol) was added benzene (20 mL). The reaction mixture was stirred at room temperature for 18 h and then the volatiles were removed *in vacuo*. The product was extracted into benzene (2 × 15 mL) and evaporation of the solution afforded an orange solid. The solid was then cooled to 0 °C and washed with pentane (2 × 15 mL) to afford ^{Me_2}SB(^{Ph}N,I*)Sc(Cl)(THF) (**2**) as a pale orange powder (0.24 g, 41%). Yellow crystals suitable for an X-ray diffraction study were obtained from a saturated pentane solution at room temperature.

^{1}H NMR (C_6D_6, 400.2 MHz, 298 K): 7.20 (2H, t, $^3J_{H\text{-}H}$ = 7.54 Hz, *m*-C_6**H**$_5$), 7.07 (2H, d, $^3J_{H\text{-}H}$ = 7.77 Hz, *o*-C_6**H**$_5$), 6.76 (1H, t, $^3J_{H\text{-}H}$ = 7.16 Hz, *p*-C_6**H**$_3$), 3.16 (4H, m, OC**H**$_2$CH$_2$), 2.82, 2.59 (3H each, s, Ind***Me**), 2.48 (6H, s, Ind***Me**), 1.93, 1.91 (3H each, s, Ind***Me**), 0.93, 0.89 (3H each, s, Si**Me**), 0.89 (4H, overlapping m, OCH$_2$C**H**$_2$) ppm.

^{13}C{^{1}H} NMR (C_6D_6, 125.8 MHz, 298 K): 153.40 (*i*-**C**$_6$H$_5$), 142.69, 136.92, 130.15, 129.77 (**Ind***), 129.55 (*m*-**C**$_6$H$_5$), 128.99, 128.59, 121.34 (**Ind***), 120.45 (*o*-**C**$_6$H$_5$), 118.59 (*p*-**C**$_6$H$_5$), 95.56 (Si-**C**Ind*), 71.84 (O**C**H$_2$CH$_2$), 25.15 (OCH$_2$**C**H$_2$), 22.07, 17.20, 16.90, 16.15, 15.84, 15.74 (Ind***Me**), 7.39, 6.52 (Si**Me**) ppm.

Anal. Calcd for $C_{54}H_{74}Cl_2N_2O_2Sc_2Si_2$: C, 64.85; H, 7.46; N, 2.80. Found: C, 55.71; H, 6.45; N, 2.52.

Synthesis of ^{Me_2}SB(^{iPr}N,I*)Sc(O-2,6-^{i}Pr-C_6H_3)(THF) (4)

To a mixture of ^{Me_2}SB(^{iPr}N,I*)Sc(Cl)(THF) (**1**, 0.46 g, 0.98 mmol) and K(O-2,6-^{i}Pr-C_6H_3) (0.23 g, 1.08 mmol) was added benzene (20 mL). The reaction mixture was stirred at room temperature for 18 h and then the volatiles were removed *in vacuo*. The product was extracted into benzene (2 × 15 mL) and evaporation of the solution afforded a pale yellow solid. The solid was then cooled to 0 °C and washed with pentane (1 × 15 mL) to afford ^{Me_2}SB(^{iPr}N,I*)Sc(O-2,6-^{i}Pr-C_6H_3)(THF) (**4**) as a very pale yellow powder (0.27 g, 44%). Colourless crystals suitable for an X-ray diffraction study were obtained from a saturated pentane solution at -23 °C.

^{1}H NMR (C_6D_6, 400.2 MHz, 298 K): 7.20 (2H, d, $^3J_{H-H}$ = 7.58 Hz, *m*-$C_6\mathbf{H}_3$), 7.0 (1H, t, $^3J_{H-H}$ = 7.52 Hz, *p*-$C_6\mathbf{H}_3$), 3.54 (3H, overlapping m, C**H**Me_2 and NC**H**Me_2), 3.23 (2H, m, OC$\mathbf{H}_2CH_2$), 3.09 (2H, m, OC$\mathbf{H}_2CH_2$), 2.61, 2.60, 2.57, 2.42 (3H each, s, Ind***Me**), 2.04 (6H, s, Ind***Me**), 1.38 (6H, d, $^3J_{H-H}$ = 6.85 Hz, CH$\mathbf{Me}_2$), 1.27 (6H, d, $^3J_{H-H}$ = 6.85 Hz, CH$\mathbf{Me}_2$), 1.18 (3H, overlapping d, $^3J_{H-H}$ = 5.96 Hz, NCH$\mathbf{Me}_2$), 1.16 (3H, overlapping d, $^3J_{H-H}$ = 5.96 Hz, NCH$\mathbf{Me}_2$), 0.98 (4H, m, $OCH_2C\mathbf{H}_2$), 0.95, 0.76 (3H each, s, Si**Me**) ppm.

^{13}C{^{1}H} NMR (C_6D_6, 125.8 MHz, 298 K): 157.72 (*i*-$\mathbf{C}_6H_3$), 140.02 (**Ind***), 136.54 (*o*-$\mathbf{C}_6H_3$), 126.47 (**Ind***), 123.43 (*m*-$\mathbf{C}_6H_3$), 118.53 (*p*-$\mathbf{C}_6H_3$), 117.67 (**Ind***), 94.37 (Si–**C**Ind*), 72.17 (O**C**H_2CH_2), 49.76 (N**C**HMe_2), 28.81, 28.13 (NCH$\mathbf{Me}_2$), 26.03 (**C**HMe_2), 25.10, 25.01 (CH$\mathbf{Me}_2$), 24.94 ($OCH_2\mathbf{C}H_2$), 21.93, 17.26, 16.96, 16.21, 15.94, 14.45 (Ind***Me**), 8.97, 8.12 (Si**Me**) ppm.

Anal. Calcd for $C_{36}H_{56}NO_2ScSi$: C, 71.13; H, 9.29; N, 2.30. Found: C, 69.18; H, 9.15; N, 2.12.

Synthesis of ^{Me_2}SB($^{i\mathrm{Pr}}$N,I*)Sc(O-2,4-^{t}Bu-C_6H_3)(THF) (5)

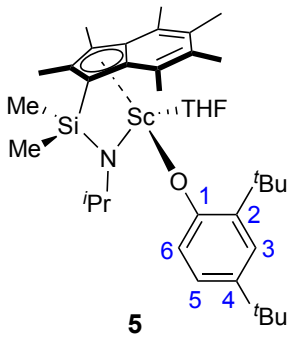

5

To a mixture of ^{Me_2}SB($^{i\mathrm{Pr}}$N,I*)Sc(Cl)(THF) (**1**, 0.50 g, 1.07 mmol) and K(O-2,4-^{t}Bu-C_6H_3) (0.29 g, 1.18 mmol) was added benzene (20 mL). The reaction mixture was stirred at room temperature for 18 h and then the volatiles were removed *in vacuo*. The product was extracted into benzene (2 × 15 mL) and evaporation of the solution afforded a pale yellow solid. The solid was then cooled to 0 °C and washed with pentane (2 × 15 mL) to afford ^{Me_2}SB($^{i\mathrm{Pr}}$N,I*)Sc(O-2,6-^{i}Pr-C_6H_3)(THF) (**4**) as a very pale yellow powder (0.23 g, 34%).

^{1}H NMR (C_6D_6, 500.3 MHz, 298 K): 7.55 (1H, d, $^4J_{H-H}$ = 2.55 Hz, 3-$C_6\mathbf{H}_3$), 7.32 (1H, dd, $^3J_{H-H}$ = 8.25 Hz, $^4J_{H-H}$ = 2.52 Hz, 5-$C_6\mathbf{H}_3$), 6.92 (1H, d, $^3J_{H-H}$ = 8.23 Hz, 6-$C_6\mathbf{H}_3$), 3.47 (1H, sept, NC**H**Me_2), 3.18 (4H, m, OC$\mathbf{H}_2CH_2$), 2.77 (3H, s, Ind***Me**), 2.59 (6H, s, Ind***Me**), 2.46, 2.04, 2.03 (3H each, s, Ind***Me**), 1.62, 1.40 (9H each, s, C$\mathbf{Me}_3$-C_6H_3), 1.27 (3H, d, $^3J_{H-H}$ = 6.22 Hz, NCH$\mathbf{Me}_2$), 1.16 (3H, d, $^3J_{H-H}$ = 6.22 Hz, NCH$\mathbf{Me}_2$), 0.99 (3H, s, Si**Me**), 0.92 (4H, m, $OCH_2C\mathbf{H}_2$), 0.73 (3H, s, Si**Me**) ppm.

^{13}C{^{1}H} NMR (C_6D_6, 125.8 MHz, 298 K): 160.40 (1-$\mathbf{C}_6H_3$), 140.23 (**Ind***), 139.64 (4-$\mathbf{C}_6H_3$), 136.44 (**Ind***), 135.39 (2-$\mathbf{C}_6H_3$), 128.59, 127.55, 126.49 (**Ind***), 123.78 (5-$\mathbf{C}_6H_3$), 123.24 (3-$\mathbf{C}_6H_3$), 123.07 (6-$\mathbf{C}_6H_3$), 117.97 (**Ind***), 94.73 (Si-**C**Ind*), 72.35 (O**C**H_2CH_2), 49.61 (N**C**HMe_2), 35.44, 34.42 (**C**Me_3-C_6H_3), 32.16, 30.31 (C$\mathbf{Me}_3$-C_6H_3), 29.67, 28.62 (NCH$\mathbf{Me}_2$), 24.82 ($OCH_2\mathbf{C}H_2$), 21.97, 17.25, 16.95, 16.27, 14.59 (Ind***Me**), 8.19, 7.80 (Si**Me**) ppm.

Synthesis of ^{Me_2}SB($^{n\mathrm{Bu}}$N,I*)Sc(O-2,6-^{i}Pr-C_6H_3)(THF) (6)

To a mixture of ^{Me_2}SB($^{n\mathrm{Bu}}$N,I*)$Li_2(THF)_{0.18}$ (0.50 g, 1.41 mmol) and $ScCl_3$·3THF (0.52 g, 1.41 mmol) was added benzene (20 mL). The reaction mixture was stirred at room temperature for 18 h, and then transferred to the benzene solution of K(O-2,6-^{i}Pr-C_6H_3) (0.34 g, 1.55 mmol). The reaction mixture was stirred at room temperature for 18 h, and then the volatiles were removed *in vacuo*. The product was extracted into benzene (2 × 15 mL) and evaporation of the solution afforded a pale yellow solid. The solid was then cooled to 0 °C and washed with pentane. A saturated pentane filtrate of **6** was stored at -23 °C given colourless crystals suitable for an X-ray diffraction study.

^{1}H NMR (C_6D_6, 400.2 MHz, 298 K): 7.20 (2H, d, $^{3}J_{H\text{-}H}$ = 7.63 Hz, *m*-$C_6\mathbf{H}_3$), 6.99 (1H, t, $^{3}J_{H\text{-}H}$ = 7.63 Hz, *p*-$C_6\mathbf{H}_3$), 3.57 (2H, m, C**H**Me_2), 3.25 (2H, overlapping m, N-$C_\alpha\mathbf{H}_2$), 3.10 (4H, overlapping m, OC$\mathbf{H}_2CH_2$), 2.61, 2.60, 2.59, 2.43 (3H each, s, Ind***Me**), 2.05 (6H, s, Ind***Me**), 1.54 (2H, m, N-$C_\beta\mathbf{H}_2$), 1.38 (6H, d, $^{3}J_{H\text{-}H}$ = 6.80 Hz, CH$\mathbf{Me}_2$), 1.32 (2H, overlapping m, N-$C_\gamma\mathbf{H}_2$), 1.27 (6H, d, $^{3}J_{H\text{-}H}$ = 6.75 Hz, CH$\mathbf{Me}_2$), 0.94 (3H, overlapping t, $NCH_2CH_2CH_2C\mathbf{H}_3$), 0.94, 0.76 (3H each, s, Si**Me**) ppm.

Synthesis of ^{Me_2}SB(^{Ph}N,I*)Sc(O-2,6-^{i}Pr-C_6H_3)(THF) (7)

To a mixture of ^{Me_2}SB(^{Ph}N,I*)Sc(Cl)(THF) (**3**, 0.50 g, 1.00 mmol) and K(O-2,6-^{i}Pr-C_6H_3) (0.24 g, 1.10 mmol) was added benzene (20 mL). The reaction mixture was stirred at room temperature for 18 h and then the volatiles were removed *in vacuo*. The product was extracted into benzene (2 × 15 mL) and evaporation of the solution afforded a pale orange solid. The solid was then cooled to 0 °C and washed with pentane (3 × 15 mL) to afford ^{Me_2}SB(^{Ph}N,I*)Sc(O-2,6-^{i}Pr-C_6H_3)(THF) (**6**) as a pale yellow powder (0.27 g, 41%).

^{1}H NMR (C_6D_6, 500.3 MHz, 298 K): 7.15 (2H, overlapping d, $^{3}J_{H\text{-}H}$ = 7.18 Hz, *m*-$C_6\mathbf{H}_3$), 7.10 (1H, t, $^{3}J_{H\text{-}H}$ = 7.96 Hz, *p*-$C_6\mathbf{H}_5$), 6.97 (1H, t, $^{3}J_{H\text{-}H}$ = 7.57 Hz, *p*-$C_6\mathbf{H}_3$), 6.82 (2H, d, $^{3}J_{H\text{-}H}$ = 7.96 Hz, *o*-$C_6\mathbf{H}_5$), 6.69 (2H, t, $^{3}J_{H\text{-}H}$ = 6.78 Hz, *m*-$C_6\mathbf{H}_5$), 3.47 (2H, sept, $^{3}J_{H\text{-}H}$ = 6.73 Hz, C**H**Me_2), 3.18 (4H, m, OC$\mathbf{H}_2CH_2$), 2.61, 2.55, 2.54, 2.02 (3H each, s, Ind***Me**), 1.98 (6H, s, Ind***Me**), 1.20 (6H, overlapping d, $^{3}J_{H\text{-}H}$ = 4.89 Hz, CH$\mathbf{Me}_2$), 1.18 (6H, overlapping d, $^{3}J_{H\text{-}H}$ = 4.89 Hz, CH$\mathbf{Me}_2$), 1.13, 0.91 (3H each, s, Si**Me**), 0.87 (4H, overlapping m, $OCH_2C\mathbf{H}_2$) ppm.

^{13}C{^{1}H} NMR (C_6D_6, 125.8 MHz, 298 K): 157.46 (*i*-$\mathbf{C}_6H_3$), 154.11 (*i*-$\mathbf{C}_6H_5$), 141.02 (**Ind***), 136.82 (*o*-$\mathbf{C}_6H_3$), 129.50, 126.57 (**Ind***), 123.33 (*m*-$\mathbf{C}_6H_3$), 120.13, 119.09 (**Ind***), 118.33 (*p*-$\mathbf{C}_6H_3$), 117.50 (**Ind***), 94.39 (Si-**C**Ind*), 72.08 (O**C**H_2CH_2), 26.42 (**C**HMe_2-C_6H_3), 25.10, 24.98 (CH$\mathbf{Me}_2$-C_6H_3), 24.33 ($OCH_2\mathbf{C}H_2$), 22.14, 17.16, 16.92, 16.23, 15.84, 14.22 (Ind***Me**), 7.71, 6.34 (Si**Me**) ppm.

Synthesis of ^{Me_2}SB(^{tBu}N,I*)Al(Cl)(THF) (8)

To a solid mixture of $AlCl_3$·THF (1.23 g, 6.00 mmol) and ^{Me_2}SB(^{tBu}N,I*)$Li_2(THF)_{0.12}$ (2.10 g, 6.00 mmol) was added benzene (30 mL). The reaction mixture was stirred at room temperature for 18 h and then the volatiles were removed *in vacuo*. The product was extracted into benzene (2 × 15 mL) and evaporation of the solution afforded a yellow solid. The solid was then washed with pentane (2 × 20 mL) to afford ^{Me_2}SB(^{tBu}N,I*)Al(Cl)(THF) (**8**) as a pale yellow solid (1.35 g, 49%). Colourless crystals suitable for an X-ray diffraction study were obtained from a saturated benzene solution at room temperature.

Isomer 1* (57%):** ^{1}H NMR (C_6D_6, 400.2 MHz, 298 K): 3.20 (4H, m, OC$\mathbf{H}_2CH_2$), 2.79, 2.72, 2.59, 2.51, 2.39, 2.37 (3H each, s, IndMe**), 1.44 (9H, s, NC$\mathbf{Me}_3$), 0.72 (4H, m, $OCH_2C\mathbf{H}_2$), 0.55, 0.34 (3H each, s, Si**Me**) ppm.

^{13}C{^{1}H} NMR (C_6D_6, 100.6 MHz, 298 K): 144.3, 142.03, 141.26, 127.18, 125.51, 125.01, 123.97 (**Ind***), 72.20 (O**C**H_2CH_2), 60.10 (Si-**C**Ind*), 51.31 (N**C**Me_3), 35.64 (NC$\mathbf{Me}_3$), 24.59 ($OCH_2\mathbf{C}H_2$), 21.62, 18.99, 17.07 16.99, 16.68, 16.05 (Ind***Me**), 7.28, 5.95 (Si**Me**) ppm.

Isomer 2* (43%):** ^{1}H NMR (C_6D_6, 400.2 MHz, 298 K): 3.37 (4H, overlapping m, OC$\mathbf{H}_2CH_2$), 3.05, 2.83, 2.63 (3H each, s, IndMe**), 2.35 (6H, s, Ind***Me**), 2.09 (3H, s, Ind***Me**), 1.43 (9H, s, NC$\mathbf{Me}_3$), 0.88 (4H, overlapping m, $OCH_2C\mathbf{H}_2$), 0.43, 0.41 (3H, s, Si**Me**) ppm.

$^{13}C\{^1H\}$ NMR (C_6D_6, 100.6 MHz, 298 K): 144.48, 140.04, 139.12, 127.53, 126.36, 125.09, 124.74 (**Ind***), 72.20 (O**C**H_2CH_2), 59.43 (Si-**C**Ind*), 51.34 (N**C**Me_3), 35.53 (NC**Me**$_3$), 25.12 (OCH$_2$**C**H$_2$), 24.55, 22.73, 18.32, 16.58, 16.19, 14.28 (Ind***Me**), 7.57, 5.64 (Si**Me**) ppm.

Anal. Calcd for $C_{25}H_{41}AlClNOSi$: C, 64.98; H, 8.94; N, 3.03. Found: C, 61.85; H, 8.90; N, 2.59.

Synthesis of ^{Me2}SB(^{tBu}N,I*)Al(O-2,6-Me-C$_6$H$_3$)(THF) (9)

To a solid mixture of ^{Me2}SB(^{tBu}N,I*)Al(Cl)(THF) (**8**, 0.50 g, 1.08 mmol) and K(O-2,6-Me-C_6H_3) (0.18 g, 1.12 mmol) was added benzene (30 mL). The reaction mixture was stirred at room temperature for 18 h and then the volatiles were removed *in vacuo*. The product was extracted into benzene (2 × 15 mL) and evaporation of the solution afforded a yellow solid. The solid was then washed with pentane (2 × 20 mL) to afford ^{Me2}SB(^{tBu}N,I*)Al (O-2,6-Me-C_6H_3)(THF) (**9**) as a pale yellow solid (0.24 g, 41%). Pale yellow crystals suitable for an X-ray diffraction study were obtained from a saturated benzene solution at room temperature.

Isomer 1* (66%):** ^{1}H NMR (C_6D_6, 400.2 MHz, 298 K): 6.85 (2H, d, $^3J_{H\text{-}H}$ = 7.4 Hz, *m*-C$_6$**H**$_3$), 6.66 (1H, t, $^3J_{H\text{-}H}$ = 7.4 Hz, *p*-C$_6$**H**$_3$), 3.65 (2H, m, OC**H**$_2$CH$_2$), 2.84, 2.73, 2.68, 2.37, 2.20, 2.18 (3H each, s, IndMe**), 1.75 (6H, br, C$_6$H$_3$**Me$_2$**), 1.47 (9H, s, NC**Me**$_3$), 0.92 (4H, m, OCH$_2$C**H**$_2$), 0.45, 0.33 (3H each, s, Si**Me**) ppm.

$^{13}C\{^1H\}$ NMR (C_6D_6, 100.6 MHz, 298 K): 155.39 (*i*-**C**$_6$H$_3$), 145.26, 140.47, 138.77 (**Ind***), 128.64 (*m*-**C**$_6$H$_3$), 126.60 (*o*-**C**$_6$H$_3$), 126.52, 124.49, 124.36 (**Ind***), 118.79 (*p*-**C**$_6$H$_3$), 73.04 (O**C**H$_2$CH$_2$), 51.09 (N**C**Me$_3$), 35.34 (NC**Me**$_3$), 24.55 (OCH$_2$**C**H$_2$), 16.88 (C$_6$H$_3$**Me$_2$**), 22.37, 18.17, 17.96, 17.19, 16.69, 16.24 (Ind***Me**), 7.72, 4.87 (Si**Me**) ppm.

Isomer 2* (34%):** ^{1}H NMR (C_6D_6, 400.2 MHz, 298 K): 6.98 (2H, d, $^3J_{H\text{-}H}$ = 7.4 Hz, *m*-C$_6$**H**$_3$), 6.76 (1H, t, $^3J_{H\text{-}H}$ = 7.4 Hz, *p*-C$_6$**H**$_3$), 3.44 (2H, m, OC**H**$_2$CH$_2$), 2.79, 2.53, 2.48, 2.40 (3H each, s, IndMe**), 2.39 (6H, s, Ind***Me**), 2.03 (6H, s, C$_6$H$_3$**Me$_2$**), 1.49 (9H, s, NC**Me**$_3$), 0.76 (4H, m, OCH$_2$C**H**$_2$), 0.47, 0.41 (3H each, s, Si**Me**) ppm.

$^{13}C\{^1H\}$ NMR (C_6D_6, 100.6 MHz, 298 K): 155.93 (*i*-**C**$_6$H$_3$), 144.18, 143.23, 141.03 (**Ind***), 128.90 (*m*-**C**$_6$H$_3$), 126.71 (*o*-**C**$_6$H$_3$), 126.79, 125.44, 124.51, 124.45 (**Ind***), 118.97 (*p*-**C**$_6$H$_3$), 72.98 (O**C**H$_2$CH$_2$), 51.15 (N**C**Me$_3$), 35.84 (NC**Me**$_3$), 24.51 (OCH$_2$**C**H$_2$), 17.60 (C$_6$H$_3$**Me$_2$**), 22.52, 17.92, 17.13, 17.05, 16.63, 15.87 (Ind***Me**), 7.28, 6.98 (Si**Me**) ppm.

Anal. Calcd for $C_{33}H_{50}AlNO_2Si$: C, 72.35; H, 9.20; N, 2.56. Found: C, 72.19; H, 8.82; N, 2.58.

Synthesis of ^{Me2}SB(^{tBu}N,I*)Al(O-2,4-^{t}Bu-C$_6$H$_3$)(THF) (10)

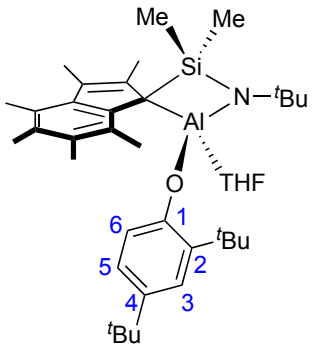

10

To a solid mixture of ^{Me2}SB(^{tBu}N,I*)Al(Cl)(THF) (**8**, 0.50 g, 1.08 mmol) and K(O-2,4-^{t}Bu-C_6H_3) (0.29 g, 1.13 mmol) was added benzene (30 mL). The reaction mixture was stirred at room temperature for 18 h and then the volatiles were removed *in vacuo*. The product was extracted into benzene (2 × 15 mL) and evaporation of the solution afforded a yellow solid. The solid was then washed with pentane (2 × 20 mL) to afford ^{Me2}SB(^{tBu}N,I*)Al (O-2,4-^{t}Bu-C_6H_3)(THF) (**10**) as a pale yellow solid (0.17 g, 24%). Pale yellow crystals suitable for an X-ray diffraction study were obtained from a saturated pentane solution at room temperature.

***Isomer 1* (55%):** ^{1}H NMR (C_6D_6, 400.2 MHz, 298 K): 7.50 (1H, d, $^3J_{H\text{-}H}$ = 2.6 Hz, 3-C$_6$**H**$_3$), 7.06 (1H, dd, $^3J_{H\text{-}H}$ = 8.3 Hz, $^4J_{H\text{-}H}$ = 2.6 Hz, 5-C$_6$**H**$_3$), 5.94 (1H, d, $^3J_{H\text{-}H}$ = 8.3 Hz, 6-C$_6$**H**$_3$), 3.42 (2H, m, OC**H**$_2$CH$_2$), 2.82, 2.62, 2.52, 2.45, 2.42, 2.41

(3H each, s, Ind*$\mathbf{Me}$), 1.65 (9H, s, 2-C$\mathbf{Me_3}$-C_6H_3), 1.50 (9H, s, NC$\mathbf{Me}_3$), 1.29 (9H, s, 4-C$\mathbf{Me_3}$-C_6H_3), 0.73 (4H, m, $OCH_2C\mathbf{H}_2$), 0.52, 0.44 (3H each, s, Si$\mathbf{Me}$) ppm.

$^{13}C\{^1H\}$ NMR (C_6D_6, 100.6 MHz, 298 K): 155.36 (1-$\mathbf{C}_6H_3$), 144.13, 142.96 (**Ind***), 140.67 (4-$\mathbf{C}_6H_3$), 139.14 (**Ind***), 136.92 (2-$\mathbf{C}_6H_3$), 126.90, 125.55, 124.64, 124.16 (**Ind***), 123.81 (5-$\mathbf{C}_6H_3$), 123.51 (3-$\mathbf{C}_6H_3$), 120.24 (6-$\mathbf{C}_6H_3$), 73.27 ($O\mathbf{C}H_2CH_2$), 51.13 (N$\mathbf{C}Me_3$), 35.95 (NC$\mathbf{Me}_3$), 35.38 (2-$\mathbf{C}Me_3$-C_6H_3), 34.33 (4-$\mathbf{C}Me_3$-C_6H_3), 32.01 (4-C$\mathbf{Me_3}$-C_6H_3), 30.07 (2-C$\mathbf{Me_3}$-C_6H_3), 24.50 ($OCH_2\mathbf{C}H_2$), 22.61, 17.44, 17.22, 17.04, 16.66, 15.90 (Ind*$\mathbf{Me}$), 7.44, 7.05 (Si$\mathbf{Me}$) ppm.

Isomer 2 **(45%):** ^1H NMR (C_6D_6, 400.2 MHz, 298 K): 7.38 (1H, d, $^3J_{H\text{-}H}$ = 2.6 Hz, 3-$C_6\mathbf{H}_3$), 6.51 (1H, dd, $^3J_{H\text{-}H}$ = 8.3 Hz, $^4J_{H\text{-}H}$ = 2.6 Hz, 5-$C_6\mathbf{H}_3$), 5.35 (1H, d, $^3J_{H\text{-}H}$ = 8.3 Hz, 6-$C_6\mathbf{H}_3$), 3.60 (2H, m, $O\mathbf{C}H_2CH_2$), 2.86, 2.78, 2.70, 2.40 (3H each, s, Ind*$\mathbf{Me}$), 2.19 (6H, s, Ind*$\mathbf{Me}$), 1.64 (9H, s, 2-C$\mathbf{Me_3}$-C_6H_3), 1.50 (9H, s, NC$\mathbf{Me}_3$), 1.17 (9H, s, 4-C$\mathbf{Me_3}$-C_6H_3), 0.89 (4H, m, $OCH_2C\mathbf{H}_2$), 0.47, 0.39 (3H each, s, Si$\mathbf{Me}$) ppm.

$^{13}C\{^1H\}$ NMR (C_6D_6, 100.6 MHz, 298 K): 154.95 (1-$\mathbf{C}_6H_3$), 144.52, 141.01 (**Ind***), 140.31 (4-$\mathbf{C}_6H_3$), 140.00 (**Ind***), 135.76 (2-$\mathbf{C}_6H_3$), 126.77, 124.60, 124.34 (**Ind***), 124.10 (5-$\mathbf{C}_6H_3$), 122.89 (3-$\mathbf{C}_6H_3$), 120.24 (6-$\mathbf{C}_6H_3$), 73.09 ($O\mathbf{C}H_2CH_2$), 51.12 (N$\mathbf{C}Me_3$), 35.65 (NC$\mathbf{Me}_3$), 35.30 (2-$\mathbf{C}Me_3$-C_6H_3), 34.18 (4-$\mathbf{C}Me_3$-C_6H_3), 31.89 (4-C$\mathbf{Me_3}$-C_6H_3), 30.16 (2-C$\mathbf{Me_3}$-C_6H_3), 24.57 ($OCH_2\mathbf{C}H_2$), 22.35, 18.01, 17.22, 16.92, 16.69, 16.32 (Ind*$\mathbf{Me}$), 7.74, 5.50 (Si$\mathbf{Me}$) ppm.

Anal. Calcd for $C_{39}H_{62}AlNO_2Si$: C, 74.12; H, 9.89; N, 2.22. Found: C, 64.68; H, 6.13; N, 2.54.

Representative NMR spectra of ^{Me_2}SB(^{R}N,I*)Li$_2$(THF)$_x$ and complexes 1–10

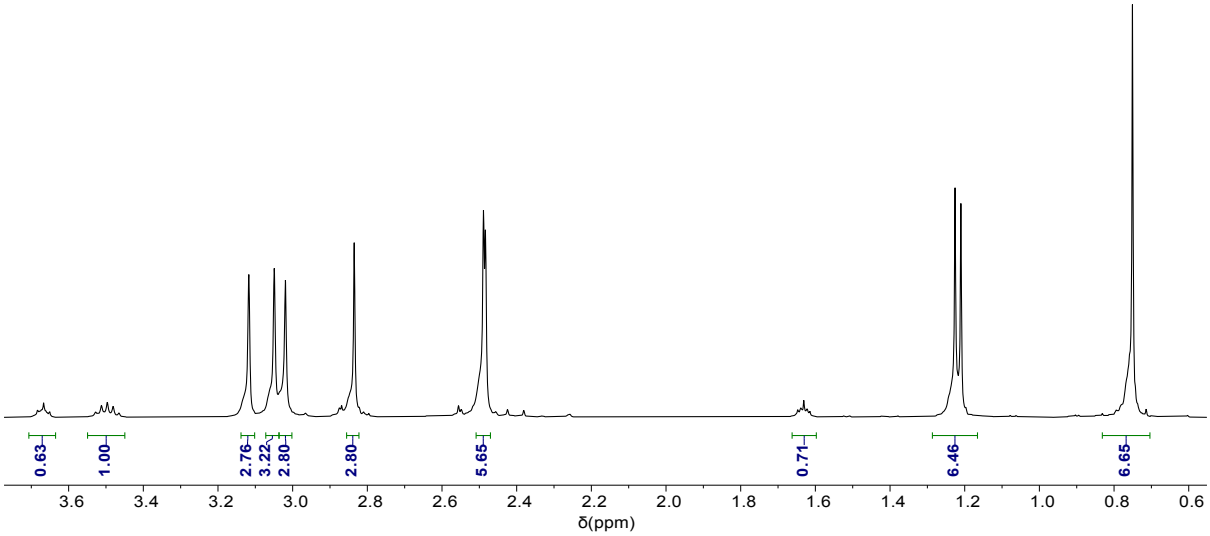

Fig. S1 ^{1}H NMR spectrum (C_5D_5N, 400.2 MHz, 298 K) of ^{Me_2}SB(^{iPr}N,I*)Li$_2$(THF)$_{0.17}$. Solvent resonances at 8.73, 7.59 and 7.22 ppm excluded for clarity.

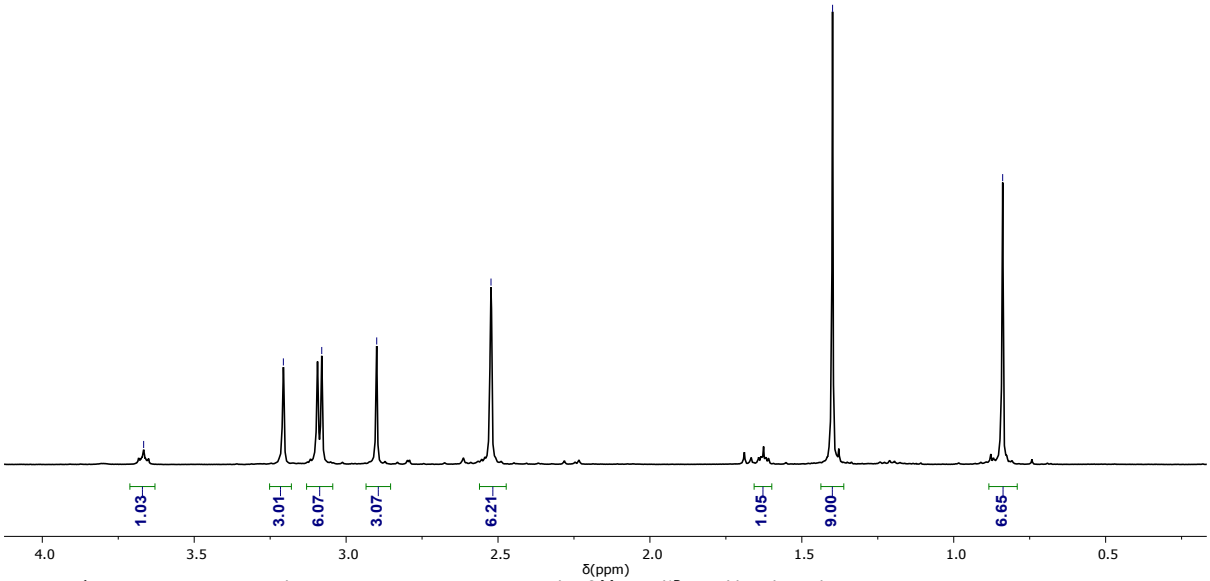

Fig. S2 ^{1}H NMR spectrum (C_5D_5N, 400.2 MHz, 298 K) of ^{Me_2}SB(^{tBu}N,I*)Li$_2$(THF)$_{0.25}$. Solvent resonances at 8.73, 7.59 and 7.22 ppm excluded for clarity.

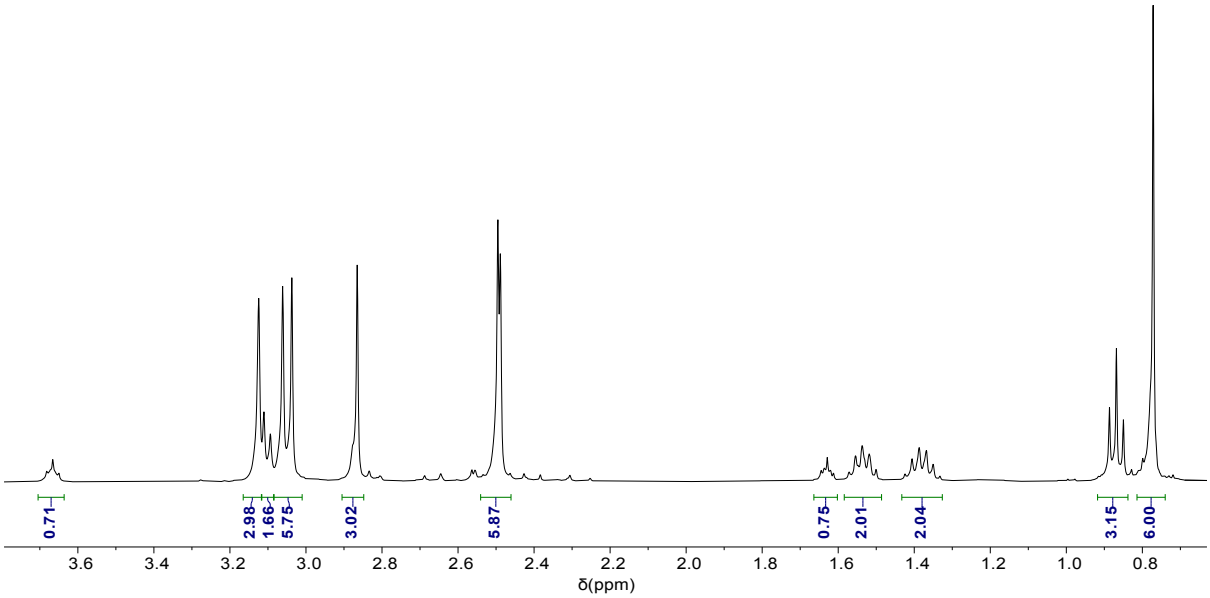

Fig. S3 ^{1}H NMR spectrum (C_5D_5N, 400.2 MHz, 298 K) of ^{Me_2}SB($^{n\text{Bu}}$N,I*)$Li_2(THF)_{0.18}$. Solvent resonances at 8.73, 7.59 and 7.22 ppm excluded for clarity.

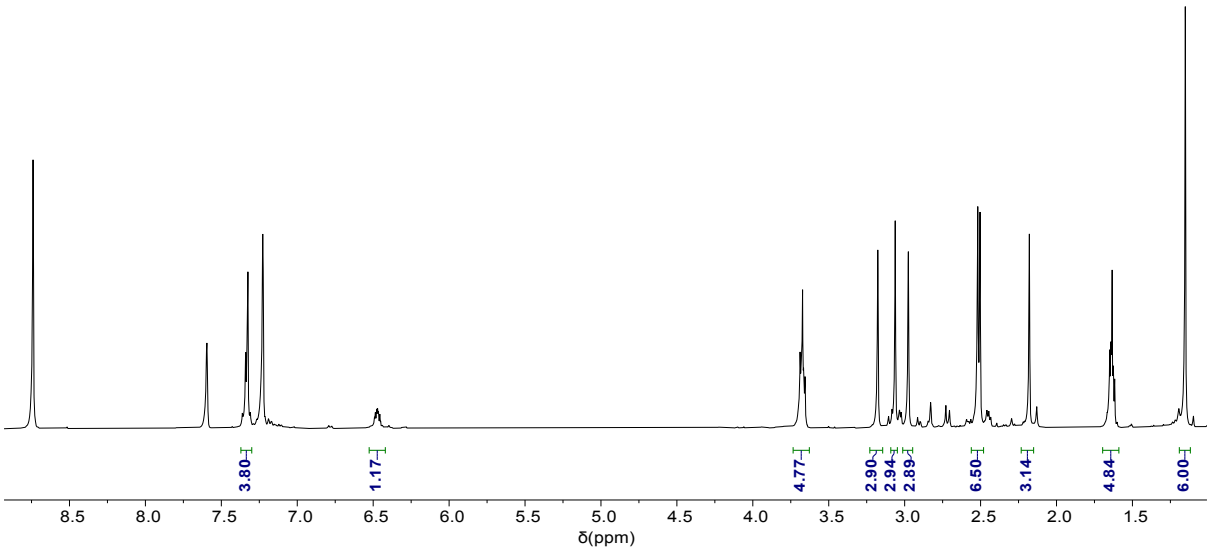

Fig. S4 ^{1}H NMR spectrum (C_5D_5N, 400.2 MHz, 298 K) of ^{Me_2}SB(^{Ph}N,I*)$Li_2(THF)_{0.90}$.

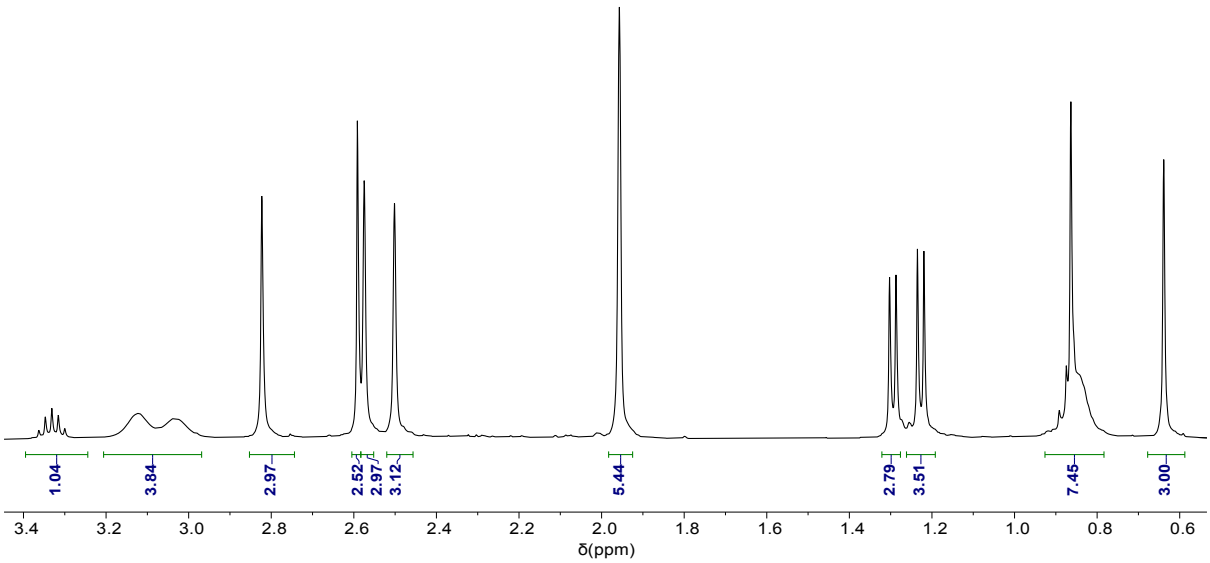

Fig. S5 ^{1}H NMR spectrum (C_6D_6, 400.2 MHz, 298 K) of ^{Me_2}SB(^{iPr}N,I*)Sc(Cl)(THF) (**1**). Solvent resonance at 7.16 ppm excluded for clarity.

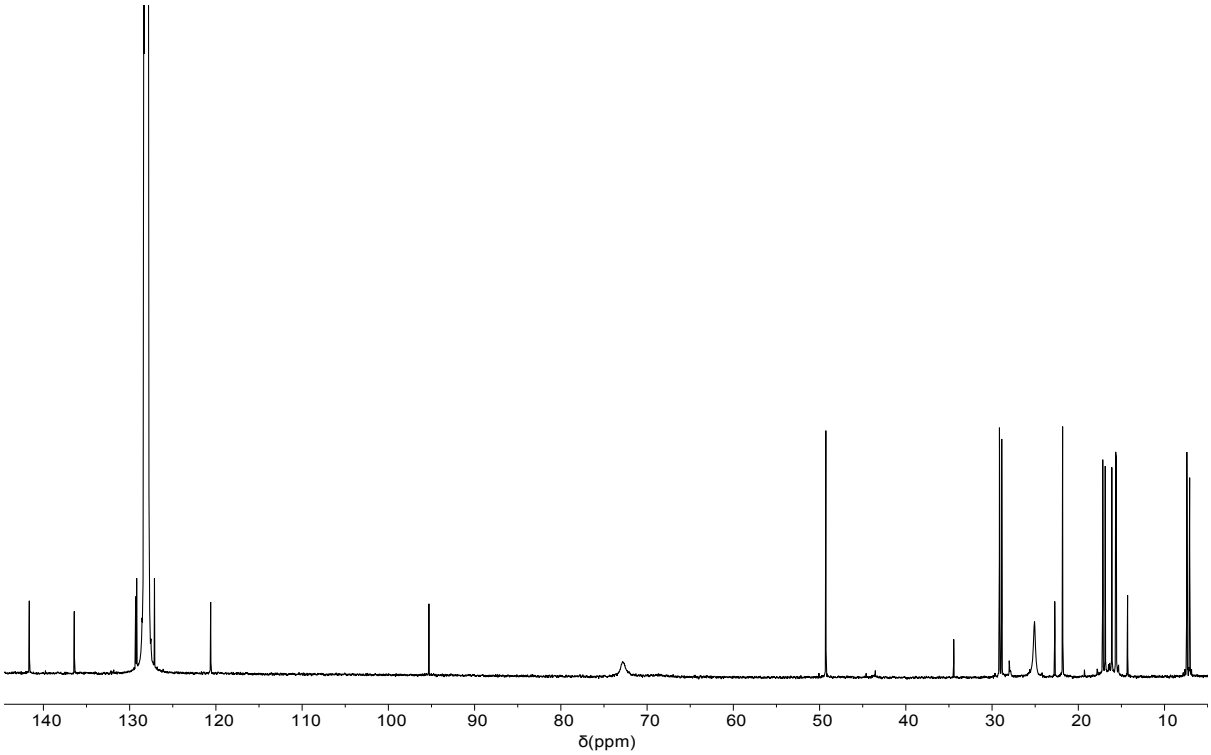

Fig. S6 ^{13}C{^{1}H} NMR spectrum (C_6D_6, 125.8 MHz, 298 K) of ^{Me_2}SB(^{iPr}N,I*)Sc(Cl)(THF) (**1**).

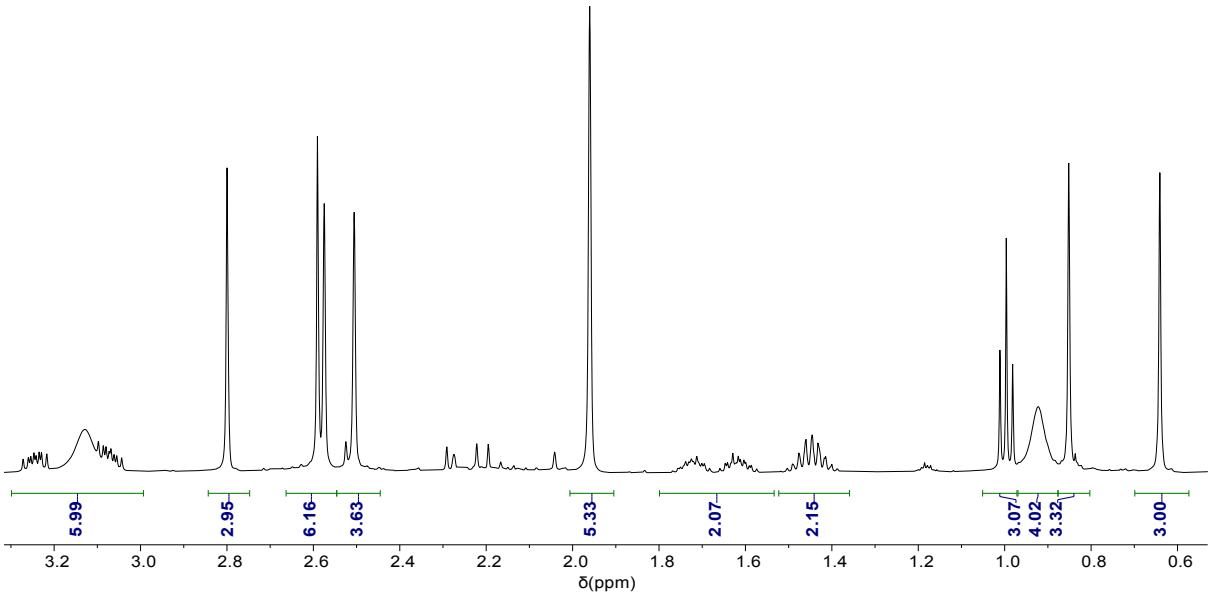

Fig. S7 ^{1}H NMR spectrum (C_6D_6, 400.2 MHz, 298 K) of $^{Me}_2$SB($^{n\text{Bu}}$N,I*)Sc(Cl)(THF) (**2**). Solvent resonance at 7.16 ppm excluded for clarity.

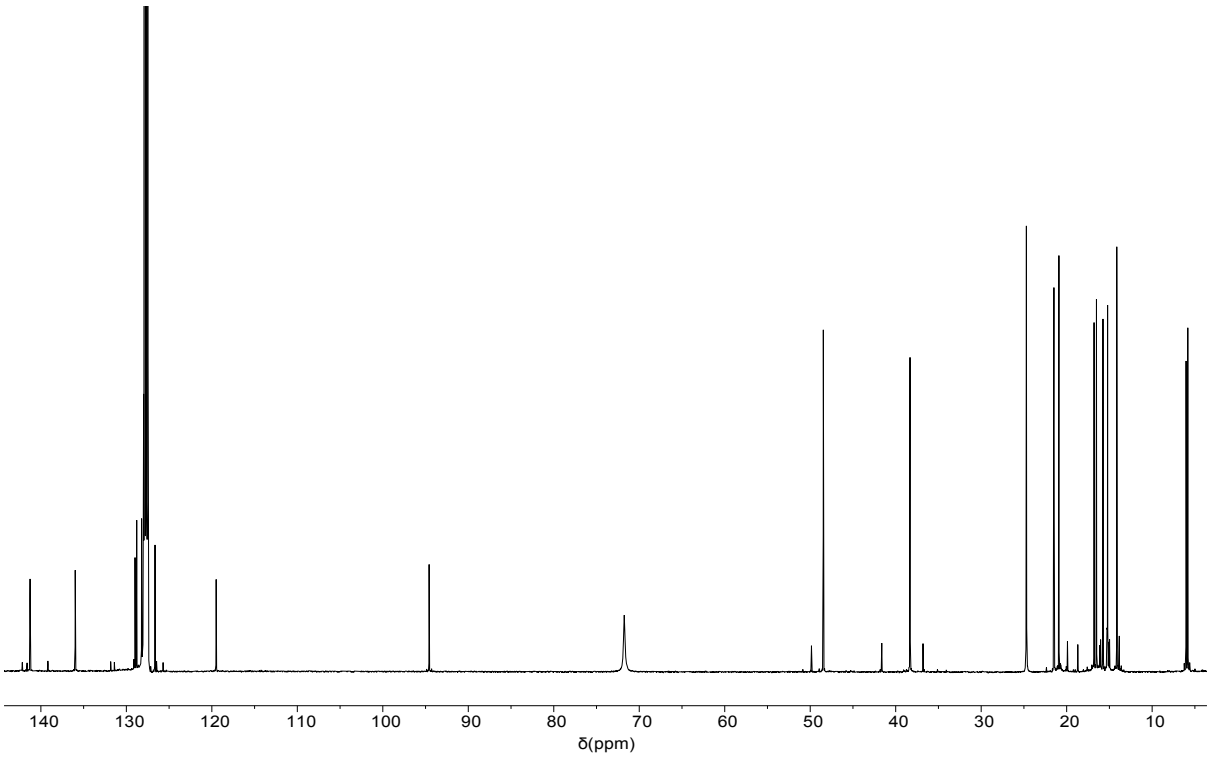

Fig. S8 ^{13}C{^{1}H} NMR spectrum (C_6D_6, 125.8 MHz, 298 K) of $^{Me}_2$SB($^{n\text{Bu}}$N,I*)Sc(Cl)(THF) (**2**).

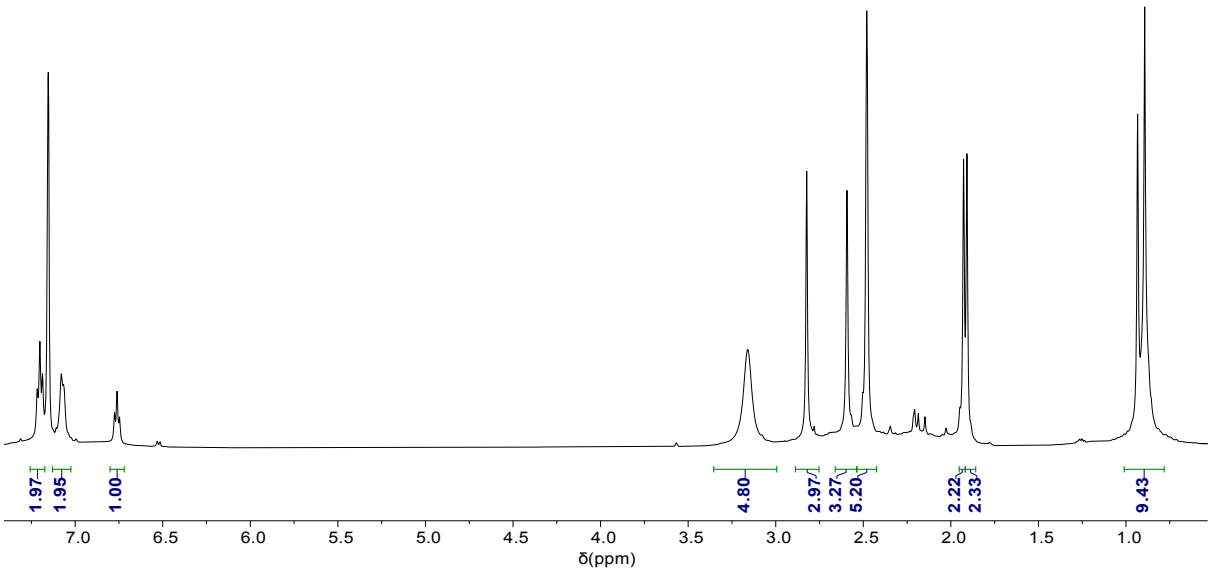

Fig. S9 ^{1}H NMR spectrum (C_6D_6, 400.2 MHz, 298 K) of ^{Me_2}SB(^{Ph}N,I*)Sc(Cl)(THF) (**3**).

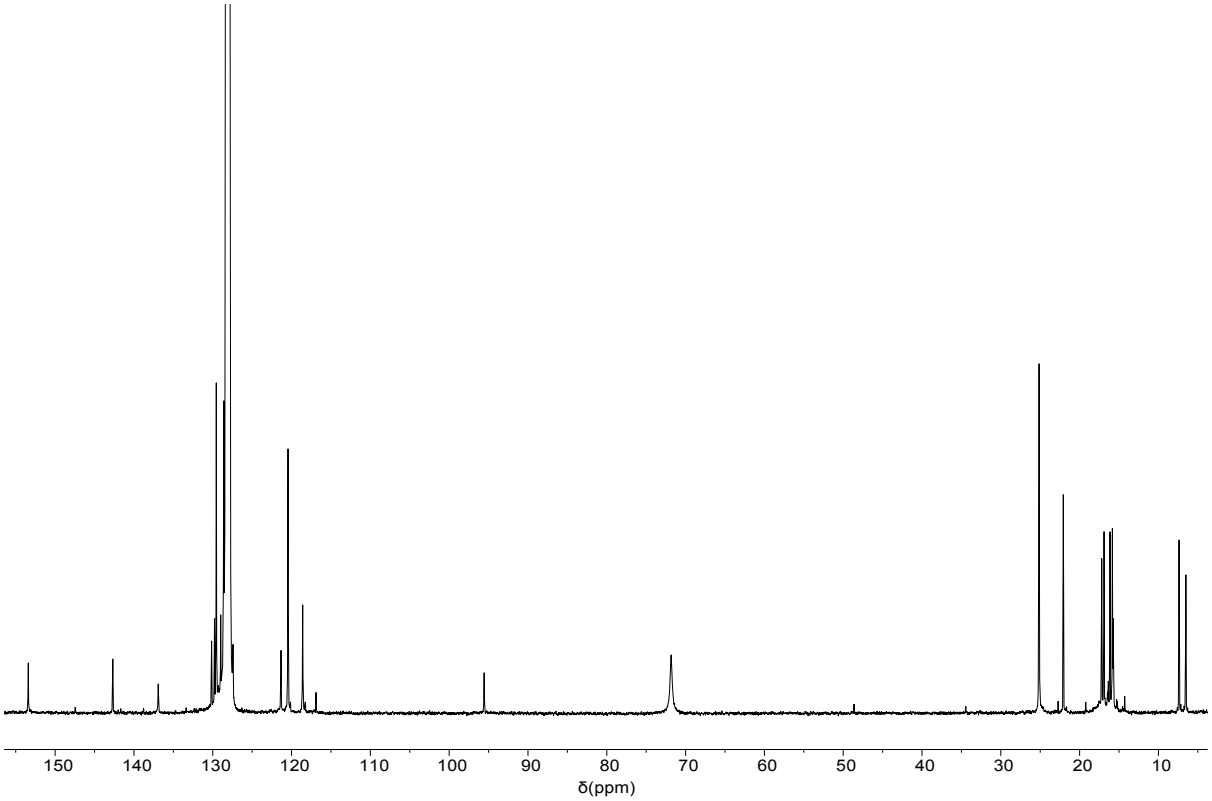

Fig. S10 ^{13}C{^{1}H} NMR spectrum (C_6D_6, 125.8 MHz, 298 K) of ^{Me_2}SB(^{Ph}N,I*)Sc(Cl)(THF) (**3**).

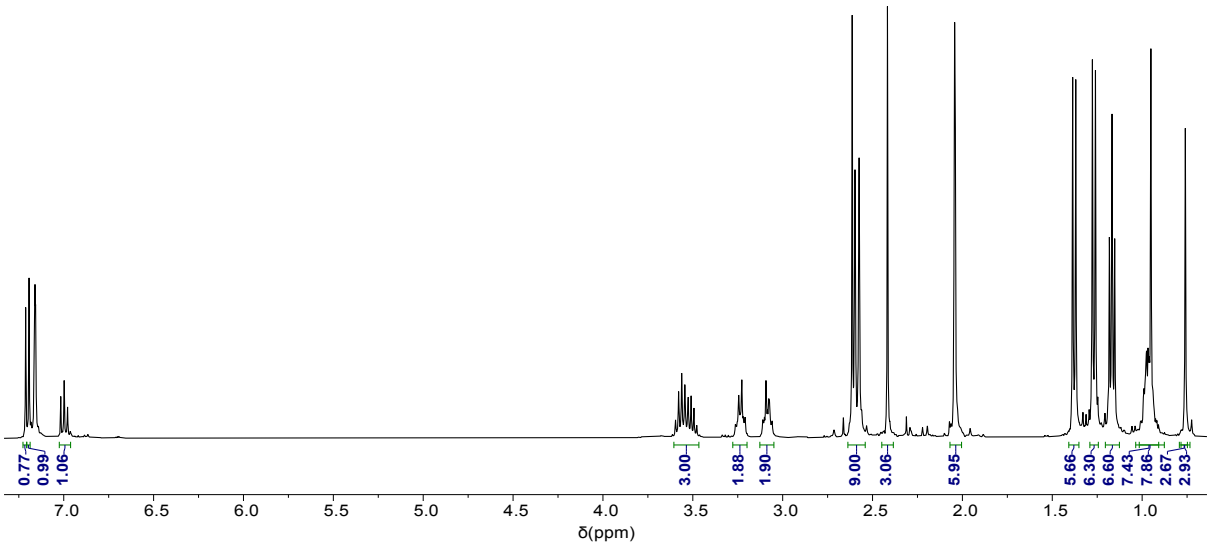

Fig. S11 ^{1}H NMR spectrum (C_6D_6, 400.2 MHz, 298 K) of ^{Me_2}SB(^{iPr}N,I*)Sc(O-2,6-^{i}Pr-C_6H_3)(THF) (**4**).

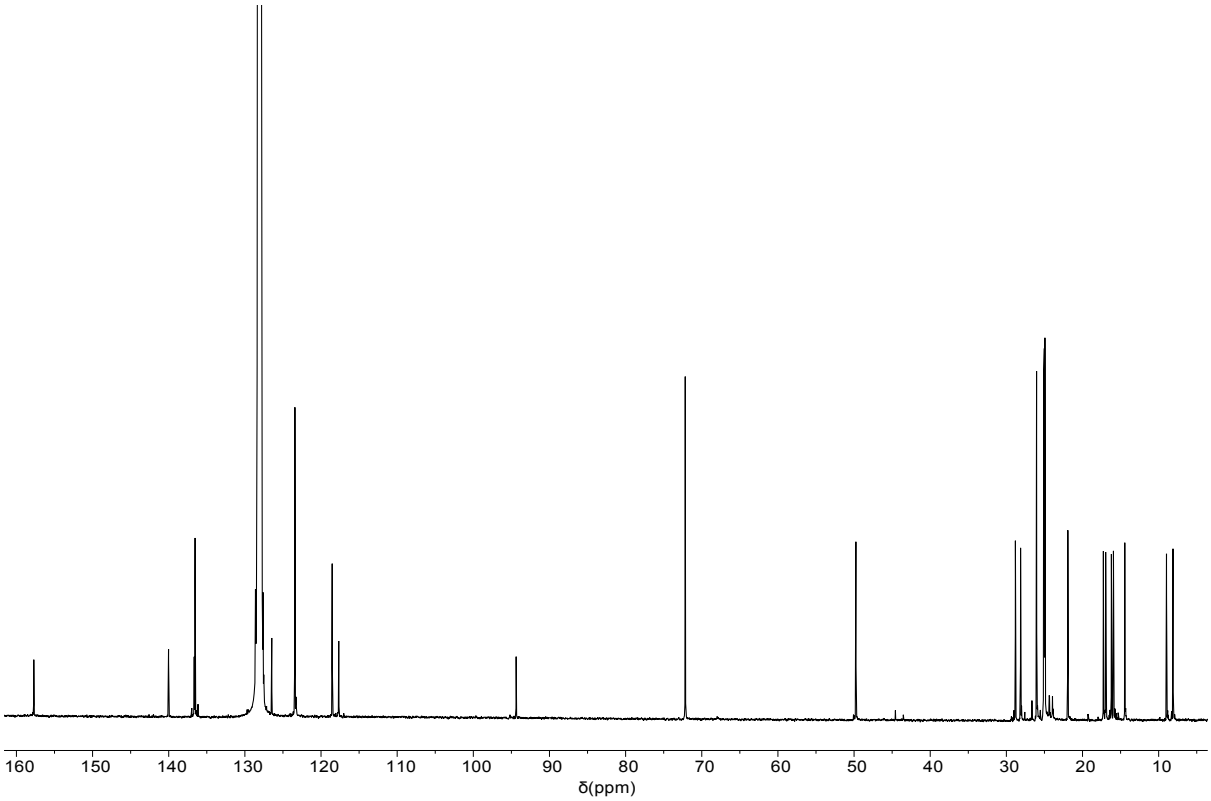

Fig. S12 ^{13}C{^{1}H} NMR spectrum (C_6D_6, 125.8 MHz, 298 K) of ^{Me_2}SB(^{iPr}N,I*)Sc(O-2,6-^{i}Pr-C_6H_3)(THF) (**4**).

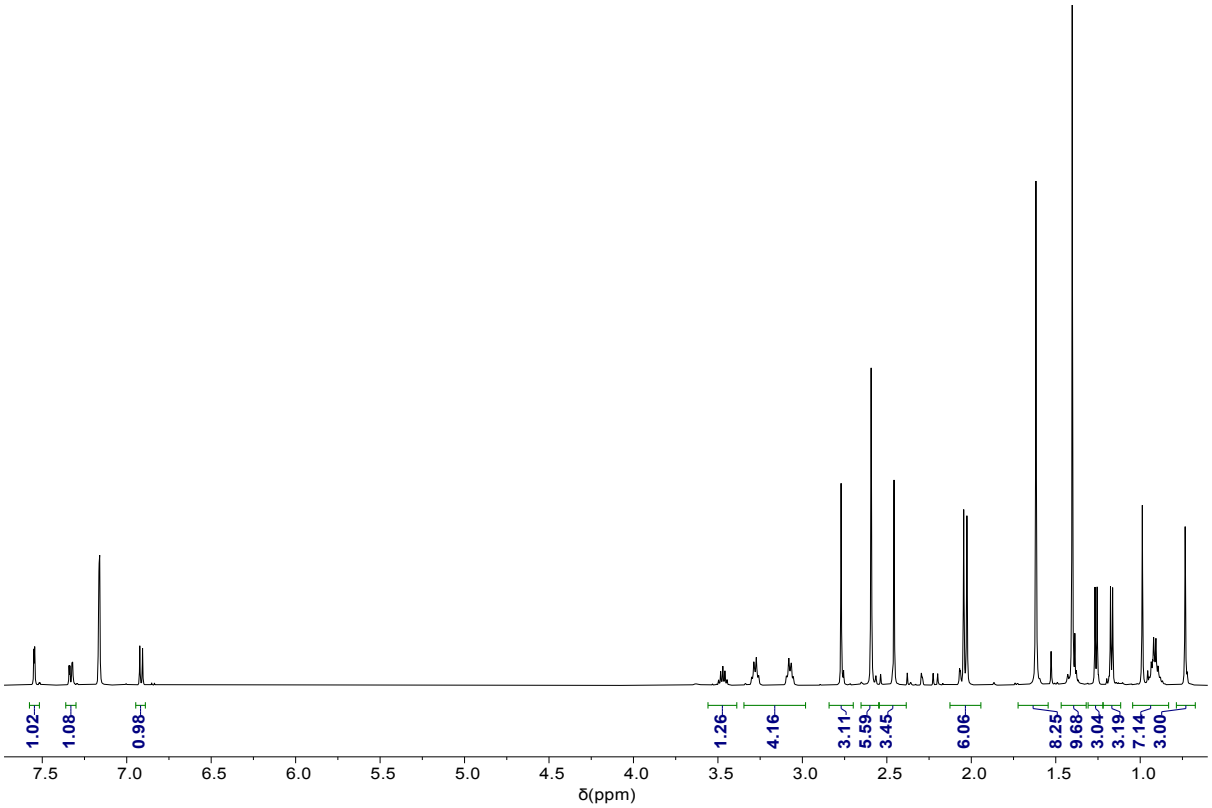

Fig. S13 ^{1}H NMR spectrum (C_6D_6, 125.8 MHz, 298 K) of $^{Me_2}SB(^{iPr}N,I^*)Sc(O\text{-}2,4\text{-}^{t}Bu\text{-}C_6H_3)(THF)$ (**5**).

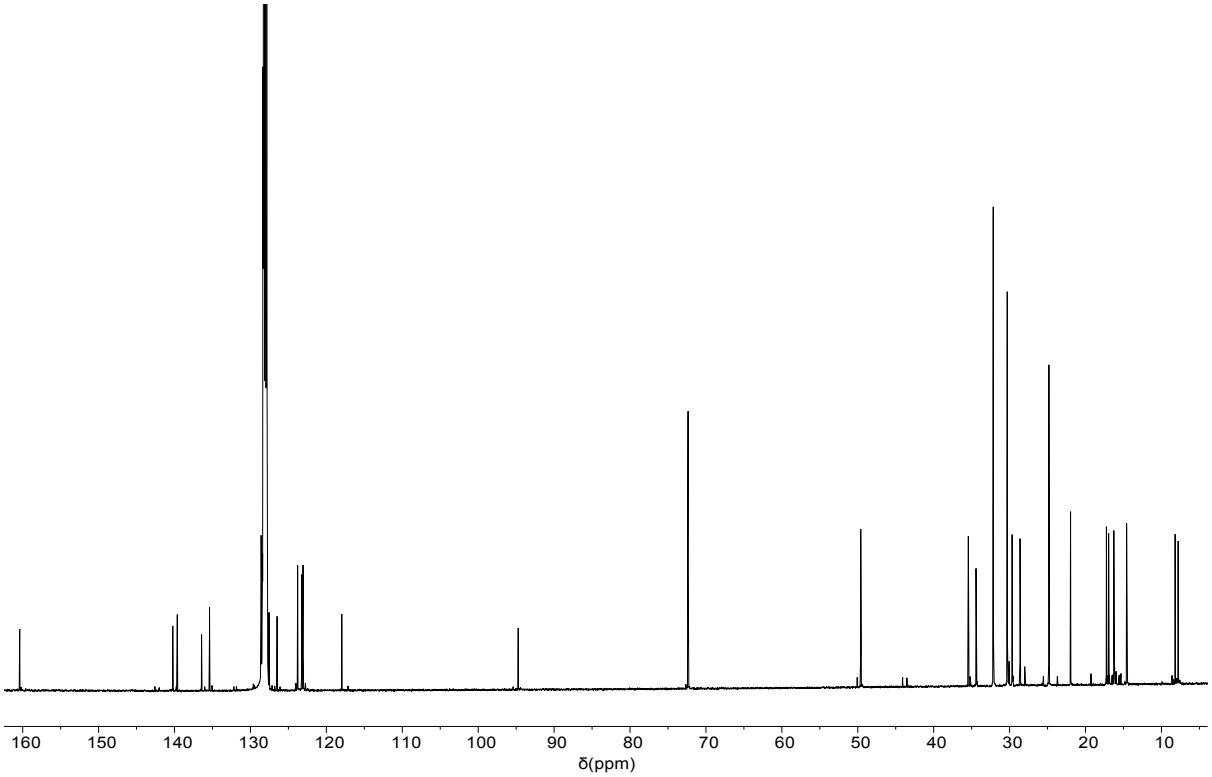

Fig. S14 $^{13}C\{^{1}H\}$ NMR spectrum (C_6D_6, 125.8 MHz, 298 K) of $^{Me_2}SB(^{iPr}N,I^*)Sc(O\text{-}2,4\text{-}^{t}Bu\text{-}C_6H_3)(THF)$ (**5**).

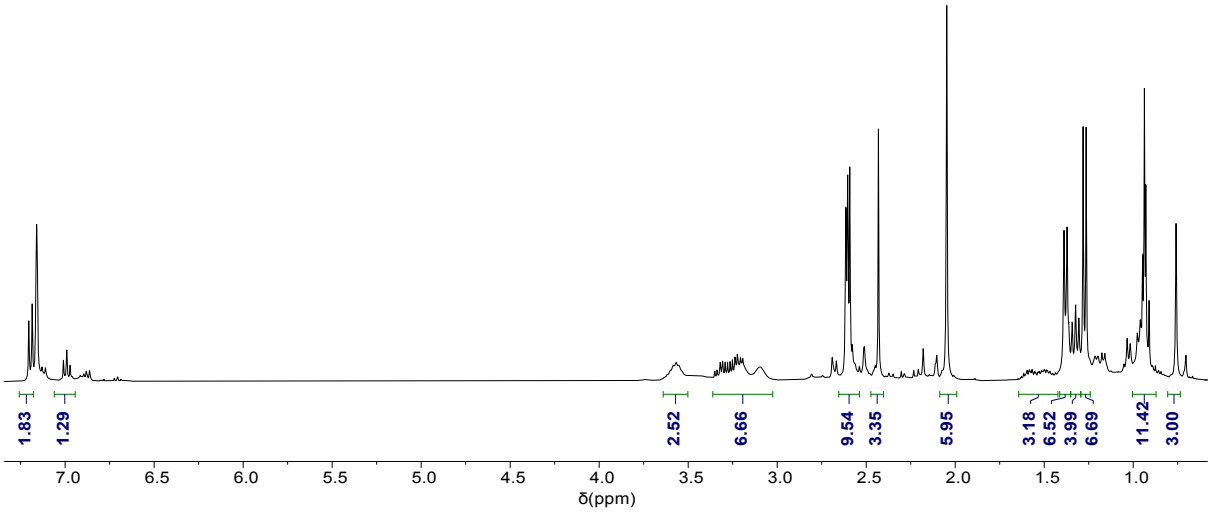

Fig. S15 ^{1}H NMR spectrum (C_6D_6, 125.8 MHz, 298 K) of $^{Me}_2$SB($^{n\text{Bu}}$N,I*)Sc(O-2,6-^{i}Pr-C_6H_3)(THF) (**6**).

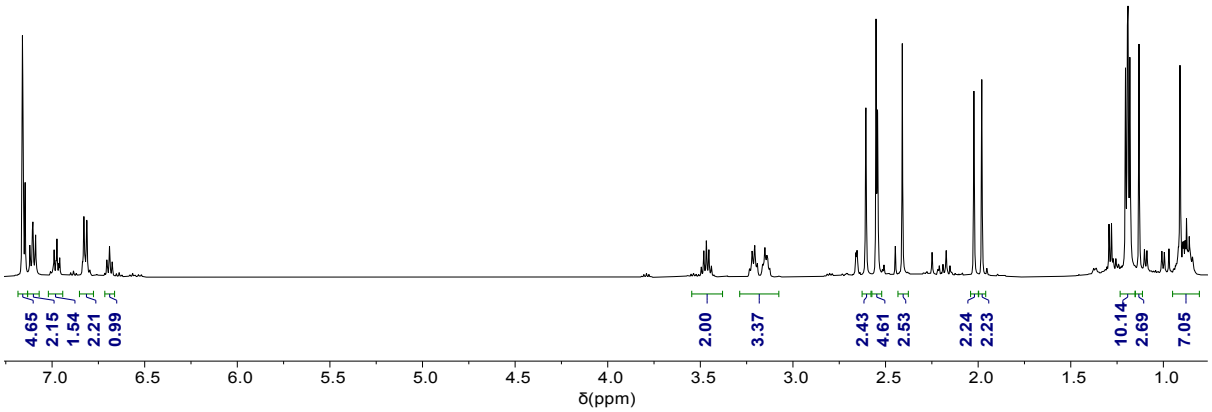

Fig. S16 ^{1}H NMR spectrum (C_6D_6, 125.8 MHz, 298 K) of $^{Me_2}SB(^{Ph}N,I^*)Sc(O\text{-}2,6\text{-}^{i}Pr\text{-}C_6H_3)(THF)$ (**7**).

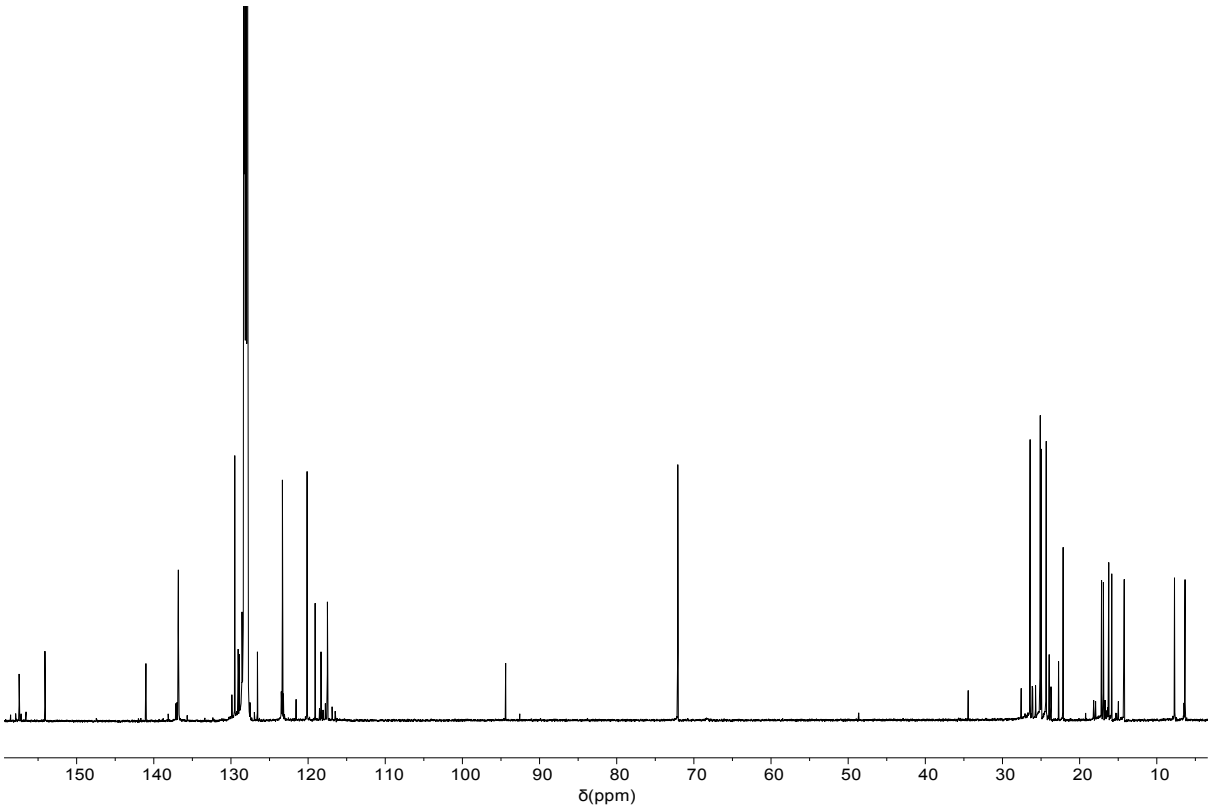

Fig. S17 $^{13}C\{^{1}H\}$ NMR spectrum (C_6D_6, 125.8 MHz, 298 K) of $^{Me_2}SB(^{Ph}N,I^*)Sc(O\text{-}2,6\text{-}^{i}Pr\text{-}C_6H_3)(THF)$ (**7**).

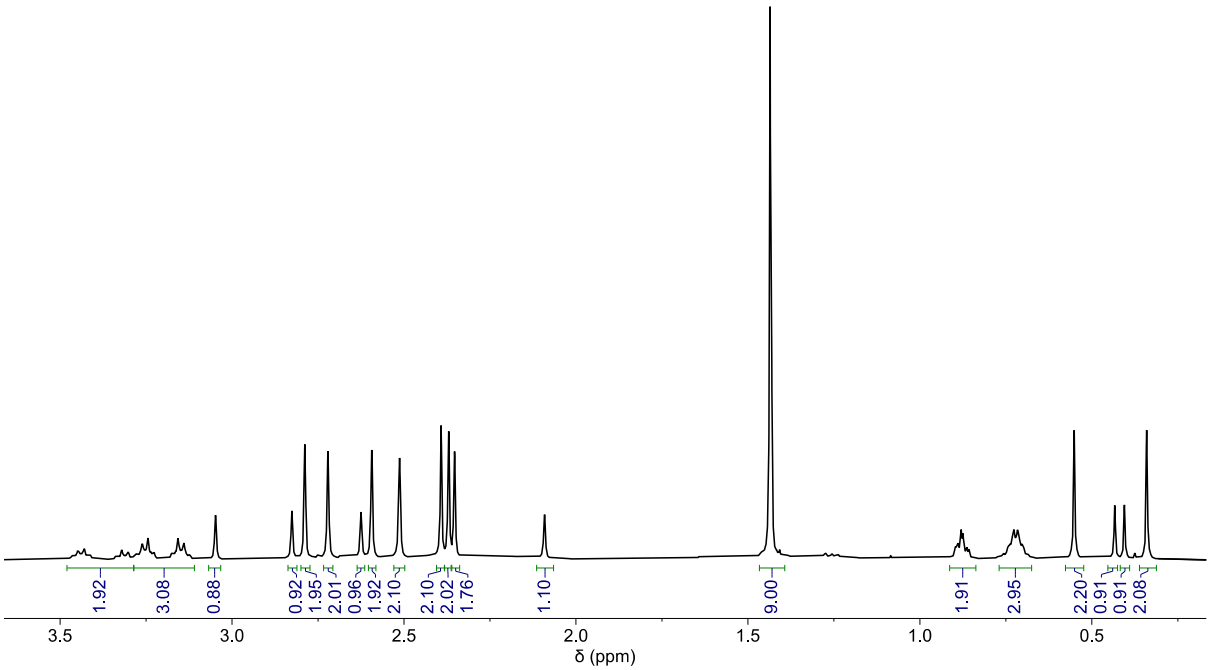

Fig. S18 ^{1}H NMR spectrum (C_6D_6, 125.8 MHz, 298 K) of ^{Me_2}SB(^{tBu}N,I*)Al(Cl)(THF) (**8**). Solvent resonance at 7.16 ppm excluded for clarity.

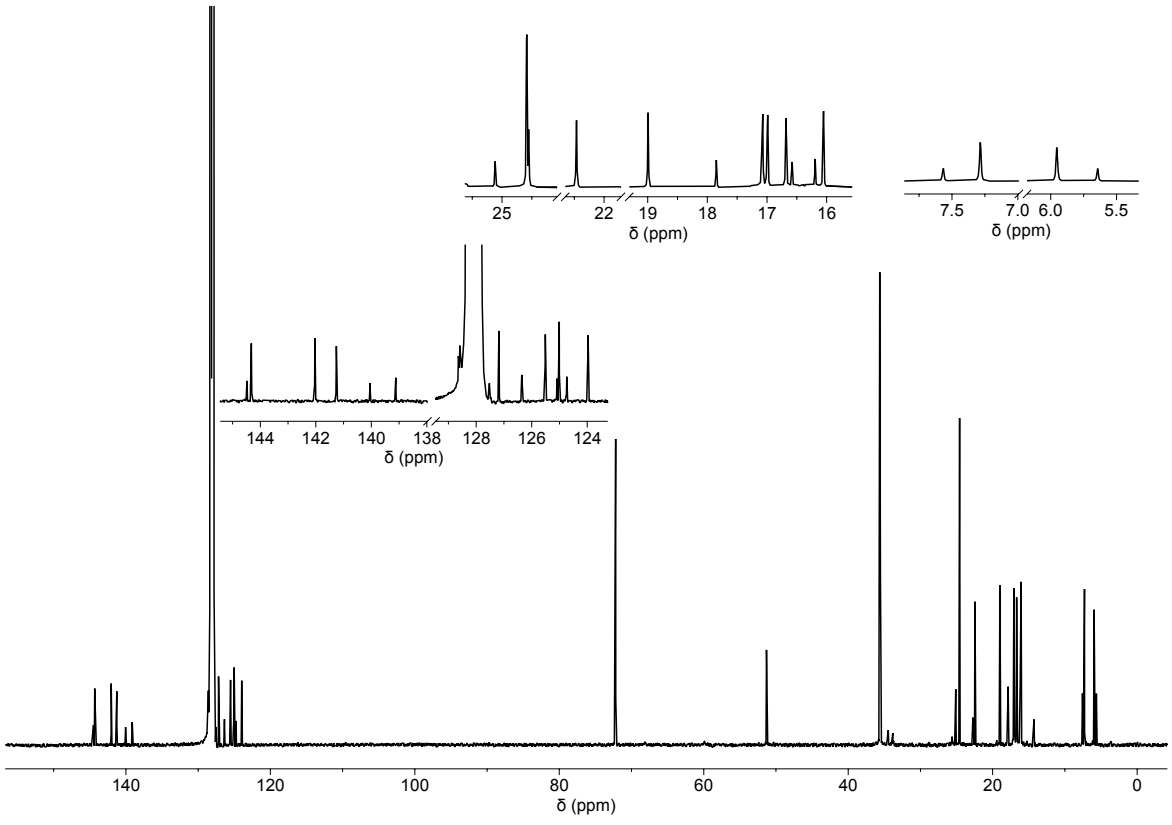

Fig. S19 ^{13}C{^{1}H} NMR spectrum (C_6D_6, 125.8 MHz, 298 K) of ^{Me_2}SB(^{tBu}N,I*)Al(Cl)(THF) (**8**).

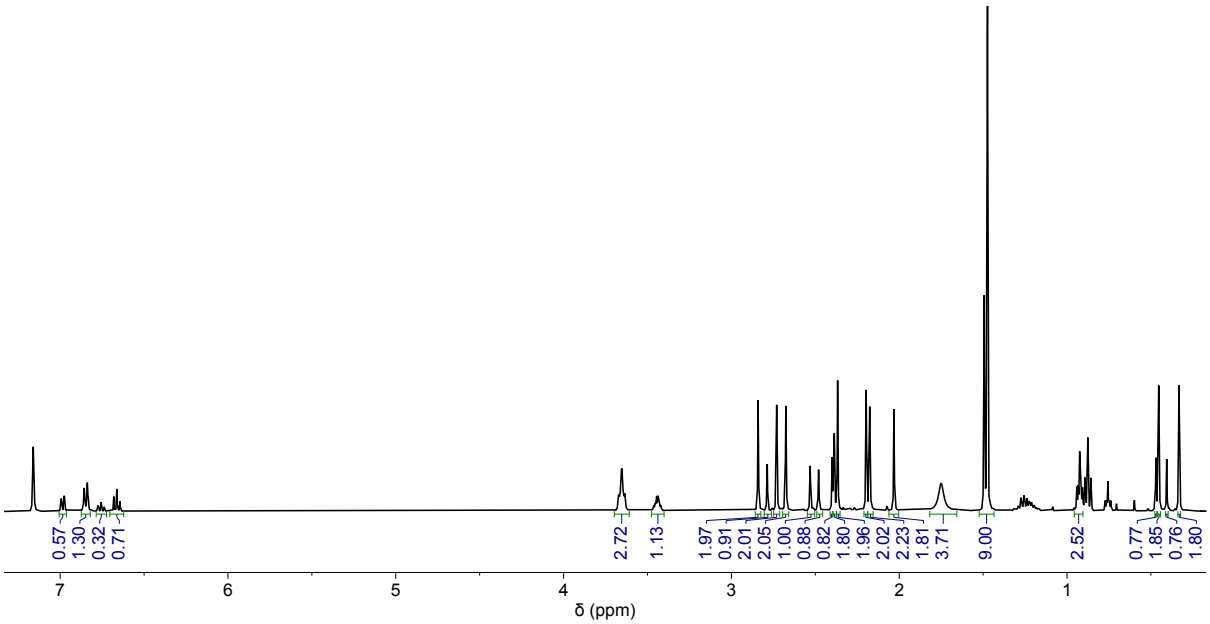

Fig. S20 ^{1}H NMR spectrum (C_6D_6, 125.8 MHz, 298 K) of ^{Me_2}SB(^{tBu}N,I*)Al(O-2,6-Me-C_6H_3)(THF) (**9**).

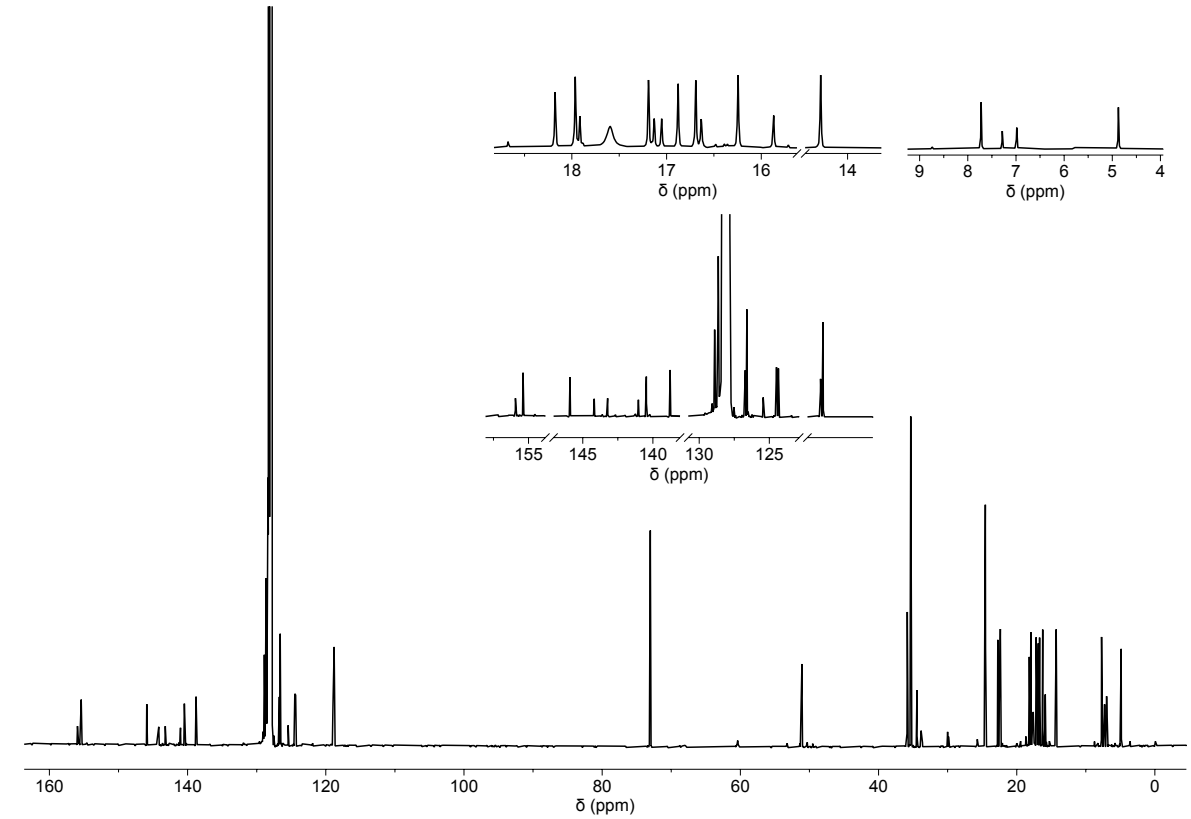

Fig. S21 ^{13}C{^{1}H} NMR spectrum (C_6D_6, 125.8 MHz, 298 K) of ^{Me_2}SB(^{tBu}N,I*)Al(O-2,6-Me-C_6H_3)(THF) (**9**).

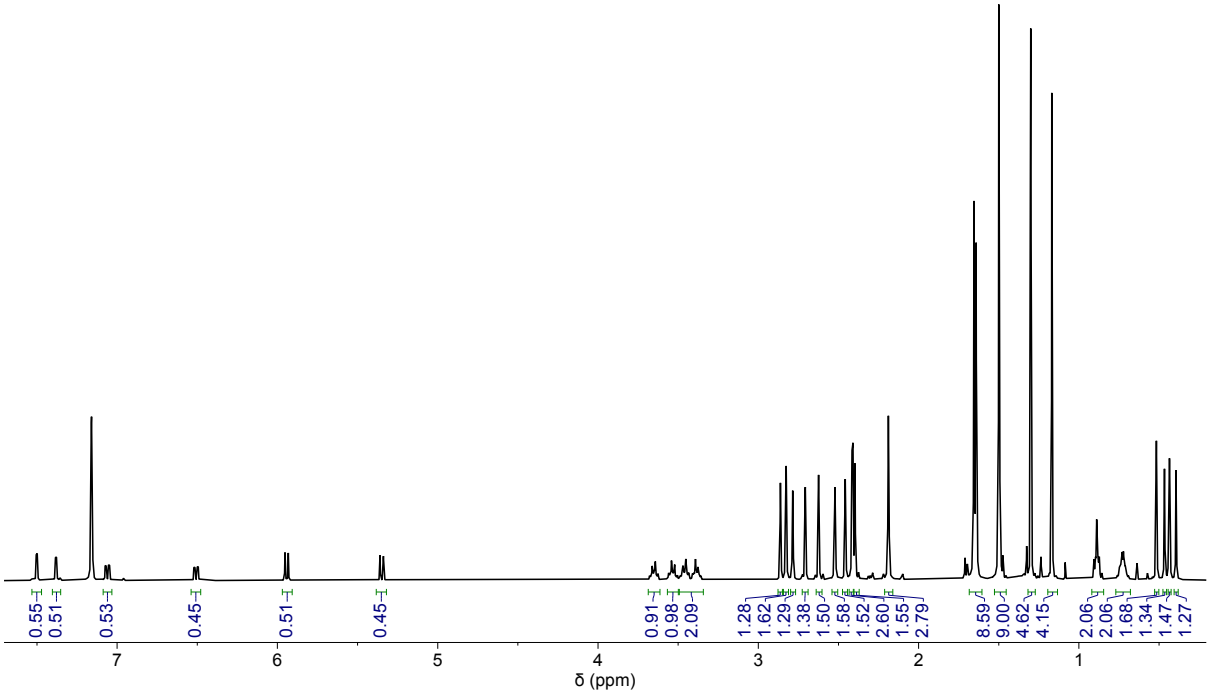

Fig. S22 ^{1}H NMR spectrum (C_6D_6, 125.8 MHz, 298 K) of $^{Me_2}SB(^{tBu}N,I^*)Al(O\text{-}2,4\text{-}^{t}Bu\text{-}C_6H_3)(THF)$ (**10**).

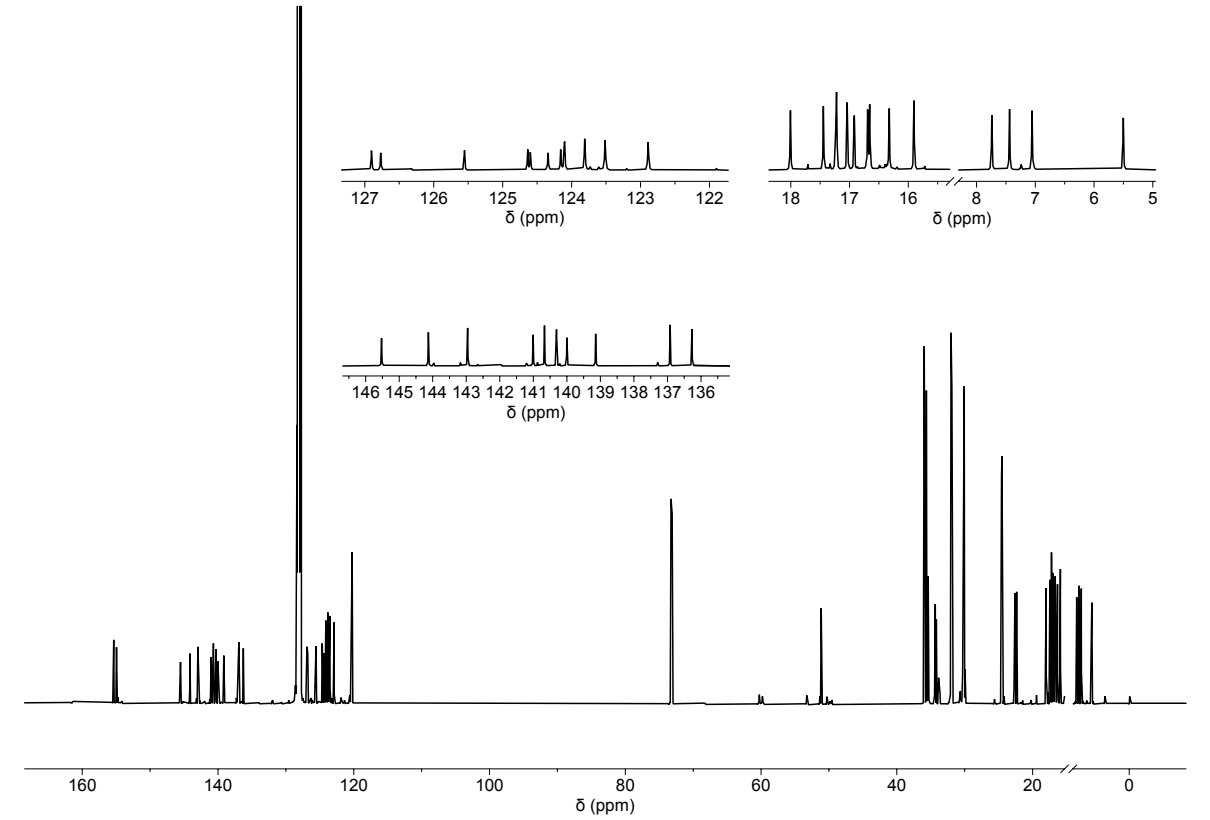

Fig. S23 $^{13}C\{^{1}H\}$ NMR spectrum (C_6D_6, 125.8 MHz, 298 K) of $^{Me_2}SB(^{tBu}N,I^*)Al(O\text{-}2,6\text{-}^{t}Bu\text{-}C_6H_3)(THF)$ (**10**).

Homonuclear decoupled $^{1}H\{^{1}H\}$ NMR spectrum of PLA synthesised by the ROP of *L*- or *rac*-lactide using $^{Me}_{2}$SB(^{iPr}N,I*)Sc(Cl)(THF) (1) with benzyl alcohol.

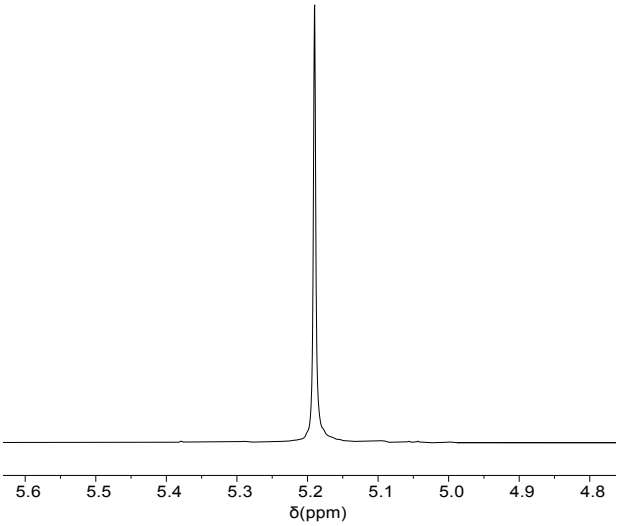

Fig. S24 $^{1}H\{^{1}H\}$ NMR spectrum ($CDCl_3$, 400.2 MHz, 298 K) of PLA synthesised from ROP of *L*-lactide with $^{Me}_{2}$SB(^{iPr}N,I*)Sc(Cl)(THF) (**1**) with benzyl alcohol. Conditions: $[L\text{-LA}]_0$:$[\mathbf{1}]_0$:$[BnOH]_0$ = 400:1:1, $[L\text{-LA}]_0$ = 0.5 M, $[\mathbf{1}]_0$ = 0.00125 M, $[BnOH]_0$ = 0.00125 M, 5.0 mL toluene at 70 °C.

Homonuclear decoupled $^1H\{^1H\}$ NMR spectra of PLA synthesised by the ROP of *L*- or *rac*-lactide using $^{Me}_2$SB(^{iPr}N,I*)Sc(O-2,6-^{i}Pr-C_6H_3)(THF) (4).

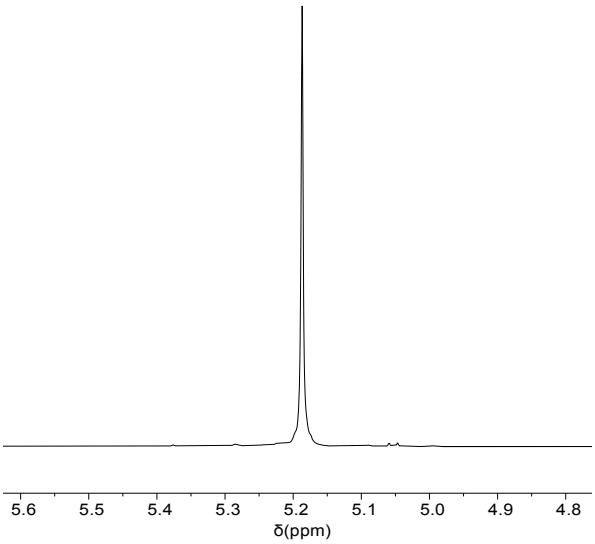

Fig. S25 $^1H\{^1H\}$ NMR spectrum ($CDCl_3$, 400.2 MHz, 298 K) of PLA synthesised from ROP of *L*-lactide with $^{Me}_2$SB(^{iPr}N,I*)Sc(O-2,6-^{i}Pr-C_6H_3)(THF) (**4**). Conditions: [*L*-LA]$_0$:[**4**]$_0$ = 600:1, [*L*-LA]$_0$ = 0.5 M, [**4**]$_0$ = 0.00083 M, 7.0 mL toluene at 70 °C.

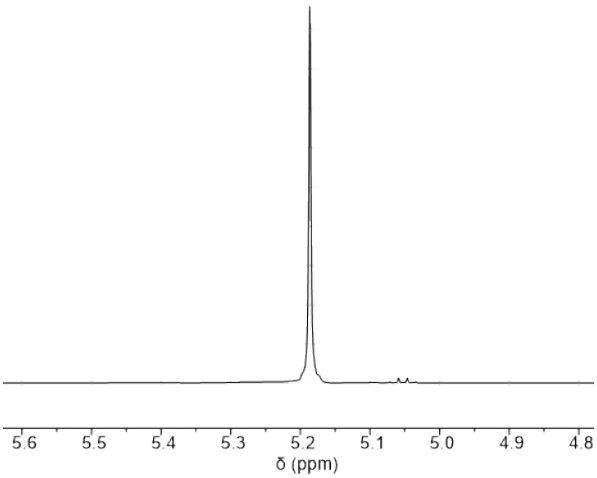

Fig. S26 $^1H\{^1H\}$ NMR spectrum ($CDCl_3$, 400.2 MHz, 298 K) of PLA synthesised from ROP of *L*-lactide with $^{Me}_2$SB(^{iPr}N,I*)Sc(O-2,6-^{i}Pr-C_6H_3)(THF) (**4**). Conditions: [*L*-LA]$_0$:[**4**]$_0$ = 800:1, [*L*-LA]$_0$ = 0.5 M, [**4**]$_0$ = 0.000625 M, 7.0 mL toluene at 70 °C.

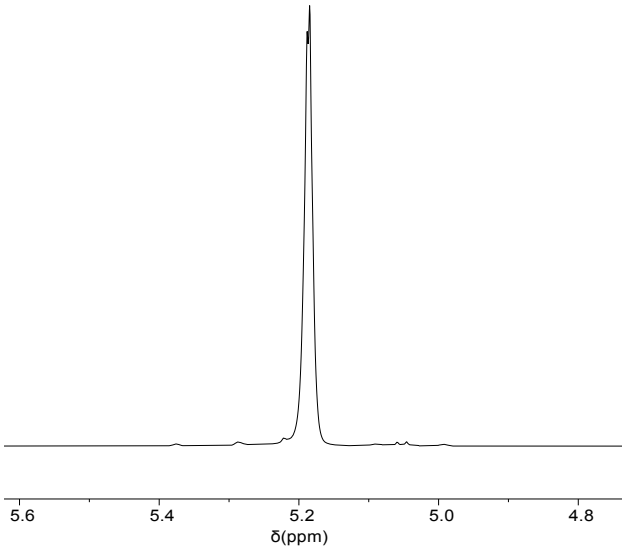

Fig. S27 $^{1}H\{^{1}H\}$ NMR spectrum ($CDCl_3$, 400.2 MHz, 298 K) of PLA synthesised from ROP of *L*-lactide with $^{Me_2}SB(^{iPr}N,I^*)Sc(O\text{-}2,6\text{-}^{i}Pr\text{-}C_6H_3)(THF)$ (**4**). Conditions: $[L\text{-LA}]_0$:$[\mathbf{4}]_0$ = 1000:1, $[L\text{-LA}]_0$ = 0.5 M, $[\mathbf{4}]_0$ = 0.0005 M, 7.0 mL toluene at 70 °C.

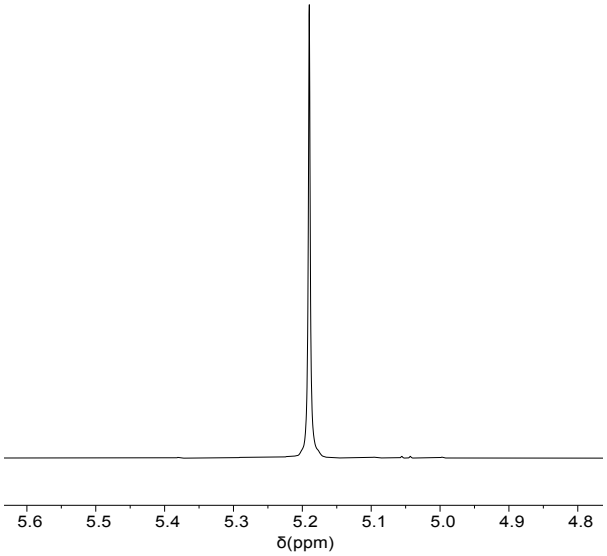

Fig. S28 $^{1}H\{^{1}H\}$ NMR spectrum ($CDCl_3$, 400.2 MHz, 298 K) of PLA synthesised from ROP of *L*-lactide with $^{Me_2}SB(^{iPr}N,I^*)Sc(O\text{-}2,6\text{-}^{i}Pr\text{-}C_6H_3)(THF)$ (**4**). Conditions: $[L\text{-LA}]_0$:$[\mathbf{4}]_0$ = 1200:1, $[L\text{-LA}]_0$ = 0.5 M, $[\mathbf{4}]_0$ = 0.000416 M, 7.0 mL toluene at 70 °C.

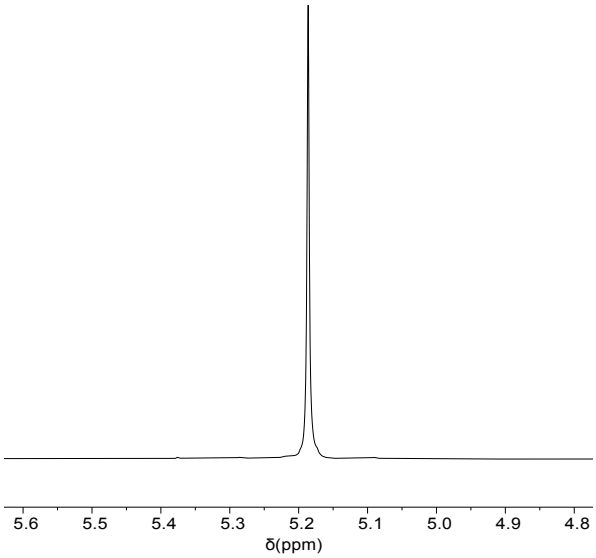

Fig. S29 $^{1}H\{^{1}H\}$ NMR spectrum ($CDCl_3$, 400.2 MHz, 298 K) of PLA synthesised from ROP of *L*-lactide with $^{Me}{}_2SB(^{iPr}N,I^*)Sc(O\text{-}2,6\text{-}^{i}Pr\text{-}C_6H_3)(THF)$ (**4**). Conditions: $[L\text{-LA}]_0$:$[\mathbf{4}]_0$ = 1000:1, $[L\text{-LA}]_0$ = 0.5 M, $[\mathbf{4}]_0$ = 0.0005 M, 7.0 mL toluene at 60 °C.

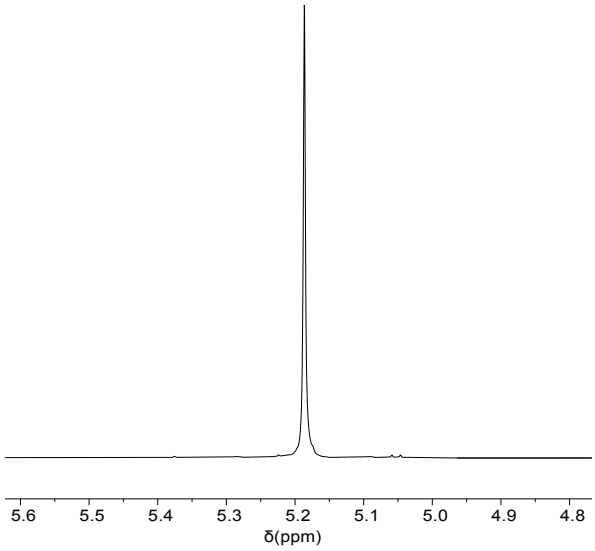

Fig. S30 $^{1}H\{^{1}H\}$ NMR spectrum ($CDCl_3$, 400.2 MHz, 298 K) of PLA synthesised from ROP of *L*-lactide with $^{Me}{}_2SB(^{iPr}N,I^*)Sc(O\text{-}2,6\text{-}^{i}Pr\text{-}C_6H_3)(THF)$ (**4**). Conditions: $[L\text{-LA}]_0$:$[\mathbf{4}]_0$ = 1000:1, $[L\text{-LA}]_0$ = 0.5 M, $[\mathbf{4}]_0$ = 0.0005 M, 7.0 mL toluene at 80 °C.

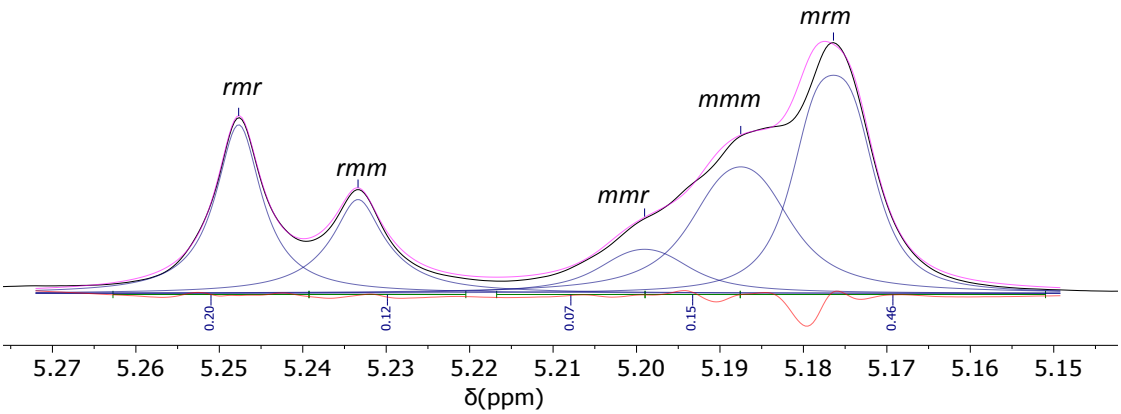

Fig. S31 $^{1}H\{^{1}H\}$ NMR spectrum ($CDCl_3$, 400.2 MHz, 298 K) of slightly heterotactic PLA (P_r =0.63) synthesised from ROP of *rac*-lactide with ^{Me_2}SB(^{iPr}N,I*)Sc(O-2,6-^{i}Pr-C_6H_3)(THF) (**4**) (batch 1). Conditions: $[rac\text{-LA}]_0$:$[\mathbf{4}]_0$ = 1000:1, $[rac\text{-LA}]_0$ = 0.5 M, $[\mathbf{4}]_0$ = 0.0005 M, 7.0 mL toluene at 70 °C.

Tetrad	Probability	P_r (deconvolution)	P_r (integration)
rmr	$P_m^2/2$	0.62	0.63
mmm	$P_m^2 + (P_rP_m/2)$	0.62	0.76
mrm	$(P_r^2 + P_rP_m)/2$	0.64	0.92
Average P_r		P_r = 0.63 ± 0.01	P_r = 0.77 ± 0.14

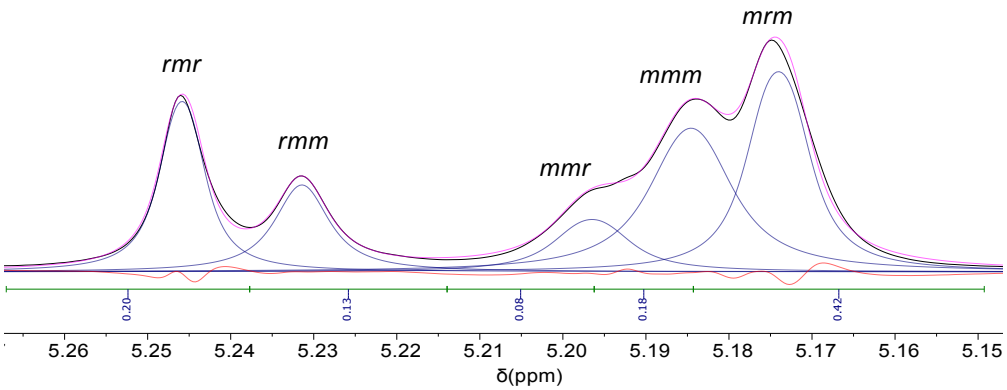

Fig. S32 $^{1}H\{^{1}H\}$ NMR spectrum ($CDCl_3$, 400.2 MHz, 298 K) of slightly heterotactic PLA (P_r =0.59) synthesised from ROP of *rac*-lactide with ^{Me_2}SB(^{iPr}N,I*)Sc(O-2,6-^{i}Pr-C_6H_3)(THF) (**4**) (batch 2). Conditions: $[rac\text{-LA}]_0$:$[\mathbf{4}]_0$ = 1000:1, $[rac\text{-LA}]_0$ = 0.5 M, $[\mathbf{4}]_0$ = 0.0005 M, 7.0 mL toluene at 70 °C.

Tetrad	Probability	P_r (deconvolution)	P_r (integration)
rmr	$P_m^2/2$	0.61	0.63
mmm	$P_m^2 + (P_rP_m/2)$	0.58	0.72
mrm	$(P_r^2 + P_rP_m)/2$	0.58	0.84
Average P_r		P_r = 0.59 ± 0.02	P_r = 0.73 ± 0.10

Homonuclear decoupled $^{1}H\{^{1}H\}$ NMR spectrum of PLA synthesised by the ROP of *L*- or *rac*-lactide using $^{Me_2}SB(^{iPr}N,I^*)Sc(O\text{-}2,4\text{-}^{t}Bu\text{-}C_6H_3)(THF)$ (5).

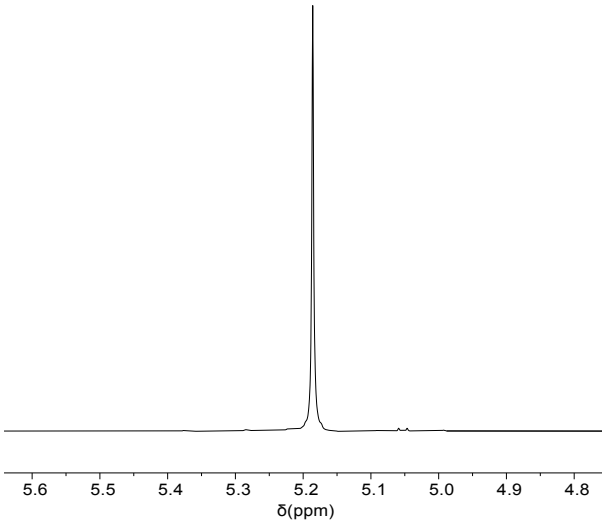

Fig. S33 $^{1}H\{^{1}H\}$ NMR spectrum ($CDCl_3$, 400.2 MHz, 298 K) of PLA synthesised from ROP of *L*-lactide with $^{Me_2}SB(^{iPr}N,I^*)Sc(O\text{-}2,4\text{-}^{t}Bu\text{-}C_6H_3)(THF)$ (**5**). Conditions: $[L\text{-LA}]_0$:$[\mathbf{5}]_0$ = 1000:1, $[L\text{-LA}]_0$ = 0.5 M, $[\mathbf{5}]_0$ = 0.0005 M, 7.0 mL toluene at 70 °C.

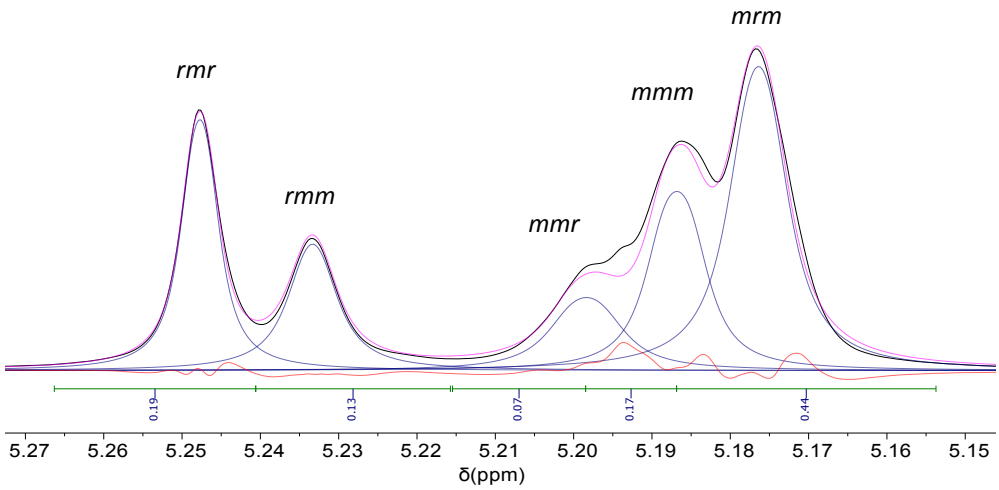

Fig. S34 $^{1}H\{^{1}H\}$ NMR spectrum ($CDCl_3$, 400.2 MHz, 298 K) of slightly heterotactic PLA (P_r =0.68) synthesised from ROP of *rac*-lactide with $^{Me_2}SB(^{iPr}N,I^*)Sc(O\text{-}2,4\text{-}^{t}Bu\text{-}C_6H_3)(THF)$ (**5**) (batch 1). Conditions: $[rac\text{-LA}]_0$:$[\mathbf{5}]_0$ = 1000:1, $[rac\text{-LA}]_0$ = 0.5 M, $[\mathbf{5}]_0$ = 0.0005 M, 7.0 mL toluene at 70 °C.

Tetrad	Probability	P_r (deconvolution)	P_r (integration)
rmr	$P_m^2/2$	0.62	0.62
mmm	$P_m^2 + (P_rP_m/2)$	0.69	0.73
mrm	$(P_r^2 + P_rP_m)/2$	0.73	0.88
Average P_r		P_r = 0.68 ± 0.06	P_r = 0.74 ± 0.13

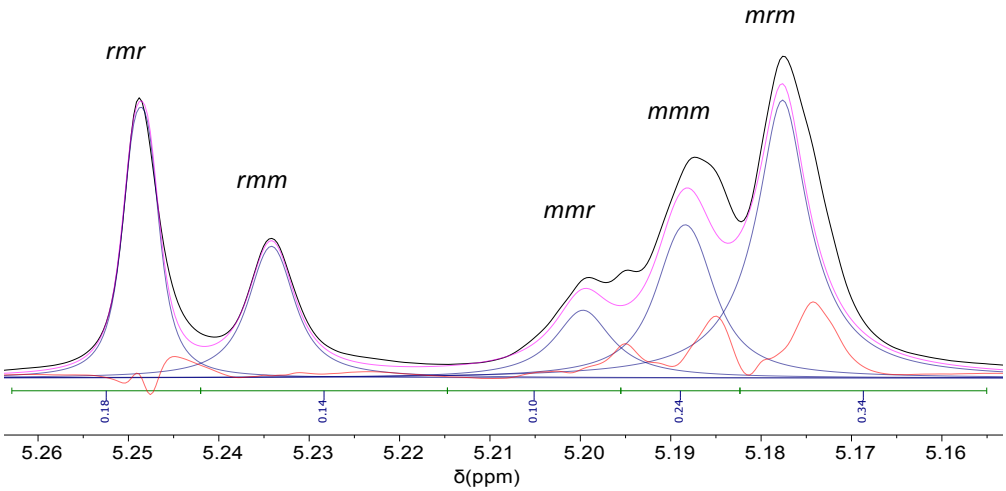

Fig. S35 $^{1}H\{^{1}H\}$ NMR spectrum ($CDCl_3$, 400.2 MHz, 298 K) of slightly heterotactic PLA (P_r =0.68) synthesised from ROP of *rac*-lactide with $^{Me_2}SB(^{iPr}N,I^*)Sc(O\text{-}2,4\text{-}^{t}Bu\text{-}C_6H_3)(THF)$ (**5**) (batch 2). Conditions: $[rac\text{-LA}]_0$:$[\mathbf{5}]_0$ = 1000:1, $[rac\text{-LA}]_0$ = 0.5 M, $[\mathbf{5}]_0$ = 0.0005 M, 7.0 mL toluene at 70 °C.

Tetrad	Probability	P_r (deconvolution)	P_r (integration)
rmr	$P_m^2/2$	0.62	0.60
mmm	$P_m^2 + (P_rP_m/2)$	0.69	0.65
mrm	$(P_r^2 + P_rP_m)/2$	0.75	0.68
Average P_r		P_r = 0.68 ± 0.07	P_r = 0.64 ± 0.04

Homonuclear decoupled $^{1}H\{^{1}H\}$ NMR spectra of PLA synthesised by the ROP of *L*- or *rac*-lactide using $^{Me_2}SB(^{Ph}N,I^*)Sc(O\text{-}2,6\text{-}^{i}Pr\text{-}C_6H_3)(THF)$ (7).

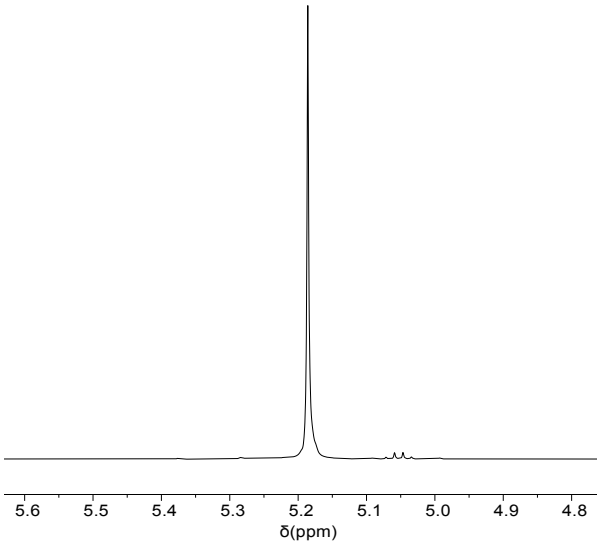

Fig. S36 $^{1}H\{^{1}H\}$ NMR spectrum ($CDCl_3$, 400.2 MHz, 298 K) of PLA synthesised from ROP of *L*-lactide with $^{Me_2}SB(^{Ph}N,I^*)Sc(O\text{-}2,6\text{-}^{i}Pr\text{-}C_6H_3)(THF)$ (**7**). Conditions: $[L\text{-LA}]_0:[\mathbf{7}]_0 = 1000:1$, $[L\text{-LA}]_0 = 0.5$ M, $[\mathbf{7}]_0 = 0.0005$ M, 7.0 mL toluene at 70 °C.

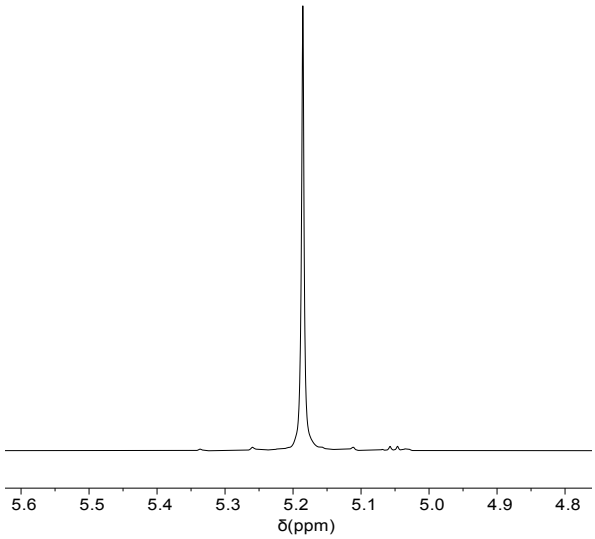

Fig. S37 $^{1}H\{^{1}H\}$ NMR spectrum ($CDCl_3$, 400.2 MHz, 298 K) of PLA synthesised from ROP of *L*-lactide with $^{Me_2}SB(^{Ph}N,I^*)Sc(O\text{-}2,6\text{-}^{i}Pr\text{-}C_6H_3)(THF)$ (**7**). Conditions: $[L\text{-LA}]_0:[\mathbf{7}]_0 = 1000:1$, $[L\text{-LA}]_0 = 0.5$ M, $[\mathbf{7}]_0 = 0.0005$ M, 7.0 mL toluene at 100 °C.

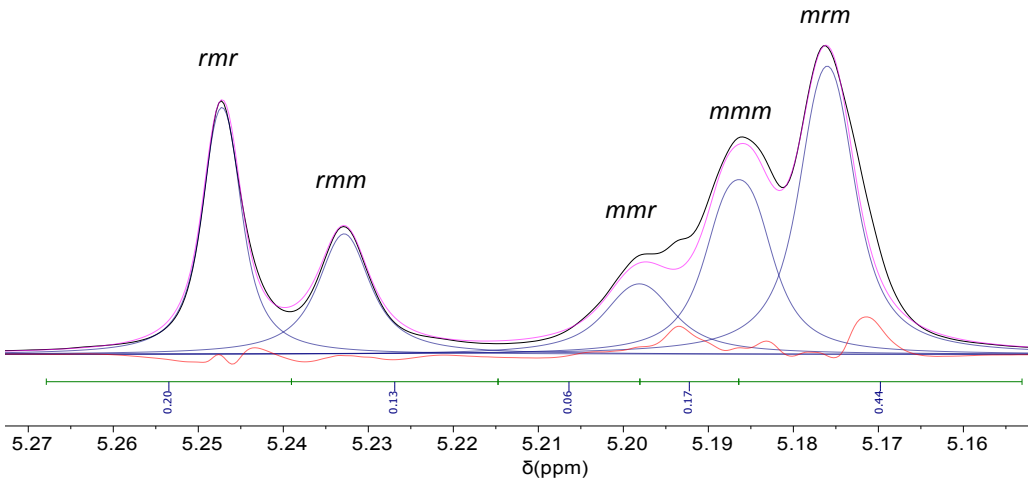

Fig. S38 $^{1}H\{^{1}H\}$ NMR spectrum ($CDCl_3$, 400.2 MHz, 298 K) of slightly heterotactic PLA (P_r =0.66) synthesised from ROP of *rac*-lactide with $^{Me_2}SB(^{Ph}N,I^*)Sc(O\text{-}2,6\text{-}^{i}Pr\text{-}C_6H_3)(THF)$ (**7**) (batch 1). Conditions: $[rac\text{-LA}]_0$:$[\mathbf{7}]_0$ = 1000:1, $[rac\text{-LA}]_0$ = 0.5 M, $[\mathbf{7}]_0$ = 0.0005 M, 7.0 mL toluene at 70 °C.

Tetrad	Probability	P_r (deconvolution)	P_r (integration)
rmr	$P_m^2/2$	0.63	0.63
mmm	$P_m^2 + (P_rP_m/2)$	0.67	0.73
mrm	$(P_r^2 + P_rP_m)/2$	0.67	0.88
Average P_r		P_r = 0.66 ± 0.02	P_r = 0.75 ± 0.12

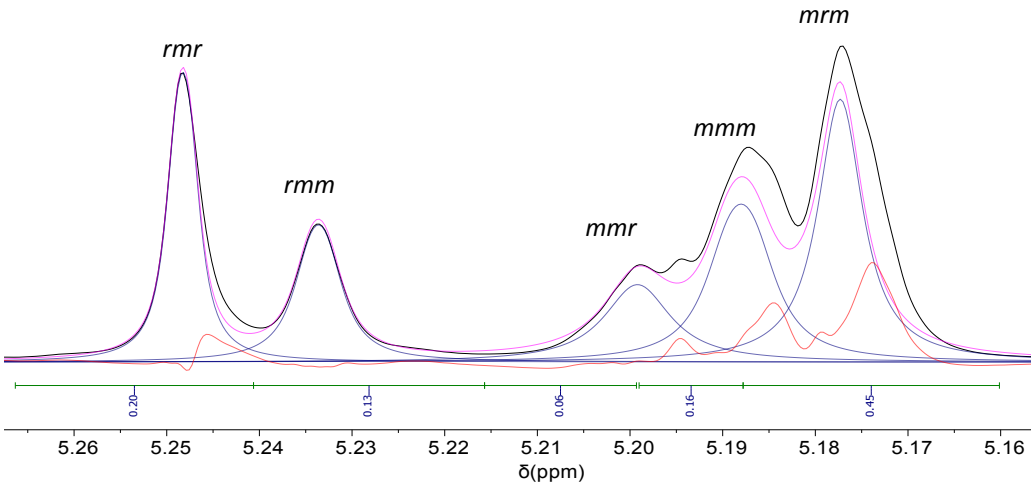

Fig. S39 $^{1}H\{^{1}H\}$ NMR spectrum ($CDCl_3$, 400.2 MHz, 298 K) of slightly heterotactic PLA (P_r =0.63) synthesised from ROP of *rac*-lactide with $^{Me_2}SB(^{Ph}N,I^*)Sc(O\text{-}2,6\text{-}^{i}Pr\text{-}C_6H_3)(THF)$ (**7**) (batch 2). Conditions: $[rac\text{-LA}]_0$:$[\mathbf{7}]_0$ = 1000:1, $[rac\text{-LA}]_0$ = 0.5 M, $[\mathbf{7}]_0$ = 0.0005 M, 7.0 mL toluene at 70 °C.

Tetrad	Probability	P_r (deconvolution)	P_r (integration)
rmr	$P_m^2/2$	0.63	0.63
mmm	$P_m^2 + (P_rP_m/2)$	0.66	0.75
mrm	$(P_r^2 + P_rP_m)/2$	0.60	0.90
Average P_r		P_r = 0.63 ± 0.03	P_r = 0.76 ± 0.13

Homonuclear decoupled $^{1}H\{^{1}H\}$ NMR spectrum of PLA synthesised by the ROP of *L*- or *rac*-lactide using $^{Me}{}_2SB(^{tBu}N,I^*)Al(O\text{-}2,6\text{-}Me\text{-}C_6H_3)(THF)$ (9)

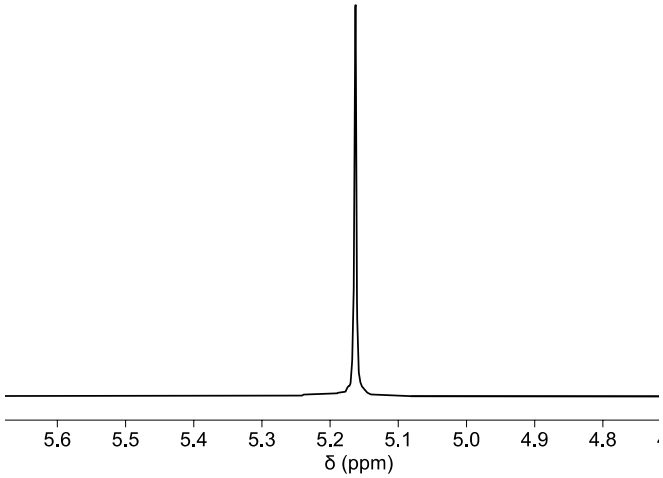

Fig. S40 $^{1}H\{^{1}H\}$ NMR spectrum ($CDCl_3$, 400.2 MHz, 298 K) of PLA synthesised from ROP of *L*-LA using $^{Me}{}_2SB(^{tBu}N,I^*)Al(O\text{-}2,6\text{-}Me\text{-}C_6H_3)(THF)$ (**9**). Conditions: $[L\text{-LA}]_0$:$[\mathbf{9}]_0$ = 100:1, $[L\text{-LA}]_0$ = 0.5 M, $[\mathbf{9}]_0$ = 0.005 M, 4.0 mL toluene at 100 °C.

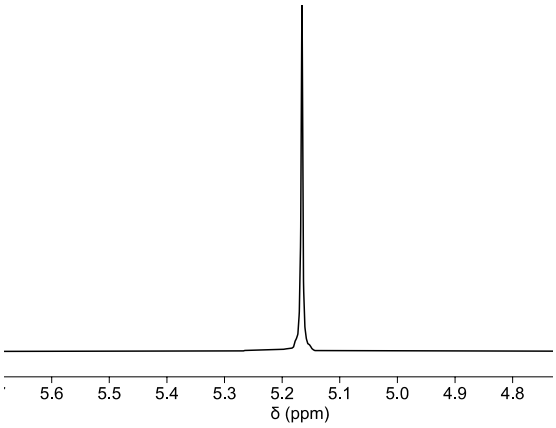

Fig. S41 $^{1}H\{^{1}H\}$ NMR spectrum ($CDCl_3$, 400.2 MHz, 298 K) of PLA synthesised from ROP of *L*-LA using $^{Me}{}_2SB(^{tBu}N,I^*)Al(O\text{-}2,6\text{-}Me\text{-}C_6H_3)(THF)$ (**9**). Conditions: $[L\text{-LA}]_0$:$[\mathbf{9}]_0$ = 100:1, $[L\text{-LA}]_0$ = 0.5 M, $[\mathbf{9}]_0$ = 0.005 M, 4.0 mL toluene at 90 °C.

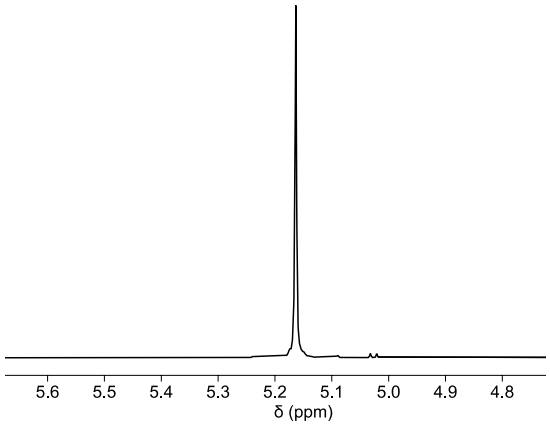

Fig. S42 $^{1}H\{^{1}H\}$ NMR spectrum ($CDCl_3$, 400.2 MHz, 298 K) of PLA synthesised from ROP of *L*-LA using $^{Me}_2SB(^{tBu}N,I^*)Al(O\text{-}2,6\text{-}Me\text{-}C_6H_3)(THF)$ (**9**). Conditions: $[L\text{-LA}]_0$:$[\mathbf{9}]_0$ = 100:1, $[L\text{-LA}]_0$ = 0.5 M, $[\mathbf{9}]_0$ = 0.005 M, 4.0 mL toluene at 70 °C.

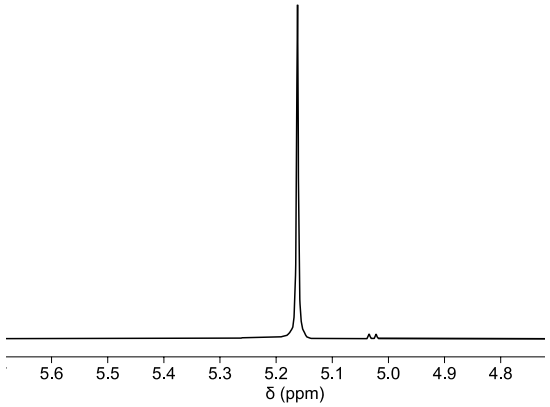

Fig. S43 $^{1}H\{^{1}H\}$ NMR spectrum ($CDCl_3$, 400.2 MHz, 298 K) of PLA synthesised from ROP of *L*-LA using $^{Me}_2SB(^{tBu}N,I^*)Al(O\text{-}2,6\text{-}Me\text{-}C_6H_3)(THF)$ (**9**). Conditions: $[L\text{-LA}]_0$:$[\mathbf{9}]_0$ = 200:1, $[L\text{-LA}]_0$ = 0.5 M, $[\mathbf{9}]_0$ = 0.0025 M, 4.0 mL toluene at 100 °C.

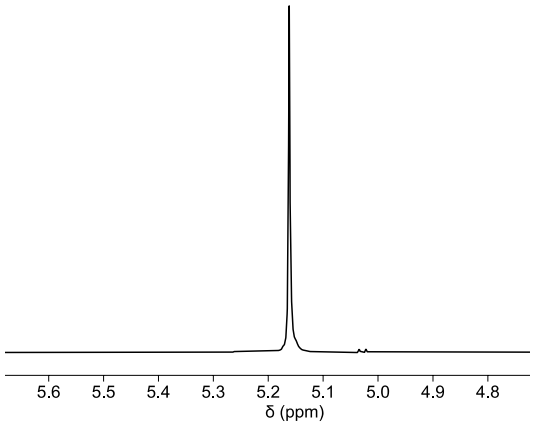

Fig. S44 $^{1}H\{^{1}H\}$ NMR spectrum ($CDCl_3$, 400.2 MHz, 298 K) of PLA synthesised from ROP of *L*-LA using $^{Me}{}_2SB(^{tBu}N,I^*)Al(O\text{-}2,6\text{-}Me\text{-}C_6H_3)(THF)$ (**9**). Conditions: $[L\text{-LA}]_0$:$[\mathbf{9}]_0$ = 300:1, $[L\text{-LA}]_0$ = 0.5 M, $[\mathbf{9}]_0$ = 0.0016 M, 4.0 mL toluene at 100 °C.

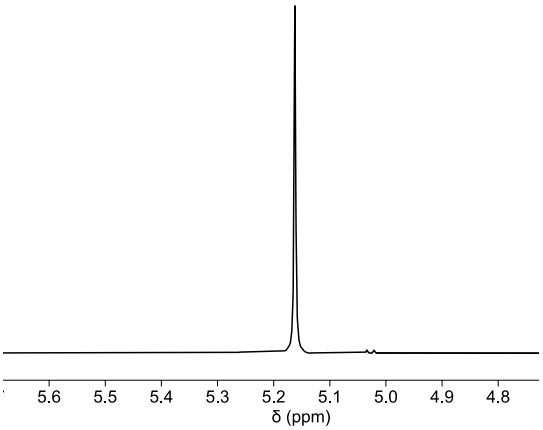

Fig. S45 $^{1}H\{^{1}H\}$ NMR spectrum ($CDCl_3$, 400.2 MHz, 298 K) of PLA synthesised from ROP of *L*-LA using $^{Me}{}_2SB(^{tBu}N,I^*)Al(O\text{-}2,6\text{-}Me\text{-}C_6H_3)(THF)$ (**9**). Conditions: $[L\text{-LA}]_0$:$[\mathbf{9}]_0$ = 500:1, $[L\text{-LA}]_0$ = 0.5 M, $[\mathbf{9}]_0$ = 0.001 M, 4.0 mL toluene at 100 °C.

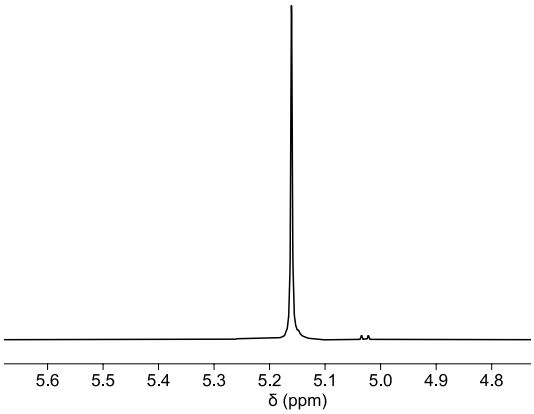

Fig. S46 $^{1}H\{^{1}H\}$ NMR spectrum ($CDCl_3$, 400.2 MHz, 298 K) of PLA synthesised from ROP of *L*-LA using $^{Me}_2SB(^{tBu}N,I^*)Al(O\text{-}2,6\text{-}Me\text{-}C_6H_3)(THF)$ (**9**). Conditions: $[L\text{-LA}]_0$:$[\mathbf{9}]_0$ = 700:1, $[L\text{-LA}]_0$ = 0.5 M, $[\mathbf{9}]_0$ = 0.0007 M, 4.0 mL toluene at 100 °C.

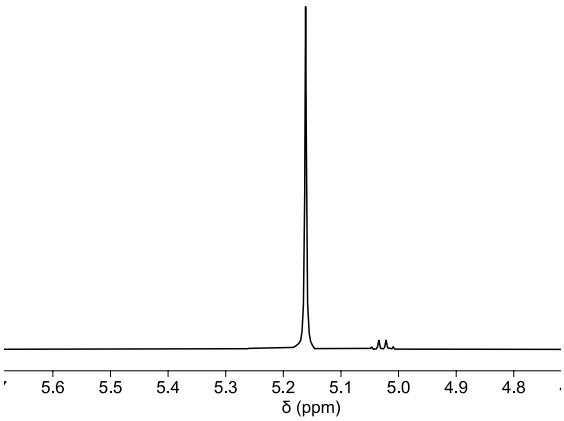

Fig. S47 $^{1}H\{^{1}H\}$ NMR spectrum ($CDCl_3$, 400.2 MHz, 298 K) of PLA synthesised from ROP of *L*-LA using $^{Me}_2SB(^{tBu}N,I^*)Al(O\text{-}2,6\text{-}Me\text{-}C_6H_3)(THF)$ (**9**). Conditions: $[L\text{-LA}]_0$:$[\mathbf{9}]_0$ = 1000:1, $[L\text{-LA}]_0$ = 0.5 M, $[\mathbf{9}]_0$ = 0.0005 M, 4.0 mL toluene at 100 °C.

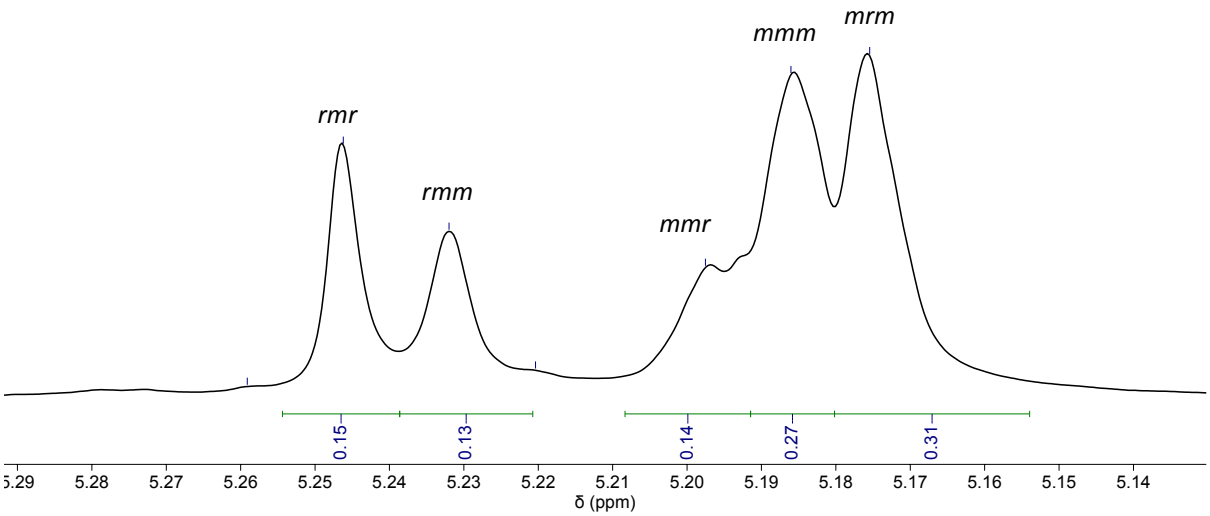

Fig. S48 $^{1}H\{^{1}H\}$ NMR spectrum ($CDCl_3$, 400.2 MHz, 298 K) of slightly heterotactic PLA (P_r =0.57) synthesised from ROP of *rac*-LA using ^{Me_2}SB(^{tBu}N,I*)Al(O-2,6-Me-C_6H_3)(THF) (**9**) (batch 1). Conditions: [*rac*-LA]$_0$:[**9**]$_0$ = 100:1, [*rac*-LA]$_0$ = 0.5 M, [**9**]$_0$ = 0.005 M, 4.0 mL toluene at 100 °C.

Tetrad	Probability	P_r (deconvolution)	P_r (integration)
rmr	$P_m^2/2$	0.51	0.55
mmm	$P_m^2 + (P_rP_m/2)$	0.55	0.61
mrm	$(P_r^2 + P_rP_m)/2$	0.66	0.62
Average P_r		P_r = 0.57 ± 0.08	P_r = 0.59 ± 0.04

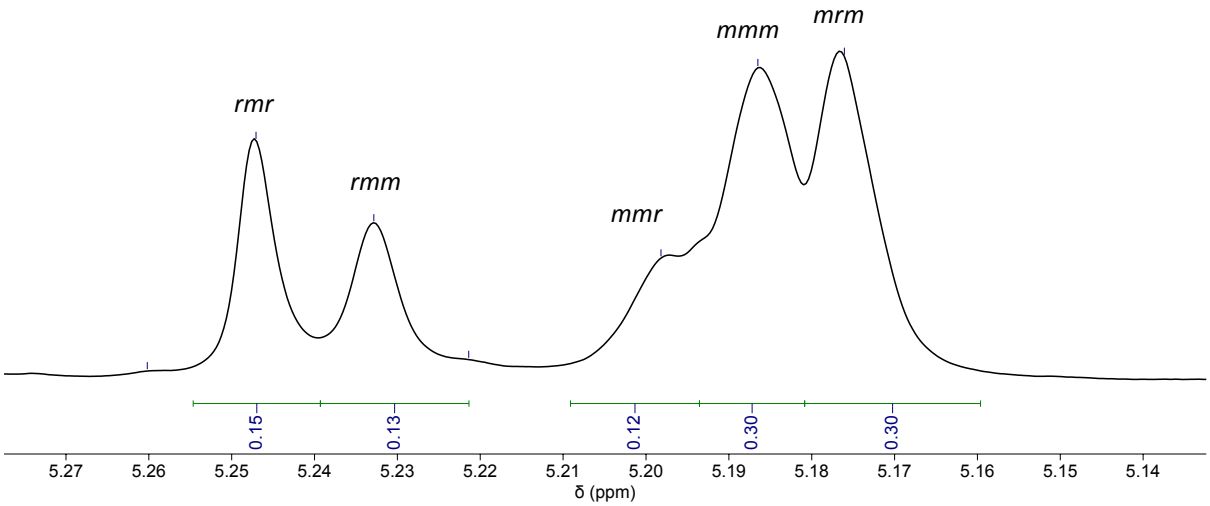

Fig. S49 $^{1}H\{^{1}H\}$ NMR spectrum ($CDCl_3$, 400.2 MHz, 298 K) of slightly heterotactic PLA (P_r =0.53) synthesised from ROP of *rac*-LA using ^{Me_2}SB(^{tBu}N,I*)Al(O-2,6-Me-C_6H_3)(THF) (**9**) (batch 2). Conditions: [*rac*-LA]$_0$:[**9**]$_0$ = 100:1, [*rac*-LA]$_0$ = 0.5 M, [**9**]$_0$ = 0.005 M, 4.0 mL toluene at 100 °C.

Tetrad	Probability	P_r (deconvolution)	P_r (integration)
rmr	$P_m^2/2$	0.53	0.55
mmm	$P_m^2 + (P_rP_m/2)$	0.51	0.58
mrm	$(P_r^2 + P_rP_m)/2$	0.55	0.60
Average P_r		P_r = 0.53 ± 0.02	P_r = 0.58 ± 0.03

Homonuclear decoupled $^{1}H\{^{1}H\}$ NMR spectrum of PLA synthesised by the ROP of *L*-lactide using $^{Me}_{2}SB(^{tBu}N,I^{*})Al(O\text{-}2,4\text{-}^{t}Bu\text{-}C_{6}H_{3})(THF)$ (10)

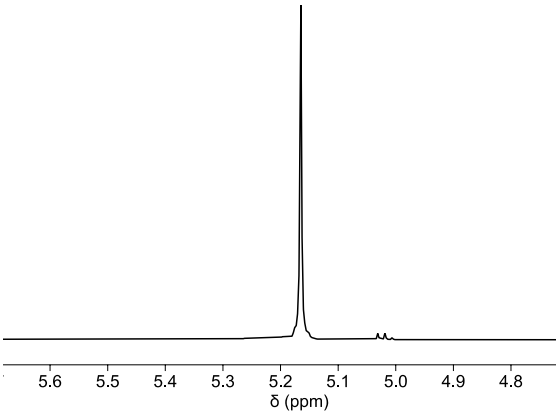

Fig. S50 $^{1}H\{^{1}H\}$ NMR spectrum ($CDCl_3$, 400.2 MHz, 298 K) of PLA synthesised from ROP of *L*-LA using $^{Me}_{2}SB(^{tBu}N,I^{*})Al(O\text{-}2,4\text{-}^{t}Bu\text{-}C_{6}H_{3})(THF)$ (**10**). Conditions: $[L\text{-LA}]_0$:$[\mathbf{10}]_0$ = 100:1, $[L\text{-LA}]_0$ = 0.5 M, $[\mathbf{10}]_0$ = 0.005 M, 4.0 mL toluene at 100 °C.

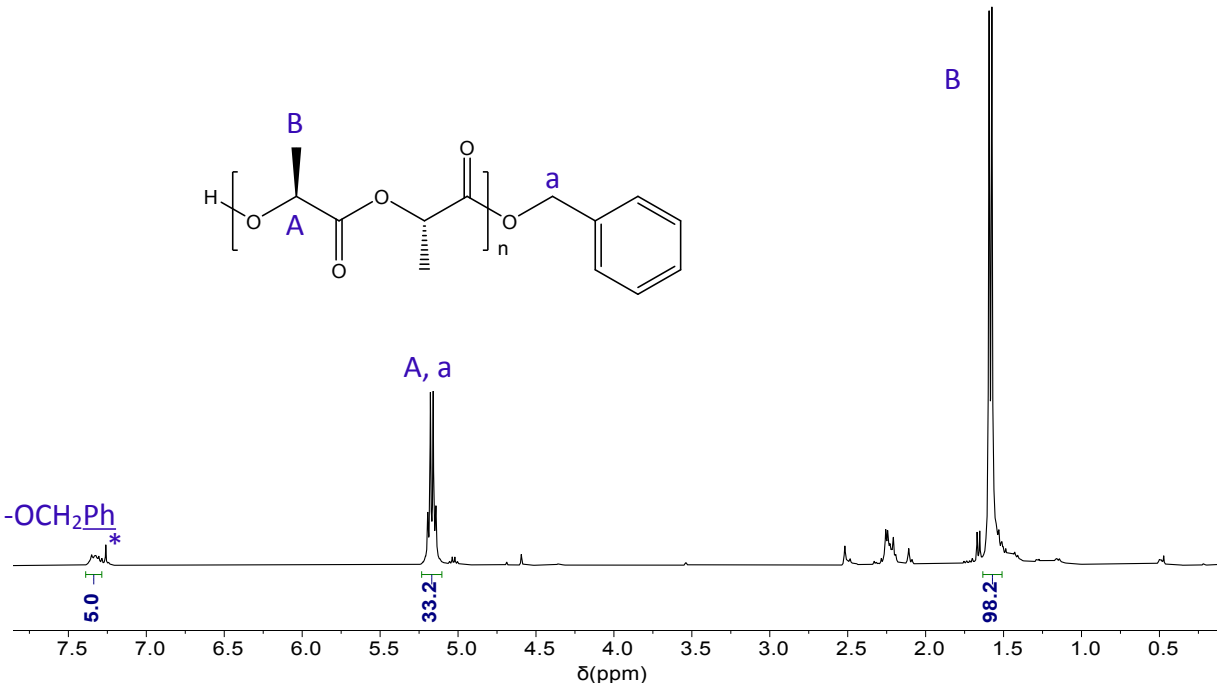

Fig. S51 ^{1}H NMR spectrum ($CDCl_3$, 400.2 MHz, 298 K) of PLA synthesised by ^{Me2}SB(^{iPr}N,I*)Sc(Cl)(THF) (**1**) with benzyl alcohol. Conditions: $[L\text{-LA}]_0$:$[\mathbf{1}]_0$:$[BnOH]_0$ = 15:1:1, $[L\text{-LA}]_0$ = 0.5 M, 0.7 mL toluene-d_8 at 70 °C. "*" denotes residual protio-solvent.

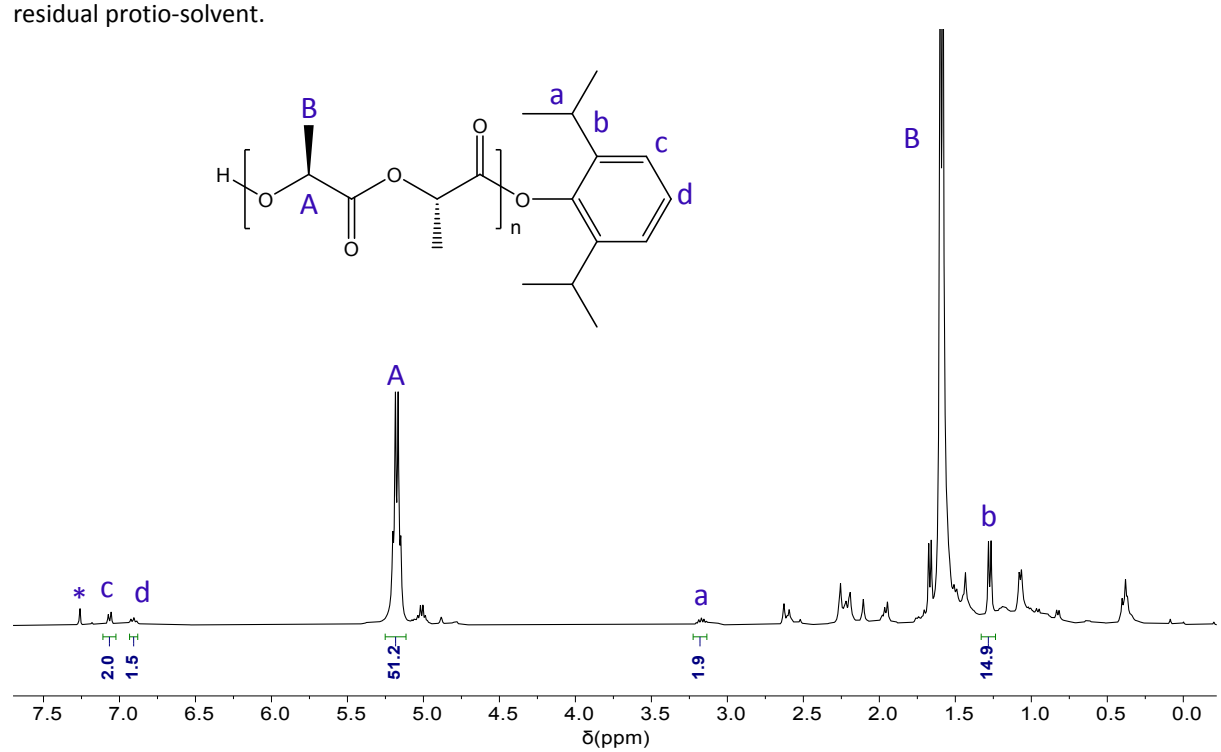

Fig. S52 ^{1}H NMR spectrum ($CDCl_3$, 400.2 MHz, 298 K) of PLA synthesised by ^{Me2}SB(^{iPr}N,I*)Sc(O-2,6-^{i}Pr-C_6H_3)(THF) (**4**). Conditions: $[L\text{-LA}]_0$:$[\mathbf{4}]_0$ = 15:1, $[L\text{-LA}]_0$ = 0.5 M, 0.7 mL toluene-d_8 at 70 °C. "*" denotes residual protio-solvent.

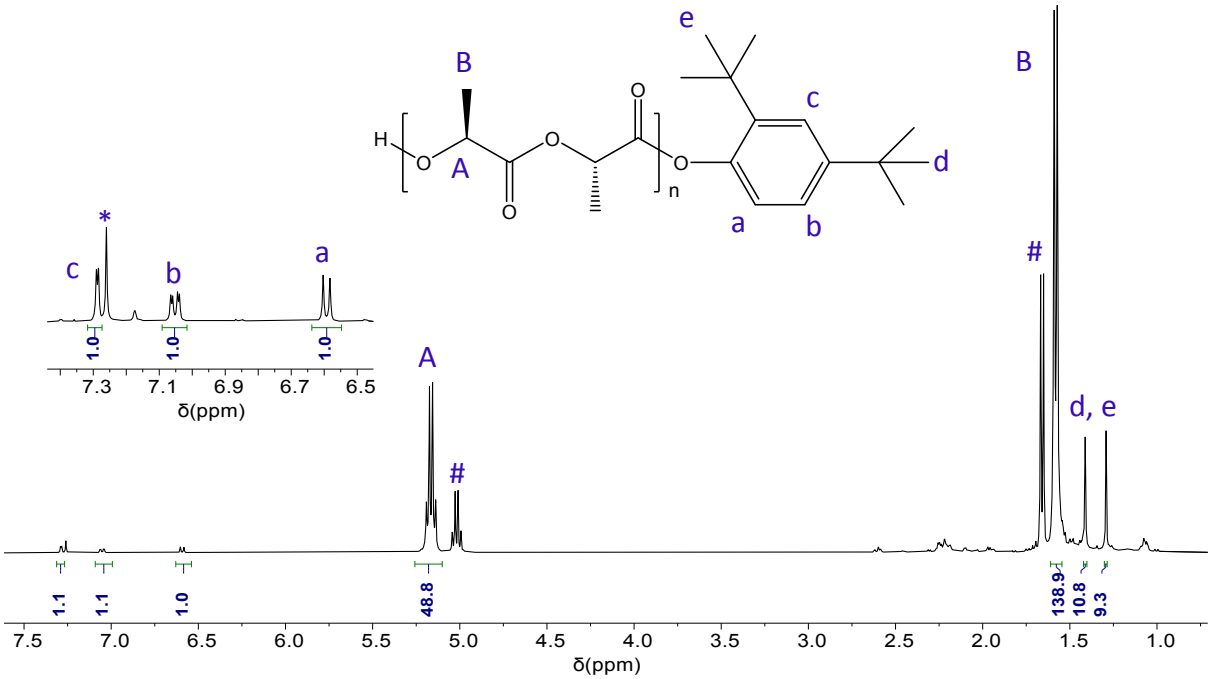

Fig. S53 ^{1}H NMR spectrum ($CDCl_3$, 400.2 MHz, 298 K) of PLA synthesised by ^{Me_2}SB(^{iPr}N,I*)Sc(O-2,4-^{t}Bu-C_6H_3)(THF) (**5**). Conditions: [*L*-LA]$_0$:[**5**]$_0$ = 15:1, [*L*-LA]$_0$ = 0.5 M, 0.7 mL toluene-d_8 at 70 °C. "*" denotes residual protio-solvent. "#" denotes *L*-lactide.

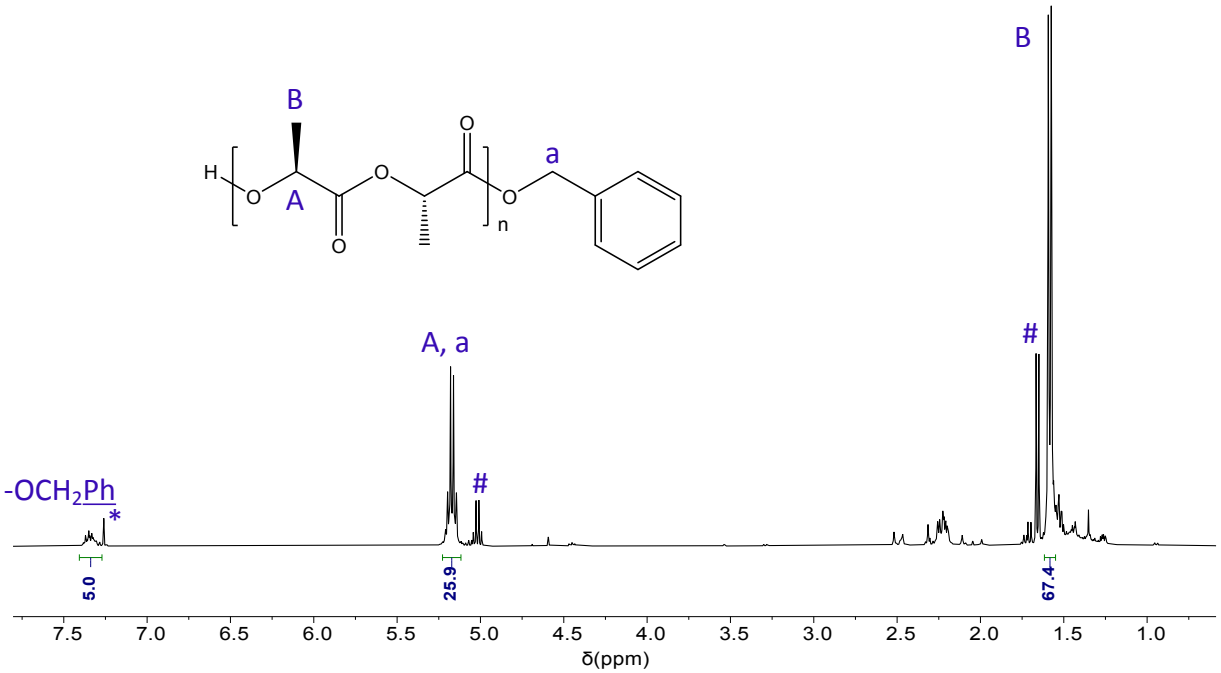

Fig. S54 ^{1}H NMR spectrum ($CDCl_3$, 400.2 MHz, 298 K) of PLA synthesised by ^{Me_2}SB(^{tBu}N,I*)Al(Cl)(THF) (**8**) with benzyl alcohol. Conditions: [*L*-LA]$_0$:[**8**]$_0$:[BnOH]$_0$ = 15:1:1, [*L*-LA]$_0$ = 0.5 M, 0.7 mL toluene-d_8 at 100 °C. "*" denotes residual protio-solvent. "#" denotes *L*-lactide.

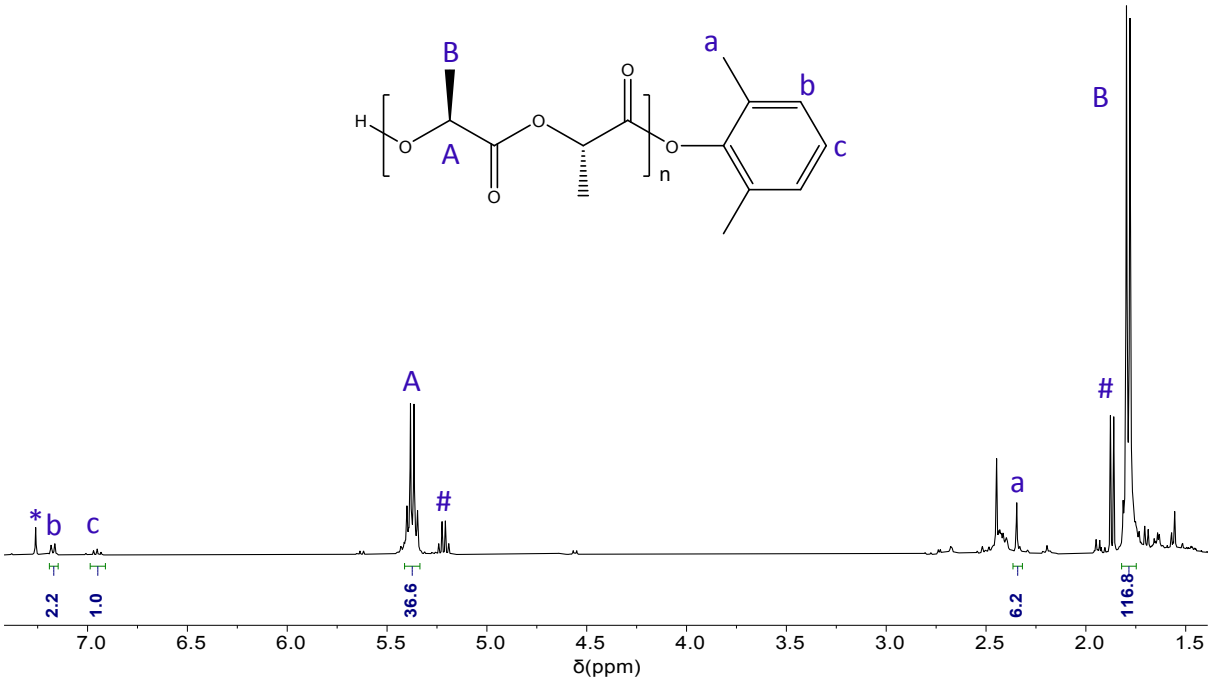

Fig. S55 ^{1}H NMR spectrum ($CDCl_3$, 400.2 MHz, 298 K) of PLA synthesised by ^{Me_2}SB(^{tBu}N,I*)Al(O-2,6-Me-C_6H_3)(THF) (**9**). Conditions: [*L*-LA]$_0$:[**9**]$_0$ = 15:1, [*L*-LA]$_0$ = 0.5 M, 0.7 mL toluene-d_8 at 100 °C. "*" denotes residual protio-solvent. "#" denotes *L*-lactide.

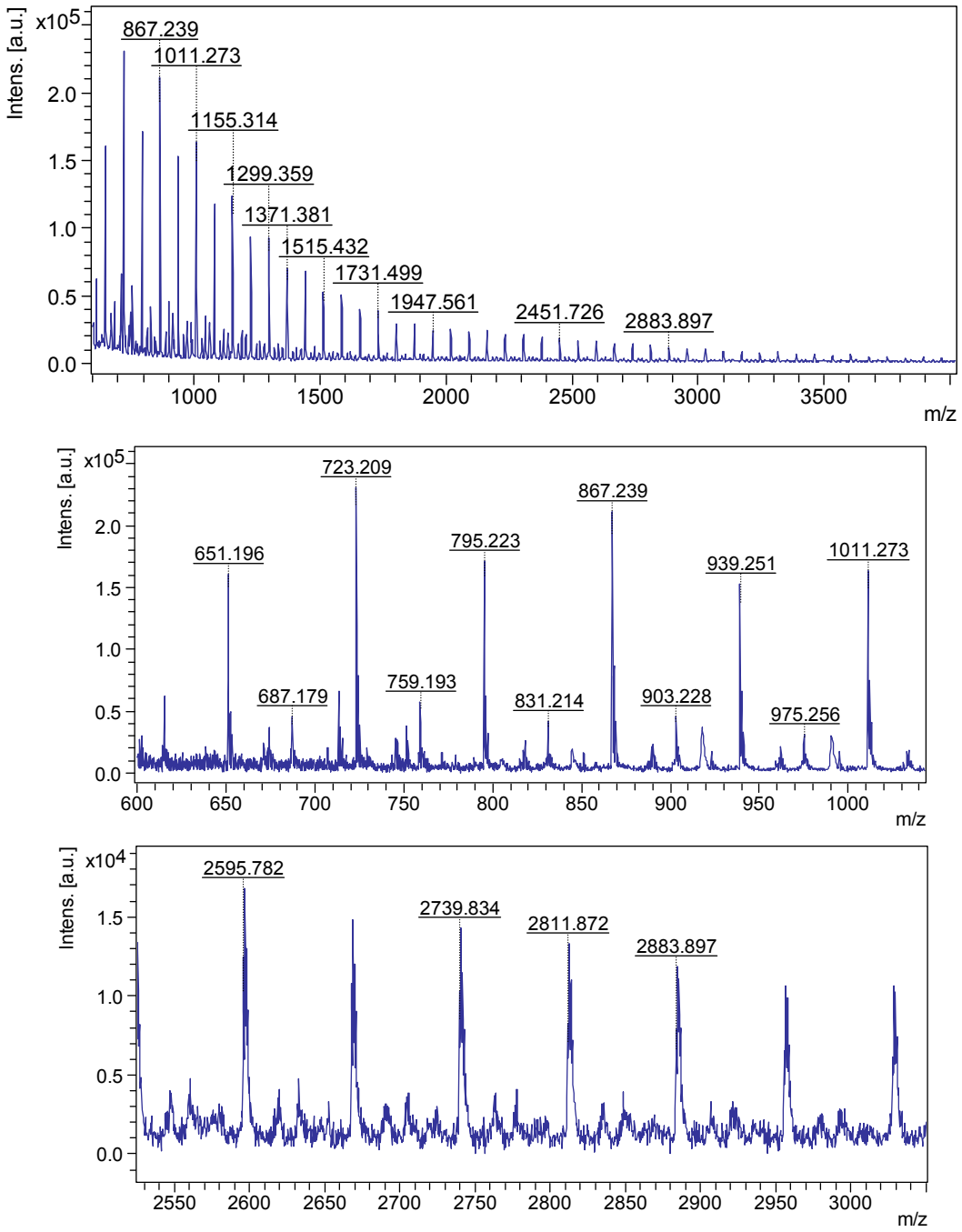

Fig. S56 MALDI-ToF MS of PLA synthesised from ^{Me_2}SB(^{iPr}N,I*)Sc(Cl)(THF) (**1**) with benzyl alcohol. The peak envelope centred at 723.2 Da corresponds to PLA with 4 units of LA terminated with –OBn and –OH groups and K^+ [144.1(4) + 108.1 + 39.1]. Δ(*m*/*z*) = 72.0 Da between peak envelopes.

Mass List (monoisotopic ions)

m/z	S/N	Quality Fac.	Res.	Intens.	Area
615.163	11	6007	2224	51005	25681
651.196	33	10071	3276	147183	51730
674.245	6	886	2279	27633	15157
687.179	8	5572	2040	36332	23508
713.357	14	1488	3562	61648	22777
723.209	49	18576	3443	212809	82753
751.452	7	1001	2364	29070	17364

759.193	11	3009	2737	48827	26346
795.223	37	18125	3529	155946	68565
831.214	8	2964	2466	33612	23374
867.239	47	21674	3700	189848	90971
903.228	10	5686	2693	38130	27171
917.896	8	3443	762	30433	68368
939.251	34	18515	3679	134193	73598
975.256	7	2493	2329	24852	22988
990.46	7	2191	741	24325	67815
1011.273	39	23794	3863	145828	85461
1047.267	8	4688	2740	28450	25596
1062.939	7	2389	666	21104	72937
1083.29	28	21805	3734	100680	69052
1155.314	31	27846	3812	107320	79722
1227.326	24	18990	3600	77494	67804
1299.359	26	24840	3841	79418	71755
1371.381	20	24545	3738	58723	59917
1443.406	20	24253	3708	56971	64334
1515.432	16	24408	3604	43082	54786
1587.445	16	26147	3714	42080	57228
1659.472	13	16392	3436	31405	49584
1731.499	13	18315	3457	30482	51919
1803.52	11	19523	3486	24541	45275
1875.539	12	20532	3570	23787	46230
1947.561	11	15378	3557	19636	39830
2019.582	11	12006	3431	18620	40813
2091.62	10	8683	3440	15973	36170
2163.631	11	15412	3679	16473	36339
2235.645	10	6156	3565	13285	32626
2307.698	10	7705	3621	12918	31411
2379.698	9	6333	3780	11479	28333
2451.726	10	8945	4148	12300	28842
2523.764	9	10272	4157	10219	24702
2595.782	9	11066	4267	9996	24822
2739.834	9	4939	4389	8274	20905
2811.872	8	2398	3977	6794	20057
2883.897	7	3178	4055	6339	18350
3100.913	6		7515	8963	6466
3173.916	6		7066	8291	6696
3245.005	6		8197	7868	5617

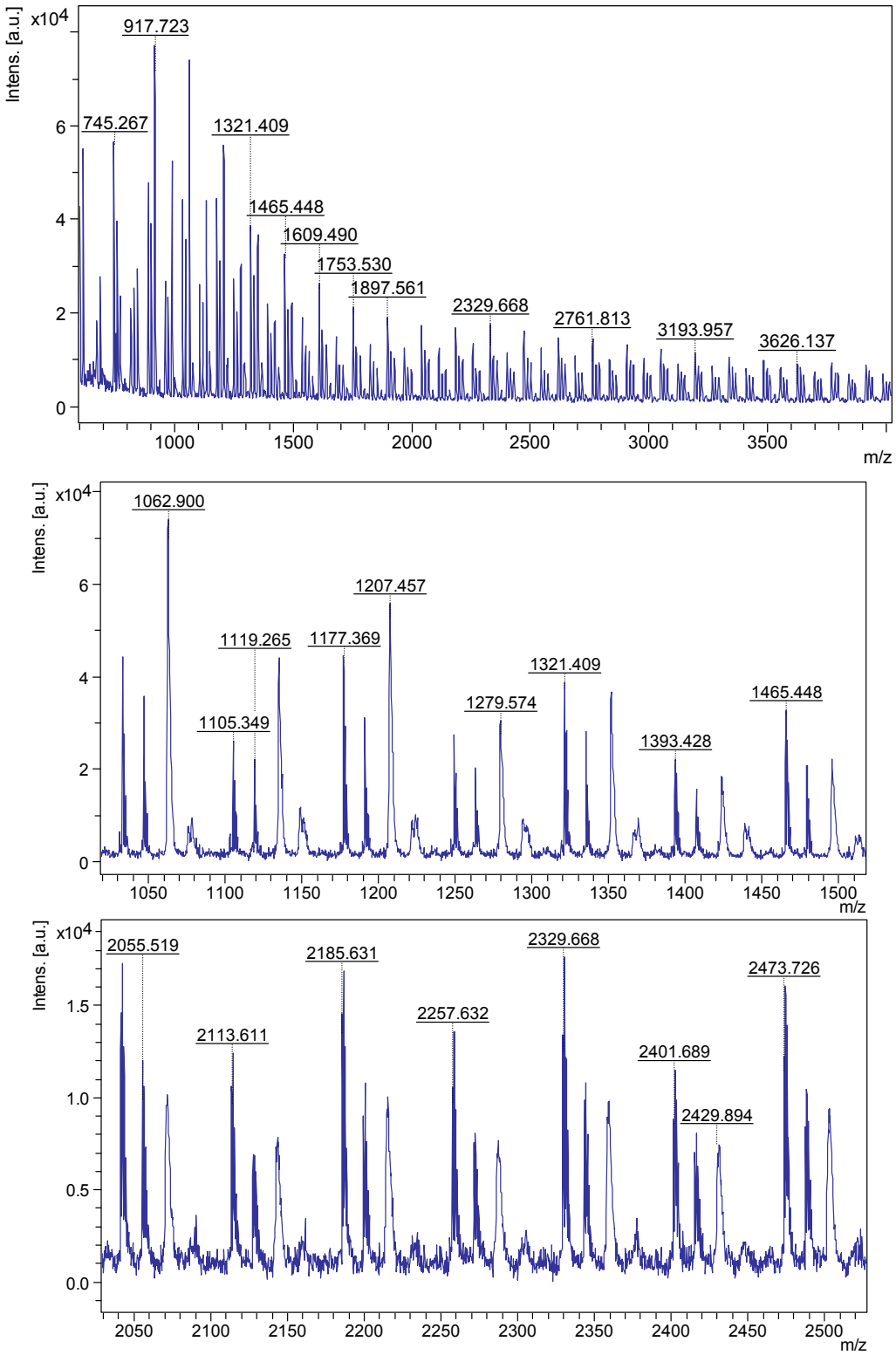

Fig. S57 MALDI-ToF MS of PLA synthesised from ^{Me_2}SB($^{i\text{Pr}}$N,I*)Sc(O-2,6-^{i}Pr-C$_6$H$_3$)(THF) (**4**). The peak envelope centred at 1105.3 Da corresponds to PLA with 7 units of LA terminated with –$^{i\text{Pr}}$NH and –OH groups and K$^+$ [144.1(7) + 59.1 + 39.1]. The peak envelope centred at 1047.2 Da corresponds to cyclic PLA with 7 units of LA and K$^+$ [144.1(7) + 39.1]. Δ(*m*/*z*) = 72.0 Da between peak envelopes.

Mass List (monoisotopic ions)

m/z	S/N	Quality Fac.	Res.	Intens.	Area
601.245	19	3218	3850	41934	10760

615.132	22	12236	3722	49403	14370
673.261	7	1126	4116	16233	4408
687.154	12	9106	2906	26018	11682
745.267	25	8771	4927	55125	15042
759.164	16	2239	4092	35630	12632
817.281	9	2718	4798	20754	6755
831.193	11	5486	3688	23256	10442
844.656	12	7801	1049	27035	38964
889.295	22	8054	5362	46314	15562
903.193	17	8855	5350	36082	12551
917.723	33	5660	1031	70781	112851
961.309	12	4160	5239	25738	10014
975.218	10	4885	4274	20560	10278
990.39	23	17581	1066	46785	84171
1033.332	20	7973	5518	41997	17194
1047.236	16	11019	6344	33310	12160
1062.9	34	18480	1125	68986	128235
1105.349	12	4786	5299	25137	12071
1119.265	10	7815	4688	19494	11031
1135.206	20	12308	1173	39976	80913
1177.369	21	9700	5898	42208	20475
1191.277	14	7899	5583	28103	14919
1207.457	27	13477	1298	51725	103928
1221.166	6	124	2291	11762	16802
1249.388	13	8204	5824	25807	14091
1263.311	9	5865	4283	16629	12620
1279.574	14	9177	1278	26710	61396
1293.694	7	458	2347	13201	20309
1321.409	19	14058	6049	36761	21350
1335.317	13	9853	5713	24059	15024
1351.655	18	19963	1393	32313	75920
1393.428	11	11317	5526	21073	14796
1407.34	7	9550	4378	13154	12163
1423.607	8	4345	1205	14226	43089
1465.448	17	13500	6041	31011	21652
1479.363	10	9414	5965	17914	12925
1495.647	10	5360	1359	17099	49730
1537.469	10	10892	5432	17296	14748
1551.376	6	8026	4816	10874	11021
1609.49	14	18174	5663	24379	21816
1623.396	8	13961	5793	14311	13033
1639.533	7	3471	1124	8666	36607
1681.505	8	13981	5008	13679	15248
1753.53	12	20084	5357	19310	21949
1767.432	7	11902	4906	10854	13871

1825.54	7	7097	5037	11032	14699
1897.561	11	19103	5585	16576	20939
1911.453	7	8618	5326	9661	13166
1969.573	7	12554	5370	10268	14144
2041.606	11	22915	5841	14583	19013
2055.519	7	9988	5780	9691	12831
2113.611	7	11528	5638	9454	13533
2185.631	11	30324	5988	13309	18631
2199.539	7	9188	5661	8061	12120
2257.632	8	19640	6158	9544	13943
2329.668	11	27301	5930	12317	19008
2343.596	7	13309	5991	7893	12084
2401.689	8	11138	6027	8345	13195
2429.894	7	804	5371	7261	13762
2473.726	11	28339	6037	11268	18262
2487.61	7	9378	5954	7046	12066
2545.729	8	13704	6069	7457	12899
2617.78	11	30764	6036	10133	17700
2631.665	7	13228	6287	6676	11533
2689.786	8	8679	5934	6635	12601
2761.813	10	24847	6161	8839	16503
2775.71	7	6822	5882	5765	11485
2833.819	7	9949	5735	5869	12714
2861.083	7	563	5997	5614	11781
2905.859	10	29532	6135	7749	15737
2919.747	7	11384	6323	5561	11234
2977.858	7	9910	6364	5456	11410
3004.714	6	70.6	5481	4911	10278
3049.901	9	26723	6132	6900	15423
3063.8	7	9866	6569	5084	10425
3121.926	7	8126	6306	4950	10981
3193.957	9	36785	6191	6068	14425
3207.852	6	7474	6360	4436	10006
3265.986	6	1711	5634	4221	11415
3337.999	8	18371	6067	5180	13657
3410.032	6	7049	5896	3881	10661
3482.065	8	7946	5812	4452	12933
3508.811	6	545	4363	3215	12455
3626.137	7	4117	5642	3914	11752
3770.186	7	6567	5967	3600	10667

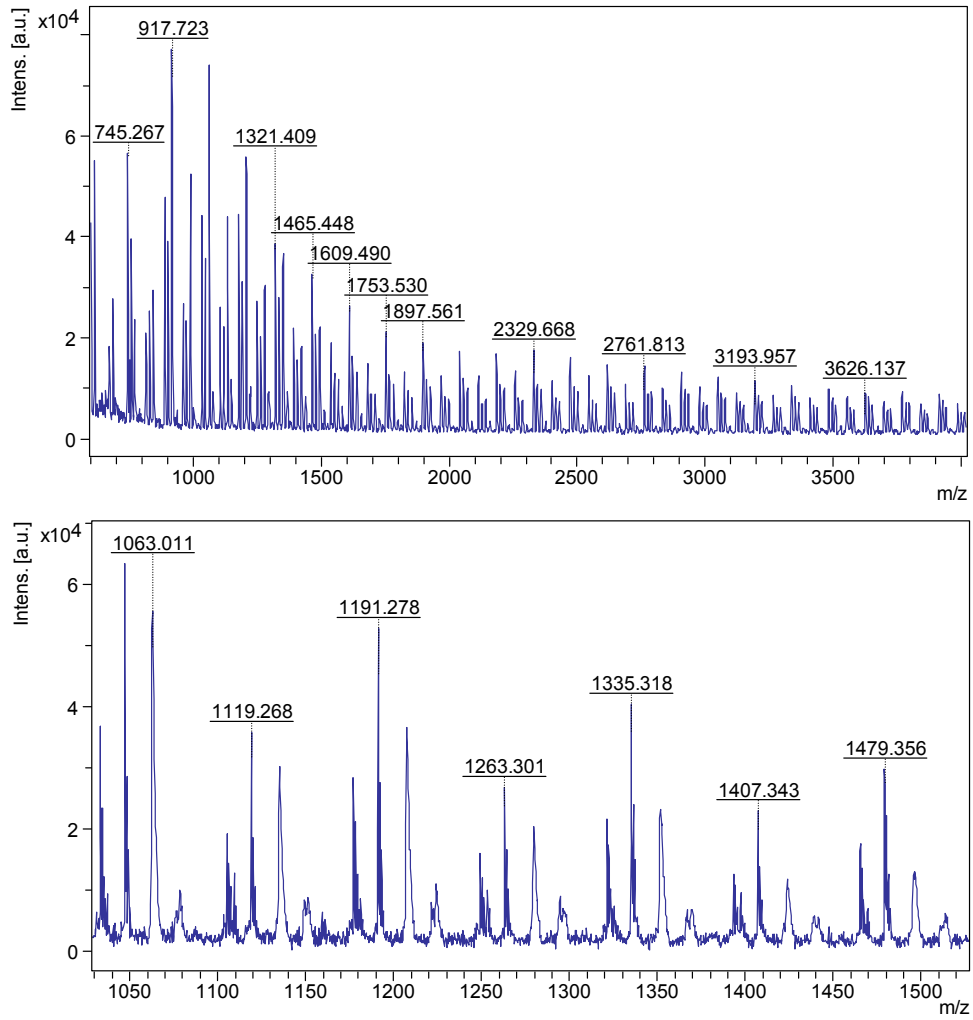

Fig. S58 MALDI-ToF MS of PLA synthesised from ^{Me_2}SB(^{iPr}N,I*)Sc(O-2,4-^{t}Bu-C_6H_3)(THF) (**5**). The peak envelope centred at 1105.3 Da corresponds to PLA with 7 units of LA terminated with –^{iPr}NH and –OH groups and K^+ [144.1(14) + 59.1 + 39.1]. The peak envelope centred at 1047.2 Da corresponds to cyclic PLA with 7 units of LA and K^+ [144.1(14) + 39.1]. Δ(*m*/*z*) = 72.0 Da between peak envelopes.

Mass List (monoisotopic ions)

m/z	S/N	Quality Fac.	Res.	Intens.	Area
601.246	26	957	3345	90305	27182
615.145	21	12929	2821	72152	28404
673.26	13	391	3624	43445	13968
687.181	17	8304	2656	55999	26548
745.268	24	2823	3782	77787	28602
751.433	8	559	3353	25029	9824
759.172	25	4040	3758	82768	32097
817.278	10	1715	3707	33140	14481
831.195	16	9889	3542	51399	24228
844.678	6	2735	874	20239	37719
889.297	15	3710	3763	45615	21979
903.204	23	8158	4347	72634	31126
917.811	19	6276	939	57345	101774
961.317	8	1941	3107	23240	15380

975.227	14	7611	4127	40479	20718
990.454	12	7191	979	36145	71818
1033.335	11	4391	3664	32082	20286
1047.242	20	8028	4655	56526	28489
1063.011	18	6670	982	48817	104747
1105.35	6	1215	3396	16876	13064
1119.268	11	6893	3759	30956	21694
1135.277	9	4488	946	23801	60887
1177.368	10	3593	3592	25186	20443
1191.278	17	10851	4528	44542	28841
1207.526	12	6749	1078	30822	77400
1263.301	9	11355	3857	22919	19482
1279.601	6	3969	927	13716	43875
1321.4	8	5427	3470	19375	20213
1335.318	14	17058	4400	35194	28800
1351.719	8	5602	1037	17491	55397
1407.343	8	11406	3968	19201	19376
1465.453	7	4859	3726	15090	17331
1479.356	12	23211	4533	26635	25785
1551.395	6	9686	4009	14099	16782
1623.412	10	22522	4467	20072	23349
1767.448	8	16278	4159	15256	22999
1911.488	8	14665	4046	12127	22047
2055.535	7	14654	4168	10299	19322
2199.567	7	3063	3753	7955	18399
2343.625	7	2942	3941	7205	17067
2487.672	6	2125	3990	6391	16290
2631.709	7	4763	4325	6208	15678
2775.742	6	2635	4393	5149	13968

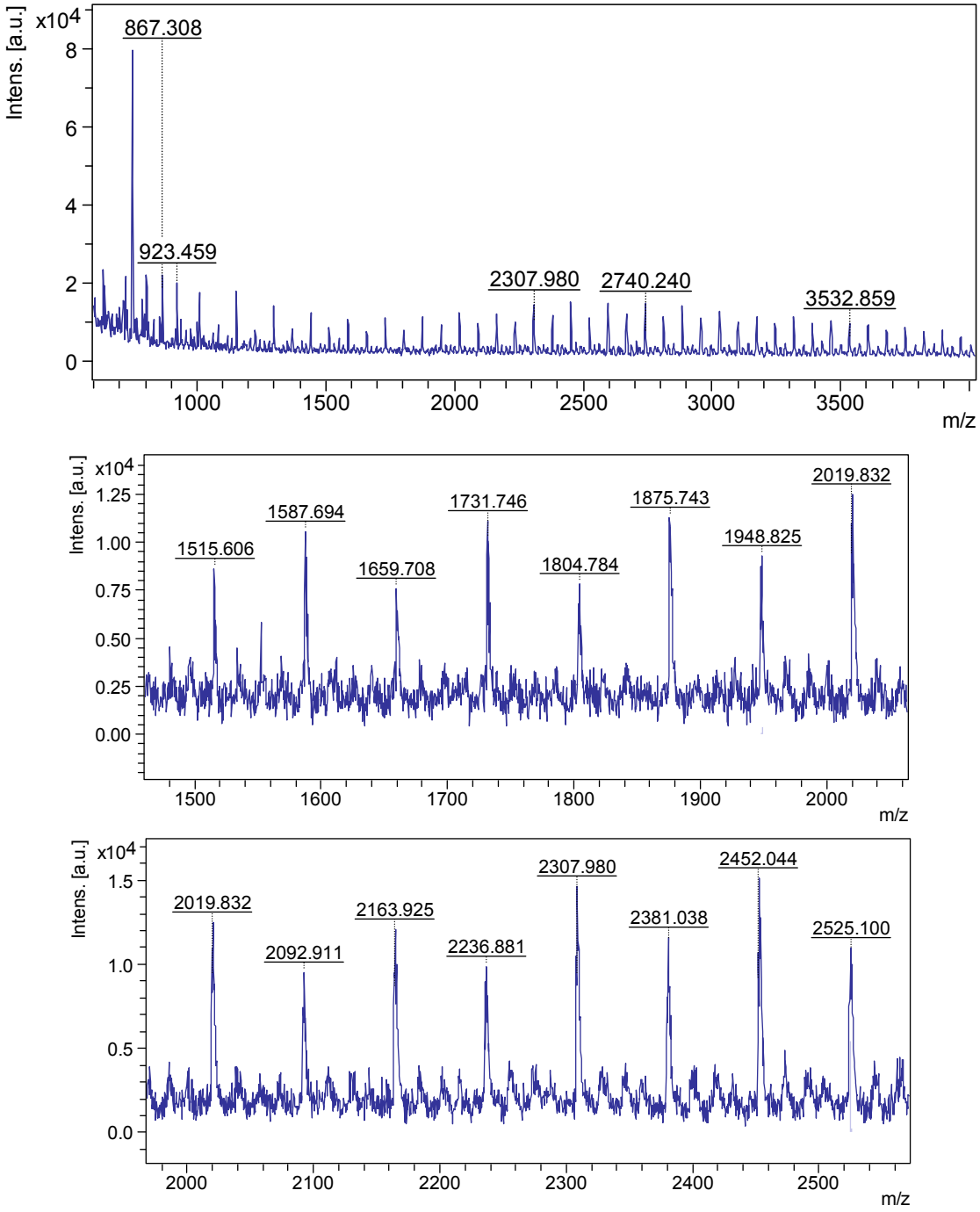

Fig. S59 MALDI-ToF MS of PLA synthesised from $^{Me}_2$SB(^{iPr}N,I*)Al(Cl)(THF) (**8**) with benzyl alcohol. The peak envelope centred at 1587.7 Da corresponds to PLA with 10 units of LA terminated with –OBn and –OH groups and K^+ [144.1(10) + 108.1 + 39.1]. Δ(*m*/*z*) = 72.0 Da between peak envelopes.

Mass List (monoisotopic ions)

m/z	S/N	Quality Fac.	Res.	Intens.	Area
751.536	25	3097	2321	74783	46009
867.308	6	1250	3214	17538	10066
923.459	7	2302	2667	19454	14679
1011.367	6	5038	2812	16499	13624
1155.454	7		4331	17833	7333
1227.473	3		3007	7937	3475

1299.505	6		3263	14104	7213
1371.538	4		3086	8393	3849
1443.568	5		5225	11740	4809
1515.606	4		3698	8646	3391
1587.694	5		3275	10546	6338
1659.708	4		3973	7560	3394
1731.746	5		4370	10139	6073
1804.784	4		2611	7847	5550
1875.743	6		4840	11277	6270
1948.825	5		5087	9291	5757
2019.832	6	9953	2885	9217	24420
2092.911	5		5337	9501	5961
2163.925	6	9382	2772	8454	25060
2236.881	5		4449	9836	6871
2307.98	7	19660	2982	9224	27179
2381.038	6		6972	11335	5841
2452.044	7	27737	3092	8941	27924
2525.1	5		4615	10789	8426
2596.118	7	8298	2930	7799	27973
2669.136	6		5150	11679	9027
2740.24	6	4284	2631	6706	27588
2813.246	6		6030	11537	8146
2884.262	6	3374	2852	6449	27308
2958.133	6		6804	10910	8396
3102.401	5		4337	9242	8264
3173.366	6		6485	11234	8550
3245.442	5		6315	9282	7128
3318.254	6		5264	11495	9980
3390.507	5		5404	9382	9303
3532.859	7	456	7710	5255	12671
3606.705	5		9416	8958	4741
3678.695	4		7976	7822	6669
3823.713	4		11356	7587	3645
3894.725	4		10656	7948	5637
3966.842	3		6694	6207	4650

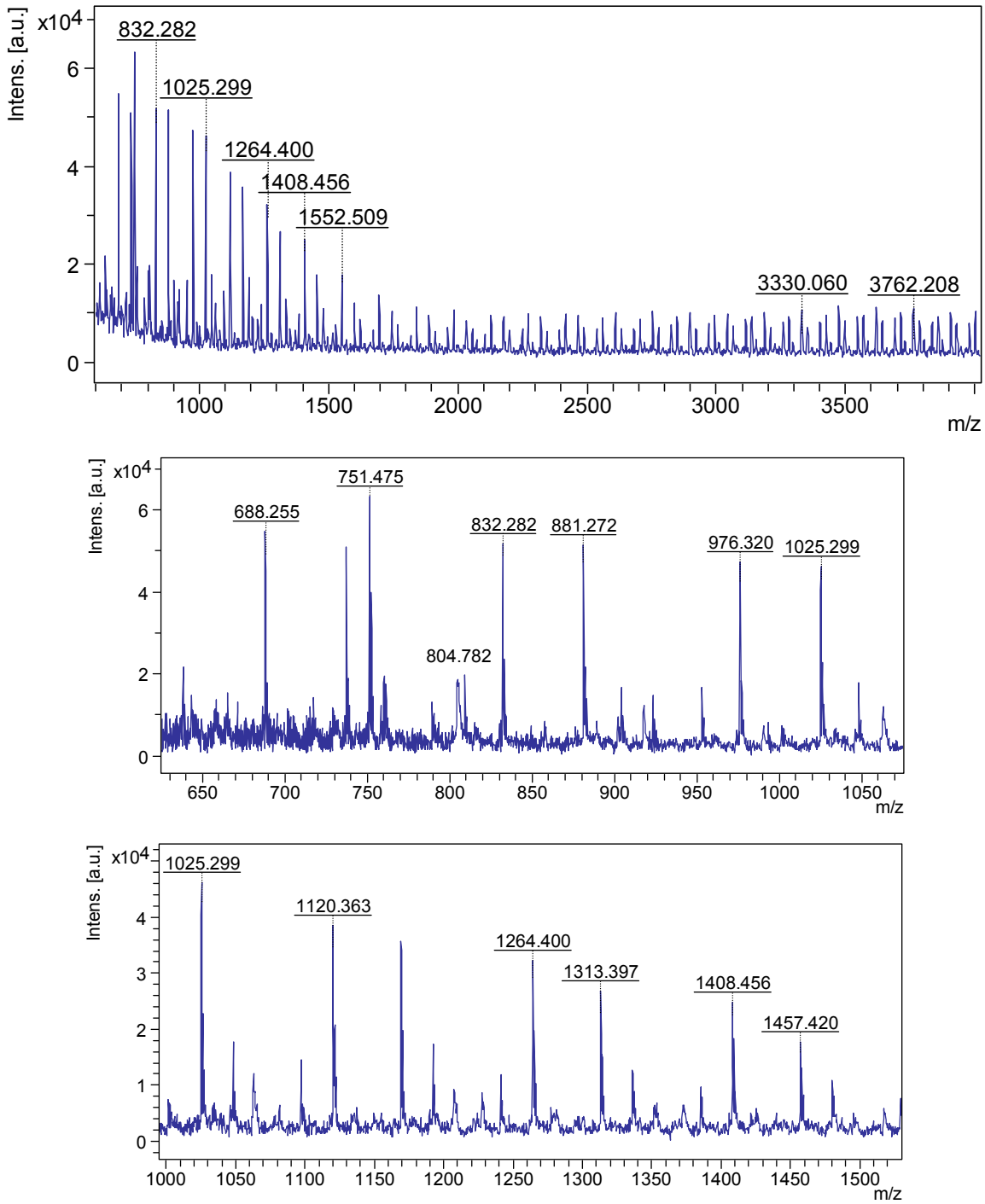

Fig. S60 MALDI-ToF MS of PLA synthesised from ^{Me2}SB(^{iPr}N,I*)AL(O-2,6-Me-C_6H_3)(THF) (**9**). The peak envelope centred at 881.3 Da corresponds to PLA with 5 units of LA terminated with –O-2,6-Me-C_6H_3 and –OH groups and K^+ [144.1(5) + 122.2 + 39.1]. The peak envelope centred at 832.1 Da corresponds to PLA with 5 units of LA terminated with –NH^{t}Bu and –OH groups and K^+ [144.1(5) + 73.1 + 39.1]. Δ(*m*/*z*) = 144.0 Da between peak envelopes.

Mass List (monoisotopic ions)

m/z	S/N	Quality Fac.	Res.	Intens.	Area
688.255	15	4438	3088	48086	19813
737.228	14	5215	3035	45047	21414
751.475	19	3104	3236	62571	27811

804.782	7	392	1002	21609	29628
832.282	15	7960	3565	47938	22467
881.272	15	6420	3498	46301	24271
976.32	14	7258	3914	41397	22843
1025.299	15	6605	4071	42015	24455
1120.363	13	9770	3874	33893	23904
1169.351	12	8374	4198	31541	22057
1264.4	11	12194	4018	28523	24063
1313.397	9	9863	4085	22176	19320
1408.456	9	12955	3973	21694	22444
1457.42	7	7030	4087	15175	16522
1552.509	7	11891	4027	15453	18733
1601.514	5		5218	11965	4636
1624.595	4		5303	8369	3154
1696.56	6		5823	13210	5866
1745.559	5		5954	10146	4288
1768.569	4		4760	7522	3404
1840.63	5		4440	10877	5642
1889.595	5		6674	9688	3419
1912.672	3		5606	6115	2226
1984.64	5		6108	10137	4328
2033.672	4		4819	7991	4216
2034.631	4		5036	8396	4668
2057.746	4		7328	6712	2803
2105.719	3		6093	5820	2640
2128.728	5		6960	9357	3717
2178.681	5		6448	9103	4735
2250.765	4		8547	6460	3025
2273.716	5		5824	9889	4991
2322.727	5		6303	9246	4285
2394.694	4		9907	6518	2706
2417.828	5		7632	8994	4878
2466.719	5		9237	9237	4138
2538.8	4		4699	6800	3479
2561.866	5		5040	9022	5461
2705.861	5		7725	8226	4559
2754.809	6		8286	10488	5517
2826.879	4		6494	7428	4399
2849.861	5		7252	9321	4879
2898.888	6		7128	9684	5888
2993.937	5		7149	8456	5426
3042.947	6		7309	9914	5597
3114.926	5		7800	8596	4780
3137.963	5		7248	9247	5909
3186.979	6		6011	10031	6122

3260.021	5		7971	8183	4989
3330.06	6	1604	5280	4866	14749
3354.01	4		5086	6960	4826
3403.07	5		6854	8155	4680
3427.133	6		8504	9582	6102
3474.102	6	3062	5420	4752	14468
3498.133	5		10736	8528	5155
3548.139	5		9726	9400	5776
3571.194	5		8912	9235	6339
3618.159	6	3445	5289	4263	13971
3643.12	5		9092	8588	5486
3692.163	5		8478	9130	5408
3715.209	6		7358	10089	6926
3762.208	6	1848	4890	3673	14139
3859.212	5		7922	9389	6565
4003.348	6		9265	10340	6929

Additional Crystallographic Data

Table S1: Selected experimental crystallographic data for complexes **2**–**4** and **6**.

Complex	$[^{Me_2}SB(^{nBu}N,I^*)Sc(Cl)(THF)]_2$ (**2**)	$[^{Me_2}SB(^{Ph}N,I^*)Sc(Cl)(THF)]_2$ (**3**)	$^{Me_2}SB(^{iPr}N,I^*)Sc(O\text{-}2,6\text{-}^{i}Pr\text{-}C_6H_3)(THF)$ (**4**)	$^{Me_2}SB(^{nBu}N,I^*)Sc(O\text{-}2,6\text{-}^{i}Pr\text{-}C_6H_3)(THF)$ (**6**)
Crystal data				
Chemical formula	$C_{50}H_{82}Cl_2N_2O_2Sc_2Si_2$	$C_{54}H_{74}Cl_2N_2O_2Sc_2Si_2$	$C_{36}H_{56}NO_2ScSi$	$C_{37}H_{58}NO_2ScSi$
M_r	960.18	1000.15	607.86	621.89
Crystal system, space group	Triclinic, *P*-1	Monoclinic, *C*2/*c*	Monoclinic, $P2_1/n$	Orthorhombic, $Pna2_1$
Temperature (K)	150	150	150	150
a, *b*, *c* (Å)	10.2397(4), 10.9358(4), 12.4015(4)	23.7263(4), 10.4153(2), 21.6239(3)	11.5970(1), 16.9523(2), 18.2920(2)	15.21080(1), 24.5048(2), 9.70340(1)
α, *β*, *γ* (°)	89.006(3), 85.166(3), 67.359(4)	90, 106.991(2), 90	90, 103.407(1) 90	90, 90, 90
V (Å^3)	1276.96(9)	5110.38(16)	3498.13(7)	3616.82(5)
Z	2	4	4	4
Radiation type	Cu *K*a	Cu *K*a	Cu *K*a	Cu *K*a
μ (mm^{-1})	3.99	4.01	2.35	2.28
Crystal size	0.25 × 0.21 × 0.13	0.26 × 0.14 × 0.11	0.35 × 0.09 × 0.06	0.43 × 0.20 × 0.13
Data Collection				
Diffractometer	SuperNova, Dual, Cu at zero, Atlas	SuperNova, Dual, Cu at zero, Atlas	SuperNova, Dual, Cu at zero, Atlas	SuperNova, Dual, Cu at zero, Atlas
Absorption correction	Gaussian *CrysAlis PRO* 1.171.39.46 (Rigaku Oxford Diffraction, 2018) Empirical absorption correction	Gaussian *CrysAlis PRO* 1.171.39.46 (Rigaku Oxford Diffraction, 2018) Empirical absorption correction using	Gaussian *CrysAlis PRO* 1.171.39.46 (Rigaku Oxford Diffraction, 2018) Numerical absorption correction based on	Gaussian *CrysAlis PRO* 1.171.39.46 (Rigaku Oxford Diffraction, 2018) Numerical absorption correction based on

	using spherical harmonics, Implemented in SCALE3 ABSPACK scaling algorithm.	spherical harmonics, Implemented in SCALE3 ABSPACK scaling algorithm.	gaussian integration over a multifaceted crystal model. Empirical absorption correction using spherical harmonics, Implemented in SCALE3 ABSPACK scaling algorithm.	gaussian integration over a multifaceted crystal model. Empirical absorption correction using spherical harmonics, Implemented in SCALE3 ABSPACK scaling algorithm.
T_{min}, T_{max}	0.841, 1.000	0.613, 1.000	0.526, 1.000	0.456, 1.000
No. of measured, independent and observed [$I > 2\sigma(I)$] reflections	15537, 5222, 4966	29495, 5223, 4871	28917, 7152, 6616	32662, 7219, 6888
R_{int}	0.019	0.028	0.026	0.023
Refinement				
$R[F^2 > 2\sigma(F^2)]$, $wR(F^2)$, S	0.034, 0.092, 1.04	0.033, 0.095, 1.07	0.034, 0.097, 1.06	0.052, 0.143, 1.05
No. of reflections	5222	5223	7152	7219
No. of parameters	280	297	384	437
No. of restraints	0	0	0	82
$(\Delta/\sigma)_{max}$	0.001	0.001	0.001	0.001
$\Delta\rho_{max}$, $\Delta\rho_{min}$ (e Å^{-3})	0.56, -0.56	0.45, -0.38	0.88, -0.31	0.58, -0.67

Computer programs: *CrysAlis PRO* 1.171.39.46 (Rigaku OD, 2018),[3] *SUPERFLIP*.,[5] *SHELXL2018*/3 (Sheldrick, 2018), *ORTEP-3 for Windows*.[6]

Table S2: Selected experimental crystallographic data for complexes **8**–**10**.

Complex	^{Me2}SB(^{tBu}N,I*)Al(Cl)(THF) (**8**)	^{Me2}SB(^{tBu}N,I*)Al(O-2,6-Me-C_6H_3)(THF) (**9**)	^{Me2}SB(^{tBu}N,I*)Al(O-2,4-^{t}Bu-C_6H_3)(THF) (**10**)
Crystal data			
Chemical formula	$C_{25}H_{41}AlClNOSi$	$C_{33}H_{50}AlNO_2Si$	$C_{39}H_{62}AlNO_2Si$
M_r	462.11	547.81	631.96
Crystal system, space group	Monoclinic, $P2_1/n$	Triclinic, P -1	Triclinic, P -1
Temperature (K)	150	150	150
a, *b*, *c* (Å)	13.0882(2), 14.3825(2), 14.3203(2)	9.1150(5), 11.4654(5), 18.1231(10)	14.9848(9), 15.2025(3), 17.3160(4)
α, *β*, *γ* (°)	90, 104.340(1), 90	75.161(4), 84.213(4), 69.169(4)	89.817(2), 84.546(3), 78.504(3)
V (Å^3)	2611.68(7)	1711.05(16)	3847.6(3)
Z	4	2	4
Radiation type	Cu *K*a	Cu *K*a	Cu *K*a
μ (mm^{-1})	2.172	1.049	0.989
Crystal size (mm)	0.451 × 0.206 × 0.109	0.315 × 0.137 × 0.057	0.161 × 0.144 × 0.031
Data collection			
Diffractometer	SuperNova, Dual, Cu at zero, Atlas	SuperNova, Dual, Cu at zero, Atlas	SuperNova, Dual, Cu at zero, Atlas
Absorption correction	Gaussian *CrysAlis PRO* 1.171.39.46 (Rigaku Oxford Diffraction, 2018) Numerical absorption correction based on gaussian integration over a multifaceted crystal model. Empirical absorption correction using spherical harmonics, Implemented in SCALE3 ABSPACK scaling algorithm	Gaussian *CrysAlis PRO* 1.171.39.46 (Rigaku Oxford Diffraction, 2018) Numerical absorption correction based on gaussian integration over a multifaceted crystal model. Empirical absorption correction using spherical harmonics, Implemented in SCALE3 ABSPACK scaling algorithm	Gaussian *CrysAlis PRO* 1.171.39.46 (Rigaku Oxford Diffraction, 2018) Numerical absorption correction based on gaussian integration over a multifaceted crystal model. Empirical absorption correction using spherical harmonics, Implemented in SCALE3 ABSPACK scaling algorithm.

T_{min}, T_{max}	0.390, 1.000	0.521, 1.000	0.695, 1.000
No. of measured, independent and observed [$I > 2\sigma(I)$] reflections	35617, 5339, 4795	13420, 6932, 5185	30411, 15496, 11671
R_{int}	0.0604	0.0468	0.0366
Refinement			
$R[F^2 > 2\sigma(F^2)]$, $wR(F^2)$, S	0.0462, 0.1322, 1.029	0.0523, 0.1480, 0.977	0.0770, 0.1778, 1.079
No. of reflections	5339	6932	15496
No. of parameters	279	356	1135
No. of restraints	0	0	1525
$(\Delta/\sigma)_{max}$	0.000	0.000	0.001
$\Delta\rho_{max}$, $\Delta\rho_{min}$ (e Å^{-3})	0.819, -0.383	0.958, -0.331	0.624, -0.884

Computer programs: *CrysAlis PRO* 1.171.39.46 (Rigaku OD, 2018),[3] *SUPERFLIP*.,[5] *SHELXL2018*/3 (Sheldrick, 2018), *ORTEP-3 for Windows*.[6]

Table S3 Selected bond lengths (Å) and angles (°) for $^{Me}_2$SB(^{nBu}N,I*)Sc(Cl)(THF) (**2**) and $^{Me}_2$SB(^{Ph}N,I*)Sc(Cl)(THF) (**3**) (E.S.D. are given in parentheses).

Complex	$^{Me}_2$SB(^{nBu}N,I*)Sc(Cl)(THF) (**2**)	$^{Me}_2$SB(^{Ph}N,I*)Sc(Cl)(THF) (**3**)
Sc(1)-I*$_{cent}$	2.1836(1)	2.1845(1)
Sc(1)-Cl(1)	2.5700(5)	2.5732(5)
Sc(1)-Cl(1´)	2.6273(5)	2.6055(5)
Sc(1)-O(1)	2.2257(12)	2.2174(12)
Sc(1)-N(1)	2.0412(14)	2.0909(14)
Sc(1)-Si(1)	2.9993(5)	3.0268(5)
N(1)-C(18)	1.457(2)	1.389(2)
I*$_{cent}$-Sc(1)-O(1)	116.05	111.15
I*$_{cent}$-Sc(1)-N(1)	102.77	102.50
Sc(1)-Cl(1)-Sc(1)	105.173(15)	102.264(15)
Δ_{M-C}	0.0482	0.0842

Table S4 Selected bond lengths (Å) and angles (°) for $^{Me}_2$SB(^{iPr}N,I*)Sc(O-2,6-^{i}Pr-C_6H_3)(THF) (**4**) and $^{Me}_2$SB(^{nBu}N,I*)Sc(O-2,6-^{i}Pr-C_6H_3)(THF) (**6**) (E.S.D. are given in parentheses).

Complex	$^{Me}_2$SB(^{iPr}N,I*)Sc(O-2,6-^{i}Pr-C_6H_3)(THF) (**4**)	$^{Me}_2$SB(^{nBu}N,I*)Sc(O-2,6-^{i}Pr-C_6H_3)(THF) (**6**)
Sc(1)-I*$_{cent}$	2.1704(1)	2.1735(1)
Sc(1)-O(1)	1.9344(10)	1.930(3)
Sc(1)-O(2)	2.1705(10)	2.125(12)
Sc(1)-N(1)	2.0458(12)	2.026(4)
Sc(1)-Si(1)	2.9797(4)	2.9565(16)
N(1)-C(18)	1.4682(19)	1.462(7)
Sc(1)-O(1)-C(OAr)[a]	176.91(9)	169.9(3)
I*$_{cent}$-Sc(1)-O(1)	121.15(1)	122.70
I*$_{cent}$-Sc(1)-O(2)	112.45(1)	112.86
I*$_{cent}$-Sc(1)-N(1)	103.82(1)	103.63
O(1)-Sc(1)-O(2)	103.94(4)	94.5(6)

[a]Sc(1)-O(1)-C(21) for **4** and Sc(1)-O(1)-C(22) for **6**.

Table S5 Selected bond lengths (Å) and angles (°) for $^{Me}{}_2$SB($^{t\text{Bu}}$N,I*)Al(Cl)(THF) (**8**) and $^{Me}{}_2$SB($^{t\text{Bu}}$N,I*)Al(O-2,6-Me-C_6H_3)(THF) (**9**) (E.S.D. are given in parentheses).

Complex	**8**	**9**
Al(1)-Cl(1)	2.1375(7)	–
Al(1)-O(1)	1.8600(13)	1.7150(15)
Al(1)-O(2)	–	1.8917(15)
Al(1)-N(1)	1.8047(15)	1.8221(18)
Al(1)-C(1)	2.0257(18)	2.027(2)
C(1)-Al(1)-Cl(1)	121.33(6)	–
C(1)-Al(1)-O(1)	110.78(7)	124.96(8)
C(1)-Al(1)-O(2)	–	115.06(8)
C(1)-Al(1)-N(1)	89.06(7)	88.36(8)
O(1)-Al(1)-O(2)	–	93.73(7)
Cl(1)-Al(1)-O(1)	99.04(5)	–
N(1)-Al(1)-O(1)	111.87(7)	128.06(8)
N(1)-Al(1)-O(2)	–	107.35(7)
N(1)-Al(1)-Cl(1)	125.14(6)	–
N(1)-Al(1)-Si(1)	41.82(5)	41.48(6)
O(1)-Al(1)-Si(1)	117.68(5)	149.08(6)
C(1)-Al(1)-Si(1)	47.70(5)	46.94(6)
Cl(1)-Al(1)-Si(1)	143.28(3)	–
Si(1)-C(1)-Al(1)	82.08(7)	82.67(8)
C(1)-Si(1)-N(1)	94.17(7)	94.34(8)
Si(1)-N(1)-Al(1)	94.37(7)	94.29(8)
Al(1)-O(1)-C(22)	–	143.72(14)

Table S6 Selected bond lengths (Å) and angles (°) for isomer 1 and 2 of $^{Me}_2$SB(^{tBu}N,I*)Al(O-2,4-^{t}Bu-C_6H_3)(THF) (**10**) (E.S.D. are given in parentheses). The values in brackets correspond to the other crystallographically independent molecule in the asymmetric unit.

Complex **10**	Isomer 1		Isomer 2	
Al(1)-O(1)	1.712(2)	[1.715(2)]	1.712(2)	[1.715(2)]
Al(1)-O(2)	1.880(2)	[1.887(2)]	1.880(2)	[1.887(2)]
Al(1)-N(1)	1.815(2)	[1.808(2)]	1.815(2)	[1.808(2)]
Al(1)-C(1)	2.051(4)	[2.093(7)]	2.032(8)	[2.030(4)]
C(1)-Al(1)-O(1)	133.04(13)	[136.1(2)]	111.5(2)	[116.72(17)]
C(1)-Al(1)-O(2)	101.68(15)	[98.4(2)]	129.1(3)	[121.45(19)]
C(1)-Al(1)-N(1)	89.13(14)	[88.0(2)]	86.8(3)	[88.17(14)]
O(1)-Al(1)-O(2)	95.14(11)	[96.65(11)]	95.14(11)	[96.65(11)]
N(1)-Al(1)-O(1)	122.68(12)	[122.58(12)]	122.68(12)	[122.58(12)]
N(1)-Al(1)-O(2)	114.65(11)	[113.55(11)]	114.65(11)	[113.55(11)]
N(1)-Al(1)-Si(1)	41.71(8)	[41.42(7)]	41.71(8)	[41.42(7)]
O(1)-Al(1)-Si(1)	144.28(10)	[140.86(10)]	144.28(10)	[140.86(10)]
C(1)-Al(1)-Si(1)	47.74(12)	[48.2(2)]	49.3(2)	[47.69(12)]
Si(1)-C(1)-Al(1)	81.13(16)	[79.7(3)]	80.4(3)	[81.96(17)]
C(1)-Si(1)-N(1)	94.87(14)	[93.9(2)]	90.0(2)	[92.95(15)]
Si(1)-N(1)-Al(1)	94.20(12)	[94.96(11)]	94.20(12)	[94.96(11)]
Al(1)-O(1)-C(22)	147.2(2)	[140.0(2)]	147.2(2)	[140.0(2)]

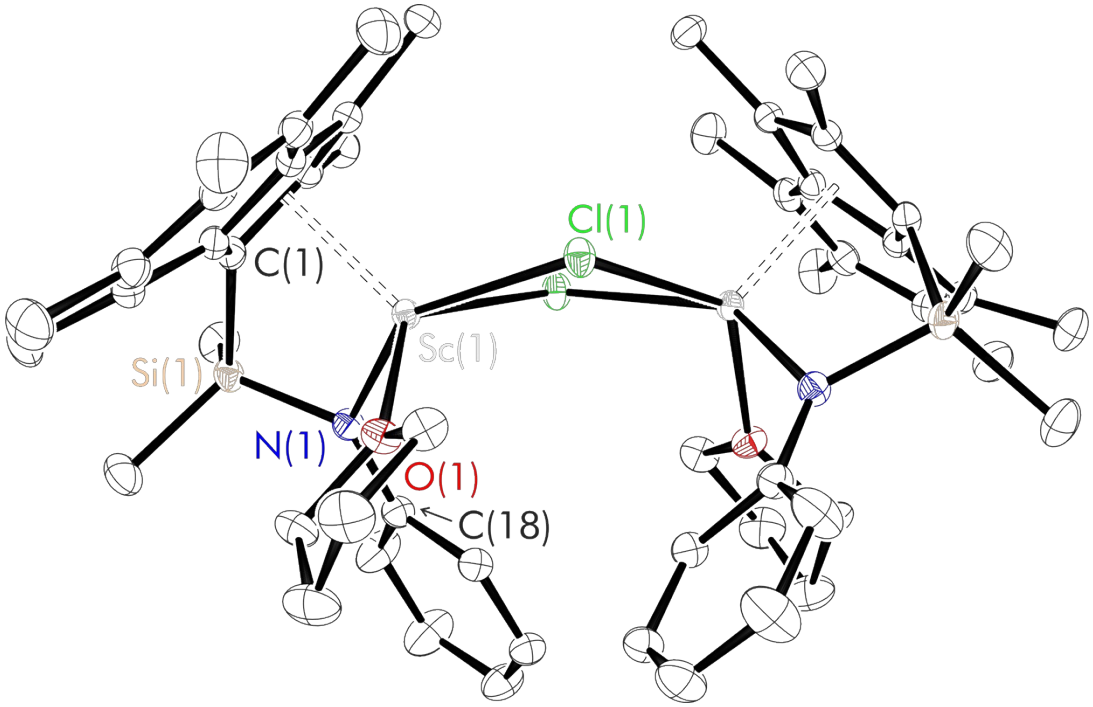

Fig. S61 Solid-state structures of ^{Me_2}SB(^{Ph}N,I*)Sc(Cl)(THF) (**3**). Ellipsoids are drawn at the 30% probability level and H atoms omitted for clarity.

Additional polymerisation data

Table S7 ROP of *L*-LA using ^{Me_2}SB(^{iPr}N,I*)Sc(Cl)(THF) (**1**) and benzyl alcohol with $[L\text{-LA}]_0$:$[\mathbf{1}]_0$:$[\text{BnOH}]_0$ = 400:1:1 at 70 °C.[a]

Time (h)	Conversion 1 (%)[b]	Time (h)	Conversion 2 (%)[b]
0.25	24	0.25	21
0.50	43	0.50	41
0.75	59	0.75	54
1.00	70	1.00	71
1.25	78	1.25	79
1.50	85	1.50	84
1.75	88	1.75	88
2.00	90	2.00	92
k_{obs} = 1.21 ± 0.03 h^{-1}. R^2 = 0.995		k_{obs} = 1.30 ± 0.03 h^{-1}. R^2 = 0.997	
M_n = 42 290 g mol^{-1}		M_n = 41 050 g mol^{-1}	
M_w/M_n = 1.17		M_w/M_n = 1.20	

[a]Conditions: $[L\text{-LA}]_0$:$[\mathbf{1}]_0$:$[\text{BnOH}]_0$ = 400:1:1, $[L\text{-LA}]_0$ = 0.5 M, 5 mL toluene at 70 °C. Aliquots were taken at given intervals. [b]Measured by ^{1}H NMR spectroscopic analyses.

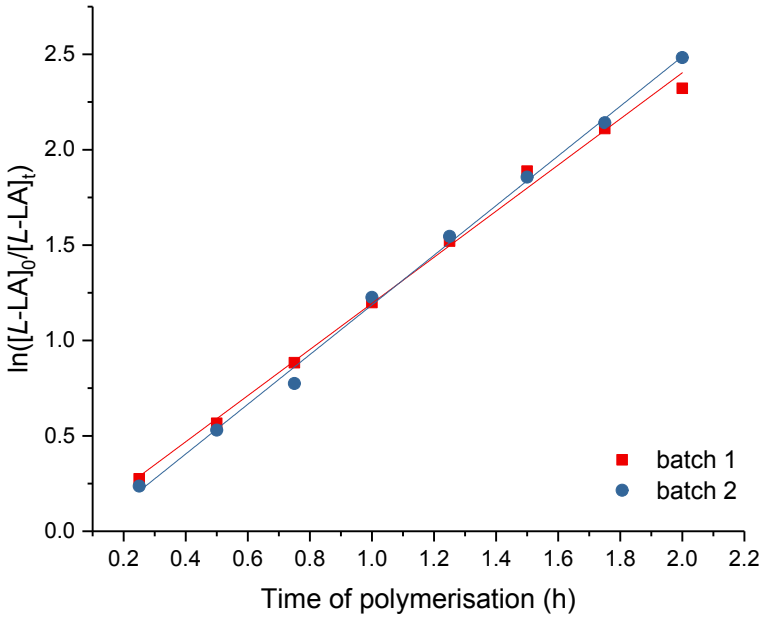

Fig. S62 Plots of $\ln([L\text{-LA}]_0/[L\text{-LA}]_t)$ *vs.* time. Red squares: batch 1 (k_{obs} = 1.21 ± 0.03 h^{-1}. R^2 = 0.995), Blue circles: batch 2 (k_{obs} = 1.30 ± 0.03 h^{-1}. R^2 = 0.997). Conditions: $[L\text{-LA}]_0$:$[\mathbf{1}]_0$:$[\text{BnOH}]_0$ = 400:1:1, $[L\text{-LA}]_0$ = 0.5 M, $[\mathbf{1}]_0$ = 0.00125 M, $[\text{BnOH}]_0$ = 0.00125 M, 5.0 mL toluene at 70 °C.

Table S8 ROP of *L*-LA using ^{Me_2}SB(^{nBu}N,I*)Sc(Cl)(THF) (**2**) and benzyl alcohol with $[L\text{-LA}]_0$:$[\mathbf{2}]_0$:$[\text{BnOH}]_0$ = 400:1:1 at 70 °C.[a]

Time (h)	Conversion 1 (%)[b]	Time (h)	Conversion 2 (%)[b]
0.25	12	0.25	13
0.50	23	0.50	25
0.75	34	0.75	36
1.00	46	1.00	46
1.25	55	1.25	57
1.50	65	1.50	68
1.75	71	1.75	72
2.00	78	2.00	76
2.25	80	2.25	83
2.50	86	2.50	87
2.75	88	2.75	89
3.00	91	3.00	94
k_{obs} = 0.89 ± 0.02 h^{-1}. R^2 = 0.994 M_n = 44 920 g mol^{-1} M_w/M_n = 1.17		k_{obs} = 0.90 ± 0.02 h^{-1}. R^2 = 0.995	

[a]Conditions: $[L\text{-LA}]_0$:$[\mathbf{2}]_0$:$[\text{BnOH}]_0$ = 400:1:1, $[L\text{-LA}]_0$ = 0.5 M, 5 mL toluene at 70 °C. Aliquots were taken at given intervals. [b]Measured by ^{1}H NMR spectroscopic analyses.

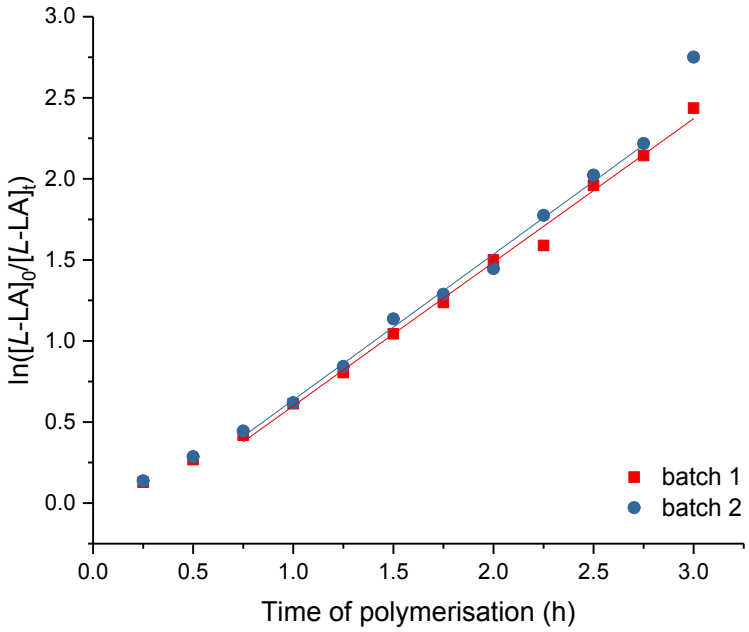

Fig. S63 Plots of $\ln([L\text{-LA}]_0/[L\text{-LA}]_t)$ *vs.* time. Red squares: batch 1 (k_{obs} = 0.89 ± 0.02 h^{-1}. R^2 = 0.994), Blue circles: batch 2 (k_{obs} = 0.90 ± 0.02 h^{-1}. R^2 = 0.995). Conditions: $[L\text{-LA}]_0$:$[\mathbf{2}]_0$:$[\text{BnOH}]_0$ = 400:1:1, $[L\text{-LA}]_0$ = 0.5 M, $[\mathbf{2}]_0$ = 0.00125 M, $[\text{BnOH}]_0$ = 0.00125 M, 5.0 mL toluene at 70 °C.

Table S9 ROP of *L*-LA using ^{Me_2}SB(^{Ph}N,I*)Sc(Cl)(THF) (**3**) and benzyl alcohol with $[L\text{-LA}]_0$:$[\mathbf{3}]_0$:$[\text{BnOH}]_0$ = 400:1:1 at 70 °C.[a]

Time (h)	Conversion 1 (%)[b]	Time (h)	Conversion 2 (%)[b]
0.5	15	0.5	15
1.0	31	1.0	28
1.5	46	1.5	43
2.0	59	2.0	56
2.5	69	2.5	66
3.0	77	3.0	74
3.5	83	3.5	81
4.0	89	4.0	89
4.5	90	4.5	89
k_{obs} = 0.57 ± 0.01 h^{-1}. R^2 = 0.999		k_{obs} = 0.54 ± 0.01 h^{-1}. R^2 = 0.998	

[a]Conditions: $[L\text{-LA}]_0$:$[\mathbf{3}]_0$:$[\text{BnOH}]_0$ = 400:1:1, $[L\text{-LA}]_0$ = 0.5 M, 5 mL toluene at 70 °C. Aliquots were taken at given intervals. [b]Measured by ^{1}H NMR spectroscopic analyses.

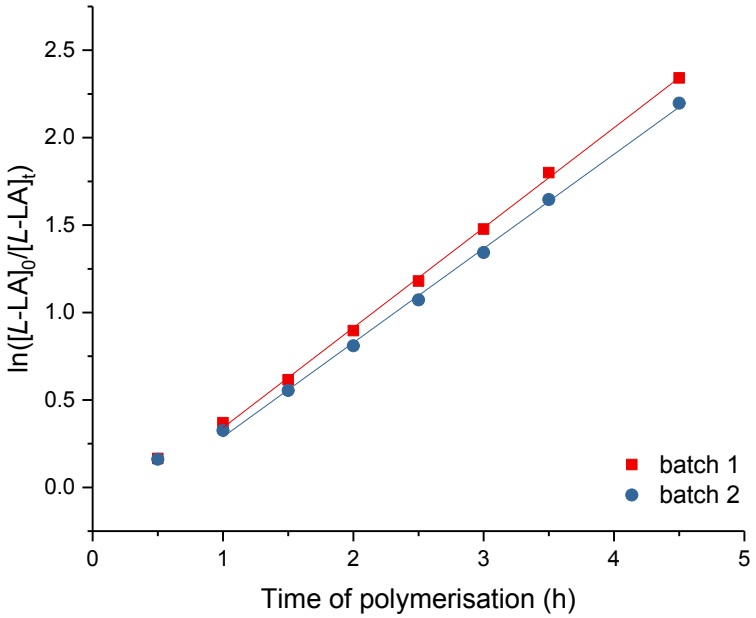

Fig. S64 Plots of $\ln([L\text{-LA}]_0/[L\text{-LA}]_t)$ *vs.* time. Red squares: batch 1 (k_{obs} = 0.57 ± 0.01 h^{-1}. R^2 = 0.999), Blue circles: batch 2 (k_{obs} = 0.54 ± 0.01 h^{-1}. R^2 = 0.998). Conditions: $[L\text{-LA}]_0$:$[\mathbf{3}]_0$:$[\text{BnOH}]_0$ = 400:1:1, $[L\text{-LA}]_0$ = 0.5 M, $[\mathbf{3}]_0$ = 0.00125 M, $[\text{BnOH}]_0$ = 0.00125 M, 5.0 mL toluene at 70 °C.

Table S10 ROP of *L*-LA using ^{Me_2}SB(^{iPr}N,I*)Sc(O-2,6-^{i}Pr-C_6H_3)(THF) (**4**) with $[L\text{-LA}]_0$:$[\mathbf{4}]_0$ = 600:1 at 70 °C.[a]

Time (h)	Conversion 1 (%)[b]	Time (h)	Conversion 2 (%)[b]
0.25	8	0.25	9
0.50	19	0.50	21
0.75	34	0.75	36
1.00	50	1.00	52
1.25	62	1.25	66
1.50	74	1.50	76
1.75	82	1.75	83
2.00	84	2.00	88
2.25	87		
k_{obs} = 1.04 ± 0.05 h^{-1}. R^2 = 0.981		k_{obs} = 1.18 ± 0.05 h^{-1}. R^2 = 0.985	
M_n = 55 380 g mol^{-1}		M_n = 49 150 g mol^{-1}	
M_w/M_n = 1.10		M_w/M_n = 1.16	

[a]Conditions: $[L\text{-LA}]_0$:$[\mathbf{4}]_0$ = 600:1, $[L\text{-LA}]_0$ = 0.5 M, 7 mL toluene at 70 °C. Aliquots were taken at given intervals. [b]Measured by ^{1}H NMR spectroscopic analyses.

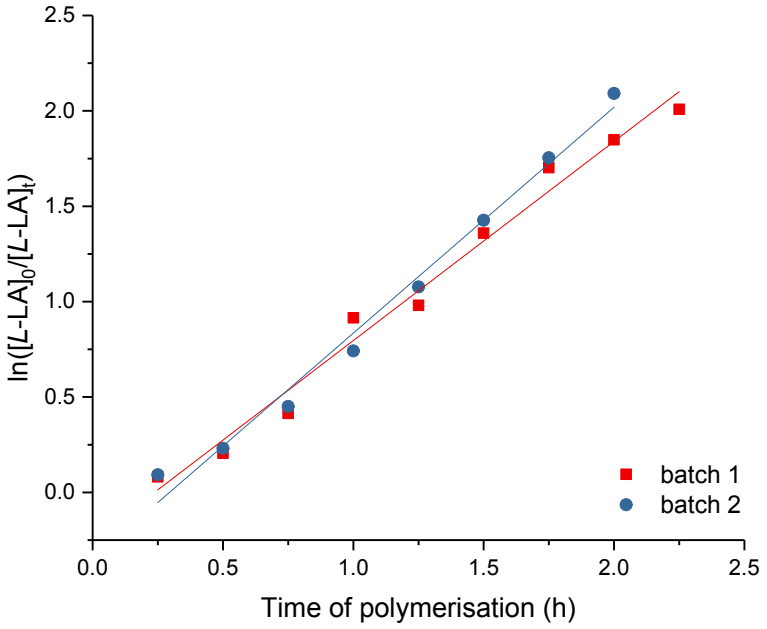

Fig. S65 Plots of $\ln([L\text{-LA}]_0/[L\text{-LA}]_t)$ *vs.* time. Red squares: batch 1 (k_{obs} = 1.04 ± 0.05 h^{-1}. R^2 = 0.981), Blue circles: batch 2 (k_{obs} = 1.18 ± 0.05 h^{-1}. R^2 = 0.985). Conditions: $[L\text{-LA}]_0$:$[\mathbf{4}]_0$ = 600:1, $[L\text{-LA}]_0$ = 0.5 M, $[\mathbf{4}]_0$ = 0.00083 M, 7.0 mL toluene at 70 °C.

Table S11 ROP of *L*-LA using ^{Me_2}SB(^{iPr}N,I*)Sc(O-2,6-^{i}Pr-C_6H_3)(THF) (**4**) with $[L\text{-LA}]_0$:$[\mathbf{4}]_0$ = 800:1 at 70 °C.[a]

Time (h)	Conversion 1 (%)[b]	Time (h)	Conversion 2 (%)[b]
0.25	5	0.25	6
0.50	11	0.50	10
0.75	19	0.75	17
1.00	28	1.00	27
1.25	40	1.25	38
1.50	51	1.50	49
1.75	60	1.75	60
2.00	67	2.00	68
2.25	74	2.25	75
2.50	79	2.50	78
2.75	83	2.75	83
3.00	86	3.00	87
k_{obs} = 0.81 ± 0.02 h^{-1}. R^2 = 0.996		k_{obs} = 0.83 ± 0.02 h^{-1}. R^2 = 0.994	
M_n = 69 700 g mol^{-1}		M_n = 71 640 g mol^{-1}	
M_w/M_n = 1.16		M_w/M_n = 1.18	

[a]Conditions: $[L\text{-LA}]_0$:$[\mathbf{4}]_0$ = 800:1, $[L\text{-LA}]_0$ = 0.5 M, 7 mL toluene at 70 °C. Aliquots were taken at given intervals.
[b]Measured by ^{1}H NMR spectroscopic analyses.

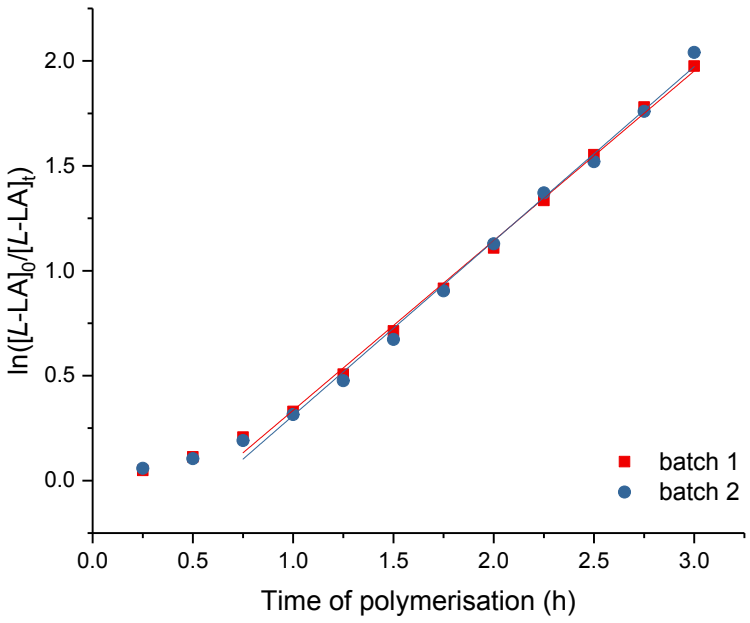

Fig. S66 Plots of $\ln([L\text{-LA}]_0/[L\text{-LA}]_t)$ *vs.* time. Red squares: batch 1 (k_{obs} = 0.81 ± 0.02 h^{-1}. R^2 = 0.996), Blue circles: batch 2 (k_{obs} = 0.83 ± 0.02 h^{-1}. R^2 = 0.994). Conditions: $[L\text{-LA}]_0$:$[\mathbf{4}]_0$ = 800:1, $[L\text{-LA}]_0$ = 0.5 M, $[\mathbf{4}]_0$ = 0.000625 M, 7.0 mL toluene at 70 °C.

Table S12 ROP of *L*-LA using ^{Me_2}SB(^{iPr}N,I*)Sc(O-2,6-^{i}Pr-C_6H_3)(THF) (**4**) with $[L\text{-LA}]_0$:$[\mathbf{4}]_0$ = 1000:1 at 70 °C.[a]

Time (h)	Conversion 1 (%)[b]	Time (h)	Conversion 2 (%)[b]
0.25	5	0.25	4
0.50	10	0.50	9
0.75	18	0.75	15
1.00	26	1.00	24
1.25	39	1.25	34
1.50	50	1.50	42
1.75	57	1.75	47
2.00	66	2.00	56
2.25	71	2.25	66
2.50	76	2.50	71
2.75	81	2.75	77
3.00	85	3.00	78
3.25	87	3.25	83
3.50	88	3.50	85
3.75	90		
4.00	91		
k_{obs} = 0.74 ± 0.01 h^{-1}. R^2 = 0.997		k_{obs} = 0.66 ± 0.02 h^{-1}. R^2 = 0.989	
M_n = 92 970 g mol^{-1}		M_n = 91 500 g mol^{-1}	
M_w/M_n = 1.15		M_w/M_n = 1.13	

[a]Conditions: $[L\text{-LA}]_0$:$[\mathbf{4}]_0$ = 1000:1, $[L\text{-LA}]_0$ = 0.5 M, 7 mL toluene at 70 °C. Aliquots were taken at given intervals.
[b]Measured by ^{1}H NMR spectroscopic analyses.

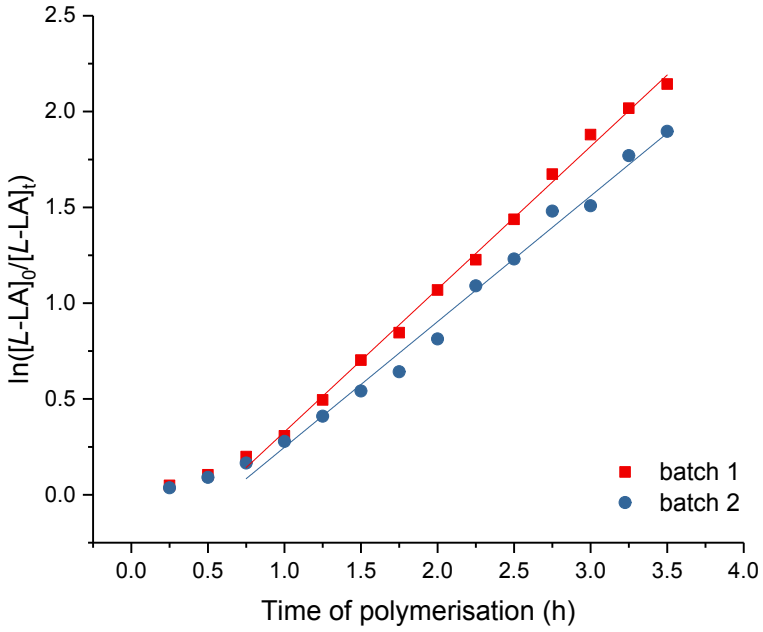

Fig. S67 Plots of $\ln([L\text{-LA}]_0/[L\text{-LA}]_t)$ *vs.* time. Red squares: batch 1 (k_{obs} = 0.74 ± 0.01 h^{-1}. R^2 = 0.997), Blue circles: batch 2 (k_{obs} = 0.66 ± 0.02 h^{-1}. R^2 = 0.989). Conditions: $[L\text{-LA}]_0$:$[\mathbf{4}]_0$ = 1000:1, $[L\text{-LA}]_0$ = 0.5 M, $[\mathbf{4}]_0$ = 0.0005 M, 7.0 mL toluene at 70 °C.

Table S13 ROP of *L*-LA using ^{Me_2}SB(^{iPr}N,I*)Sc(O-2,6-^{i}Pr-C_6H_3)(THF) (**4**) with $[L\text{-LA}]_0$:$[\mathbf{4}]_0$ = 1200:1 at 70 °C.[a]

Time (h)	Conversion 1 (%)[b]	Time (h)	Conversion 2 (%)[b]
0.5	7.	0.5	8
1.0	17	1.0	24
1.5	32	1.5	44
2.0	47	2.0	60
2.5	59	2.5	73
3.0	68	3.0	80
3.5	76	3.5	85
4.0	80	4.0	90
4.5	84	4.5	92
5.0	87	5.0	92
k_{obs} = 0.46 ± 0.01 h^{-1}. R^2 = 0.996		k_{obs} = 0.63 ± 0.01 h^{-1}. R^2 = 0.997	
M_n = 103 670 g mol^{-1}		M_n = 112 090 g mol^{-1}	
M_w/M_n = 1.14		M_w/M_n = 1.11	

[a]Conditions: $[L\text{-LA}]_0$:$[\mathbf{4}]_0$ = 1200:1, $[L\text{-LA}]_0$ = 0.5 M, 7 mL toluene at 70 °C. Aliquots were taken at given intervals.
[b]Measured by ^{1}H NMR spectroscopic analyses.

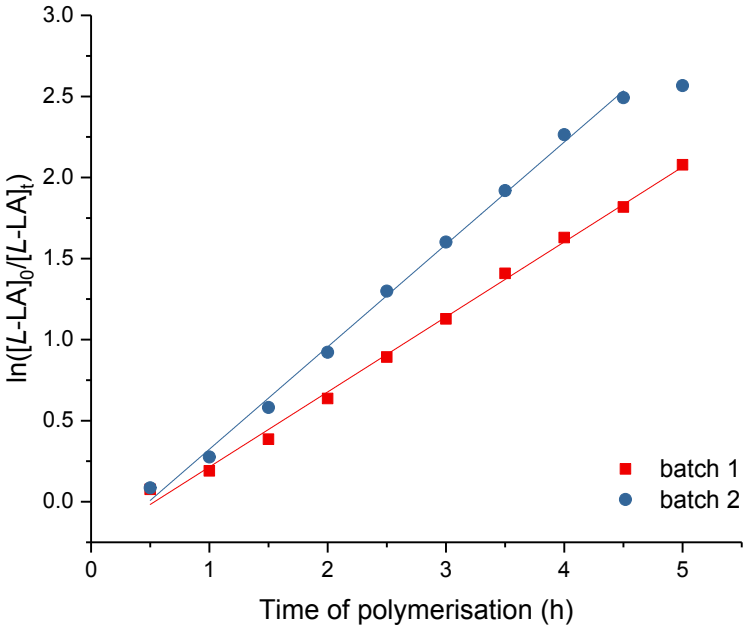

Fig. S68 Plots of $\ln([L\text{-LA}]_0/[L\text{-LA}]_t)$ *vs.* time. Red squares: batch 1 (k_{obs} = 0.46 ± 0.01 h^{-1}. R^2 = 0.996), Blue circles: batch 2 (k_{obs} = 0.63 ± 0.01 h^{-1}. R^2 = 0.997). Conditions: $[L\text{-LA}]_0$:$[\mathbf{4}]_0$ = 1200:1, $[L\text{-LA}]_0$ = 0.5 M, $[\mathbf{4}]_0$ = 0.000417 M, 7.0 mL toluene at 70 °C.

Table S14 ROP of *L*-LA using ^{Me_2}SB(^{iPr}N,I*)Sc(O-2,6-^{i}Pr-C_6H_3)(THF) (**4**) with various ratios of $[L\text{-LA}]_0$:$[\mathbf{4}]_0$.[a]

$[L\text{-LA}]_0$:$[\mathbf{4}]_0$	Time (h)	Conv. (%)[b]	k_{obs} (h^{-1})[c]	R^{2c}	M_n (GPC)[d]	M_n (calcd)[e]	M_w/M_n
1200	5.0	87	0.46 ± 0.01	0.996	103 670	151 480	1.14
	5.0	92	0.63 ± 0.01	0.997	112 090	159 851	1.11
1000	4.0	91	0.74 ± 0.01	0.997	92 970	131 252	1.15
	3.5	85	0.66 ± 0.02	0.989	91 500	122 674	1.13
800	3.0	86	0.81 ± 0.02	0.996	69 700	99 490	1.16
	3.0	87	0.83 ± 0.02	0.994	71 640	100 493	1.18
600	2.25	87	1.04 ± 0.05	0.981	55 380	75 051	1.10
	2.0	88	1.18 ± 0.06	0.985	49 150	75 976	1.16

[a]Conditions: $[L\text{-LA}]_0$:$[\mathbf{4}]_0$ as stated, $[L\text{-LA}]_0$ = 0.5 M, 7.0 mL toluene at 70 °C. Polymerisations were quenched by THF. [b]Measured by ^{1}H NMR spectroscopic analyses. [c]First order rate constant (k_{obs}) with standard error and R^2 were obtained from plots of $\ln([L\text{-LA}]_0/[L\text{-LA}]_t)$ *vs.* time. [d]Determined by GPC in THF against PS standards using the appropriate Mark-Houwink corrections.[7] [e]Calculated M_n for PLA synthesised with **4** = conv. (%) × $[L\text{-LA}]_0$:$[\mathbf{4}]_0$ × 144.1 + 178.1.

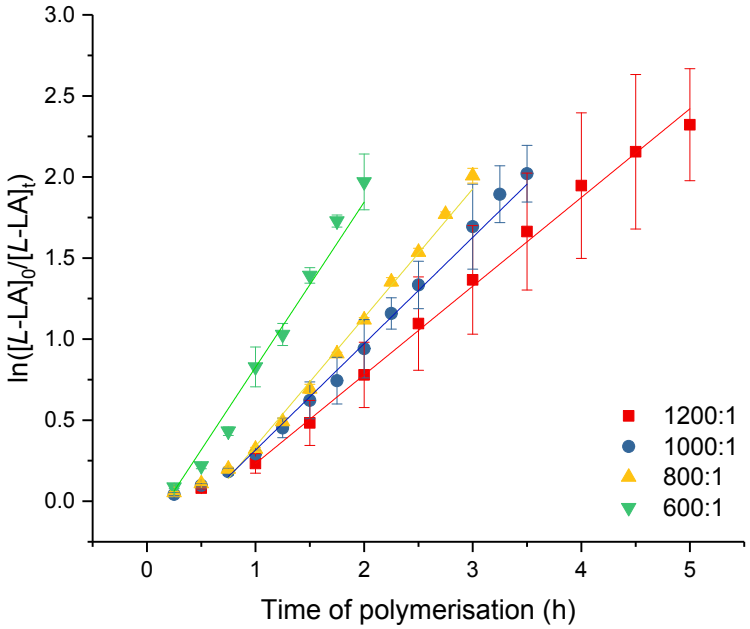

Fig. S69 Plots of $\ln([L\text{-LA}]_0/[L\text{-LA}]_t)$ *vs.* time. Red squares: 1200:1 (k_{obs} = 0.55 ± 0.01 h^{-1}. R^2 = 0.998), Blue circles: 1000:1 (k_{obs} = 0.66 ± 0.02 h^{-1}. R^2 = 0.989), Yellow triangles: 800:1 (k_{obs} = 0.79 ± 0.02 h^{-1}. R^2 = 0.995), Green triangles: 600:1 (k_{obs} = 1.02 ± 0.07 h^{-1}. R^2 = 0.966). Conditions: $[L\text{-LA}]_0$:$[\mathbf{4}]_0$ as stated, $[L\text{-LA}]_0$ = 0.5 M, 7.0 mL toluene at 70 °C. Values of $\ln([L\text{-LA}]_0/[L\text{-LA}]_t)$ with standard error were determined from duplicate experiments.

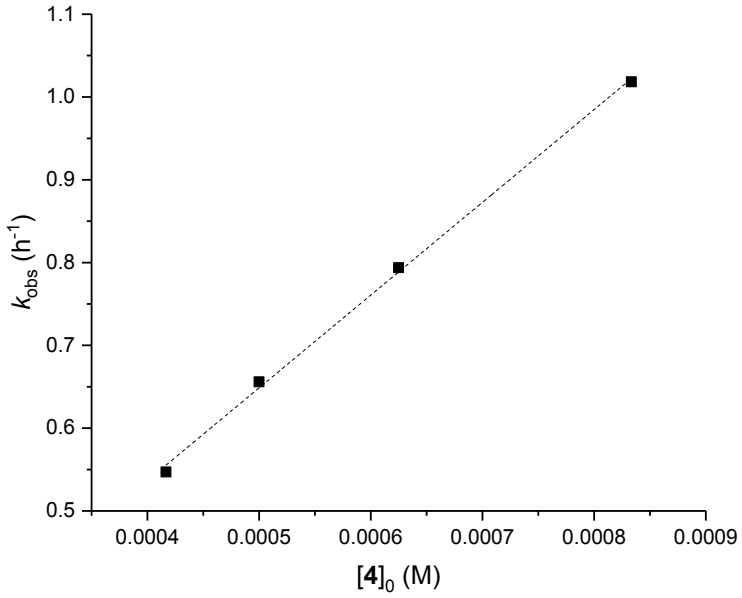

Fig. S70 Plot of k_{obs} *vs.* $[\mathbf{4}]_0$ for ROP of *L*-LA using **4**, k_p = 1120 ± 29 M^{-1} h^{-1}. R^2 = 0.998.

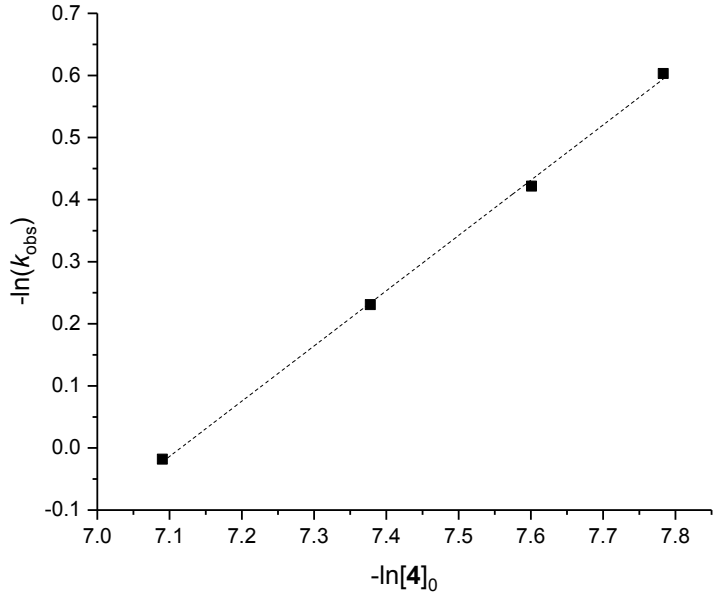

Fig. S71 Plot of $-\ln(k_{obs})$ *vs.* $-\ln([\mathbf{4}]_0)$ for ROP of *L*-LA using **4** shows that the order of reaction with respect to $[\mathbf{4}]_0$ equal to 0.89 ± 0.02. R^2 = 0.999.

Table S15 ROP of *L*-LA using ^{Me_2}SB($^{i\text{Pr}}$N,I*)Sc(O-2,6-^{i}Pr-C_6H_3)(THF) (**4**) with $[L\text{-LA}]_0$:$[\mathbf{4}]_0$ = 1000:1 at 60 °C.[a]

Time (h)	Conversion 1 (%)[b]	Time (h)	Conversion 2 (%)[b]
0.5	6	0.5	5
1.0	12	1.0	11
1.5	21	1.5	18
2.0	32	2.0	28
2.5	42	2.5	38
3.0	50	3.0	47
3.5	60	3.5	55
4.0	70	4.0	65
4.5	75	4.5	71
5.0	79	5.0	75
5.5	82	5.5	78
6.0	87	6.0	82
6.5	88	6.5	84
7.0	88	7.0	85
7.5	90	7.5	89
8.0	91	8.0	91
k_{obs} = 0.36 ± 0.01 h^{-1}. R^2 = 0.986		k_{obs} = 0.34 ± 0.01 h^{-1}. R^2 = 0.995 M_n = 105 980 g mol^{-1} M_w/M_n = 1.09	

[a]Conditions: $[L\text{-LA}]_0$:$[\mathbf{4}]_0$ = 1000:1, $[L\text{-LA}]_0$ = 0.5 M, 7 mL toluene at 60 °C. Aliquots were taken at given intervals.
[b]Measured by ^{1}H NMR spectroscopic analyses.

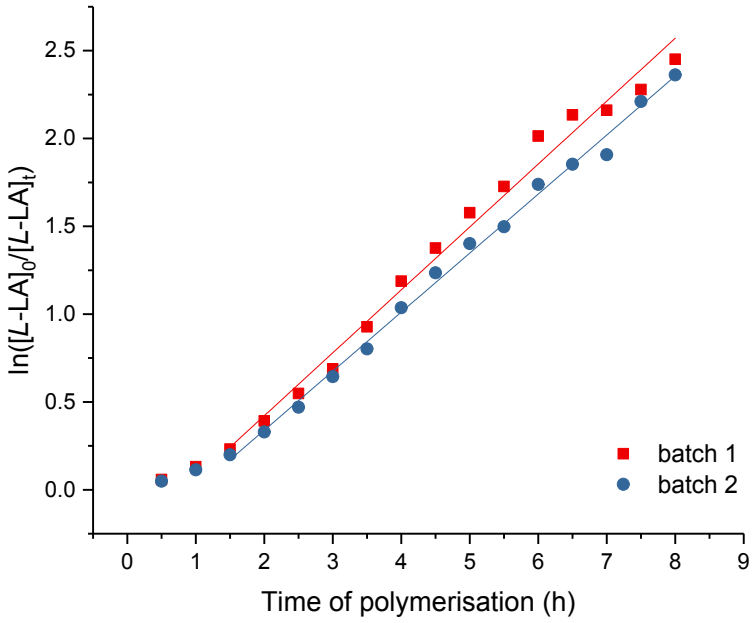

Fig. S72 Plots of $\ln([L\text{-LA}]_0/[L\text{-LA}]_t)$ *vs.* time. Red squares: batch 1 (k_{obs} = 0.36 ± 0.01 h^{-1}. R^2 = 0.986), Blue circles: batch 2 (k_{obs} = 0.34 ± 0.01 h^{-1}. R^2 = 0.995). Conditions: $[L\text{-LA}]_0$:$[\mathbf{4}]_0$ = 1000:1, $[L\text{-LA}]_0$ = 0.5 M, $[\mathbf{4}]_0$ = 0.0005 M, 7.0 mL toluene at 60 °C.

Table S16 ROP of *L*-LA using ^{Me_2}SB(^{iPr}N,I*)Sc(O-2,6-^{i}Pr-C_6H_3)(THF) (**4**) with $[L\text{-LA}]_0$:$[\mathbf{4}]_0$ = 1000:1 at 80 °C.[a]

Time (h)	Conversion 1 (%)[b]	Time (h)	Conversion 2 (%)[b]
0.25	8	0.25	9
0.50	24	0.50	25
0.75	44	0.75	44
1.00	61	1.00	61
1.25	73	1.25	73
1.50	81	1.50	82
1.75	86	1.75	86
2.00	89	2.00	89
2.25	90	2.25	91
2.50	92	2.50	92
k_{obs} = 1.28 ± 0.04 h^{-1}. R^2 = 0.994 M_n = 81 230 g mol^{-1} M_w/M_n = 1.17		k_{obs} = 1.35 ± 0.04 h^{-1}. R^2 = 0.996 M_n = 85 090 g mol^{-1} M_w/M_n = 1.18	

[a]Conditions: $[L\text{-LA}]_0$:$[\mathbf{4}]_0$ = 1000:1, $[L\text{-LA}]_0$ = 0.5 M, 7 mL toluene at 80 °C. Aliquots were taken at given intervals.
[b]Measured by ^{1}H NMR spectroscopic analyses.

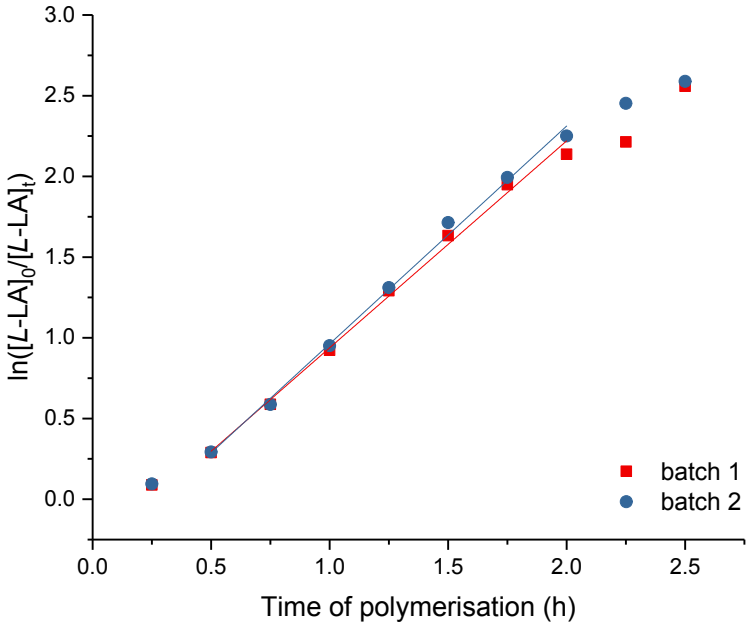

Fig. S73 Plots of $\ln([L\text{-LA}]_0/[L\text{-LA}]_t)$ *vs.* time. Red squares: batch 1 (k_{obs} = 1.28 ± 0.04 h^{-1}. R^2 = 0.994), Blue circles: batch 2 (k_{obs} = 1.35 ± 0.04 h^{-1}. R^2 = 0.996). Conditions: $[L\text{-LA}]_0$:$[\mathbf{4}]_0$ = 1000:1, $[L\text{-LA}]_0$ = 0.5 M, $[\mathbf{4}]_0$ = 0.0005 M, 7.0 mL toluene at 80 °C.

Table S17 ROP of *L*-LA using ^{Me_2}SB(^{iPr}N,I*)Sc(O-2,6-^{i}Pr-C_6H_3)(THF) (**4**) with $[L\text{-LA}]_0$:$[\mathbf{4}]_0$ = 1000:1 at 100 °C.[a]

Time (h)	Conversion 1 (%)[b]	Time (h)	Conversion 2 (%)[b]
0.083	5	0.083	4
0.167	19	0.167	15
0.250	37	0.250	29
0.333	53	0.333	45
0.417	64	0.417	55
0.500	74	0.500	69
0.583	78	0.583	73
0.667	85	0.667	81
0.750	87	0.750	83
0.833	87	0.833	85
0.917	89	0.917	86
1.000	90	1.000	88
1.083	91	1.083	88
1.167	91	1.167	86
1.250	90	1.250	90
k_{obs} = 2.91 ± 0.14 h^{-1}. R^2 = 0.980		k_{obs} = 2.68 ± 0.09 h^{-1}. R^2 = 0.989	
M_n = 70 300 g mol^{-1}		M_n = 75 280 g mol^{-1}	
M_w/M_n = 1.25		M_w/M_n = 1.19	

[a]Conditions: $[L\text{-LA}]_0$:$[\mathbf{4}]_0$ = 1000:1, $[L\text{-LA}]_0$ = 0.5 M, 7 mL toluene at 100 °C. Aliquots were taken at given intervals.
[b]Measured by ^{1}H NMR spectroscopic analyses.

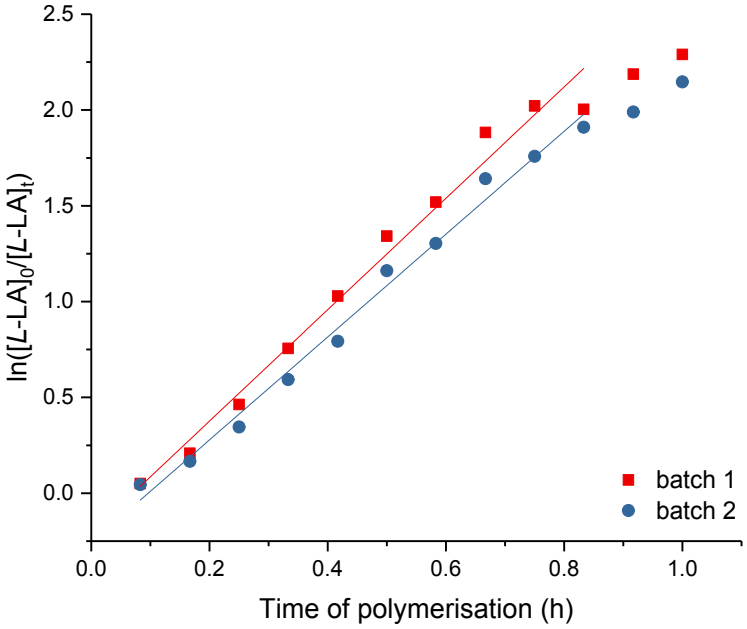

Fig. S74 Plots of $\ln([L\text{-LA}]_0/[L\text{-LA}]_t)$ *vs.* time. Red squares: batch 1 (k_{obs} = 2.91 ± 0.14 h^{-1}. R^2 = 0.980), Blue circles: batch 2 (k_{obs} = 2.68 ± 0.09 h^{-1}. R^2 = 0.989). Conditions: $[L\text{-LA}]_0$:$[\mathbf{4}]_0$ = 1000:1, $[L\text{-LA}]_0$ = 0.5 M, $[\mathbf{4}]_0$ = 0.0005 M, 7.0 mL toluene at 100 °C.

Table S18 ROP of *L*-LA using ^{Me_2}SB(^{iPr}N,I*)Sc(O-2,6-^{i}Pr-C_6H_3)(THF) (**4**) with various temperatures.[a]

T (°C)	Time (h)	Conv. (%)[b]	k_{obs} (h^{-1})[c]	R^{2c}	M_n (GPC)[d]	M_n (calcd)[e]	M_w/M_n
60	8.0	91	0.36 ± 0.01	0.986	N/A	131 857	N/A
60	8.0	91	0.34 ± 0.01	0.995	105 980	130 704	1.09
70	4.0	91	0.74 ± 0.01	0.997	92 970	131 252	1.15
70	3.5	85	0.66 ± 0.02	0.989	91 500	122 649	1.13
80	2.5	92	1.28 ± 0.04	0.994	81 230	133 284	1.17
80	2.5	92	1.35 ± 0.04	0.996	85 090	133 456	1.18
100	1.25	90	2.91 ± 0.14	0.980	70 300	130 113	1.25
100	1.25	90	2.68 ± 0.09	0.989	75 280	130 142	1.19

[a]Conditions: $[L\text{-LA}]_0$:$[\mathbf{4}]_0$ = 1000:1, $[L\text{-LA}]_0$ = 0.5 M, 7.0 mL toluene at stated temperature. Polymerisations were quenched by THF. [b]Measured by ^{1}H NMR spectroscopic analyses. [c]First order rate constant (k_{obs}) with standard error and R^2 were obtained from plots of $\ln([L\text{-LA}]_0/[L\text{-LA}]_t)$ *vs.* time. [d]Determined by GPC in THF against PS standards using the appropriate Mark-Houwink corrections.[7] [e]Calculated M_n for PLA synthesised with **4** = conv. (%) × $[L\text{-LA}]_0/[\mathbf{4}]_0$ × 144.1 + 178.1.

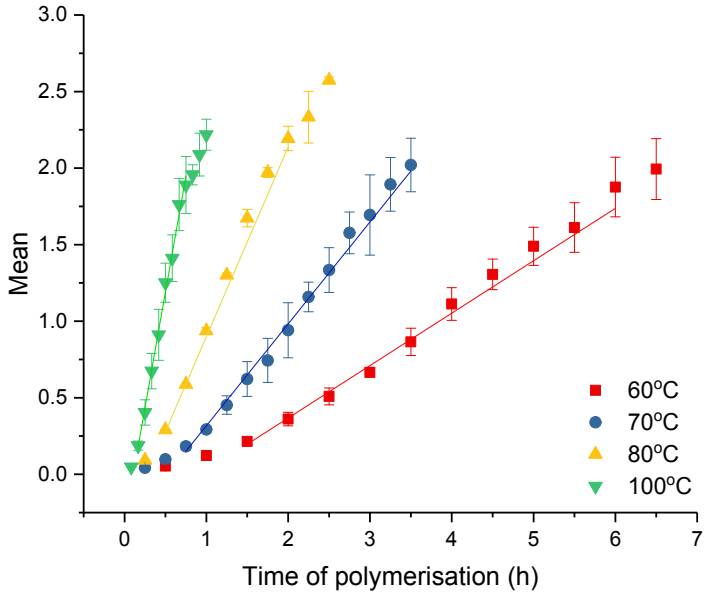

Fig. S75 Plots of $\ln([L\text{-LA}]_0/[L\text{-LA}]_t)$ *vs.* time. Red squares: 60 °C (k_{obs} = 0.34 ± 0.01 h^{-1}. R^2 = 0.988), Blue circles: 70 °C (k_{obs} = 0.67 ± 0.02 h^{-1}. R^2 = 0.989), Yellow triangles: 80 °C (k_{obs} = 1.24 ± 0.04 h^{-1}. R^2 = 0.994), Green triangles: 100 °C (k_{obs} = 3.03 ± 0.06 h^{-1}. R^2 = 0.997). Conditions: $[L\text{-LA}]_0$:$[\mathbf{4}]_0$= 1000:1, $[L\text{-LA}]_0$ = 0.5 M, 7.0 mL toluene at stated temperature. Values of $\ln([L\text{-LA}]_0/[L\text{-LA}]_t)$ with standard error were determined from duplicate experiments.

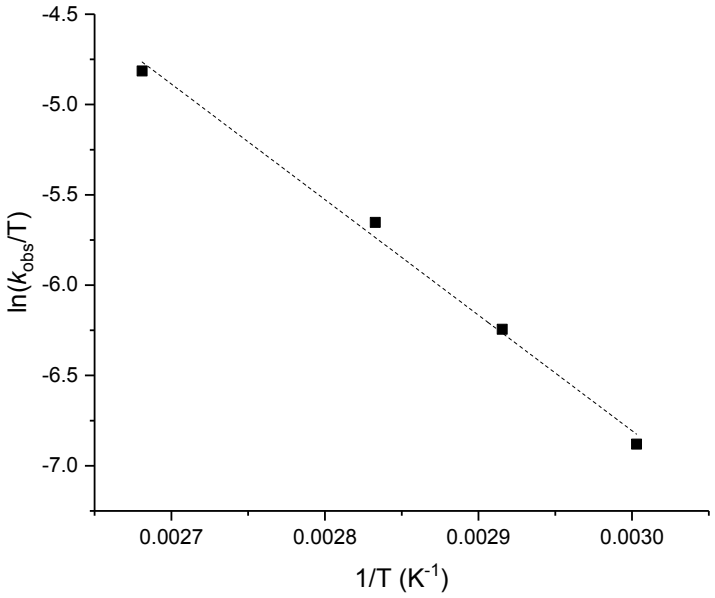

Fig. S76 Eyring plot of ln(k_{obs}/T) *vs.* 1/T. Slope = −6400 ± 339, Intercept = 12 ± 1. R^2 = 0.992. $\Delta H^{\ddagger}$ = 53 ± 3 kJ mol^{-1}, $\Delta S^{\ddagger}$ = −95 ± 8 J mol^{-1} K^{-1} and $\Delta G^{\ddagger}$ = 82 ± 20 kJ mol^{-1} for ROP of *L*-LA using ^{Me_2}SB(^{iPr}N,I*)Sc(O-2,6-^{i}Pr-C_6H_3)(THF) (**4**).

Table S19 ROP of *rac*-LA using ^{Me_2}SB(^{iPr}N,I*)Sc(O-2,6-^{i}Pr-C_6H_3)(THF) (**4**) with [*rac*-LA]$_0$:[**4**]$_0$ = 1000:1 at 70 °C.[a]

Time (h)	Conversion 1 (%)[b]	Time (h)	Conversion 2 (%)[b]
0.25	10	0.25	9
0.50	29	0.50	29
0.75	49	0.75	53
1.00	66	1.00	71
1.25	75	1.25	81
1.50	83	1.50	87
1.75	87	1.75	90
2.00	89	2.00	91
2.25	91	2.25	92
2.50	92	2.50	93
2.75	93		
3.00	95		
3.25	95		
k_{obs} = 1.27 ± 0.04 h^{-1}. R^2 = 0.992		k_{obs} = 1.44 ± 0.08 h^{-1}. R^2 = 0.981	
M_n = 83 100 g mol^{-1}		M_n = 70 280 g mol^{-1}	
M_w/M_n = 1.21		M_w/M_n = 1.21	
P_r (integration) = 0.77 ± 0.14		P_r (integration) = 0.73 ± 0.10	
P_r (deconvolution) = 0.63 ± 0.01		P_r (deconvolution) = 0.59 ± 0.02	

[a]Conditions: [*rac*-LA]$_0$:[**4**]$_0$ = 1000:1, [*rac*-LA]$_0$ = 0.5 M, 7 mL toluene at 70 °C. Aliquots were taken at given intervals. [b]Measured by ^{1}H NMR spectroscopic analyses.

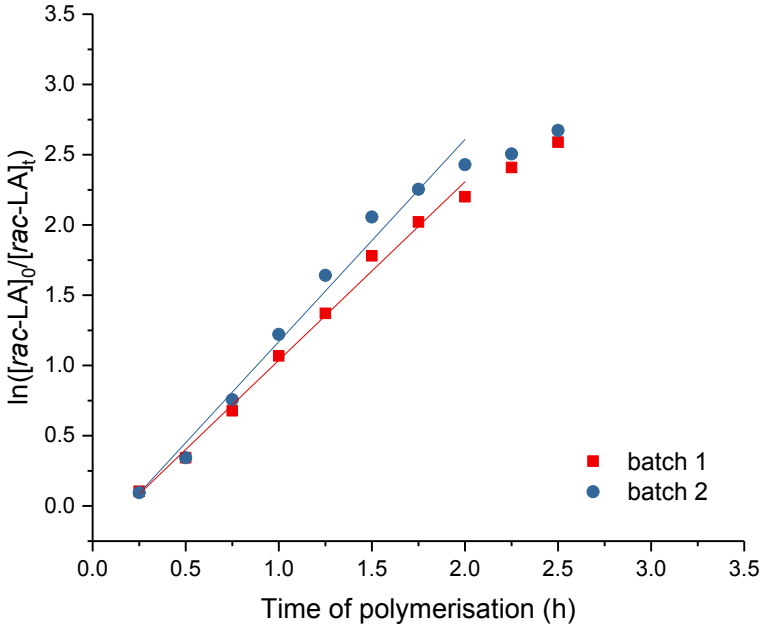

Fig. S77 Plots of ln([*rac*-LA]$_0$/[*rac*-LA]$_t$) *vs.* time. Red squares: batch 1 (k_{obs} = 1.27 ± 0.04 h^{-1}. R^2 = 0.992), Blue circles: batch 2 (k_{obs} = 1.44 ± 0.08 h^{-1}. R^2 = 0.981). Conditions: [*rac*-LA]$_0$:[**4**]$_0$ = 1000:1, [*rac*-LA]$_0$ = 0.5 M, [**4**]$_0$ = 0.0005 M, 7.0 mL toluene at 70 °C.

Table S20 ROP of *L*-LA using ^{Me_2}SB(^{iPr}N,I*)Sc(O-2,4-^{t}Bu-C_6H_3)(THF) (**5**) with $[L\text{-LA}]_0$:$[\mathbf{5}]_0$ = 1000:1 at 70 °C.[a]

Time (h)	Conversion 1 (%)[b]	Time (h)	Conversion 2 (%)[b]
0.083	14	0.083	15
0.167	55	0.167	54
0.250	74	0.250	76
0.333	85	0.333	84
0.417	89	0.417	90
0.500	91	0.500	92
k_{obs} = 6.32 ± 0.37 h^{-1}. R^2 = 0.987		k_{obs} = 6.30 ± 0.42 h^{-1}. R^2 = 0.982	
M_n = 77 560 g mol^{-1}		M_n = 72 180 g mol^{-1}	
M_w/M_n = 1.18		M_w/M_n = 1.23	

[a]Conditions: $[L\text{-LA}]_0$:$[\mathbf{5}]_0$ = 1000:1, $[L\text{-LA}]_0$ = 0.5 M, 7 mL toluene at 70 °C. Aliquots were taken at given intervals.
[b]Measured by ^{1}H NMR spectroscopic analyses.

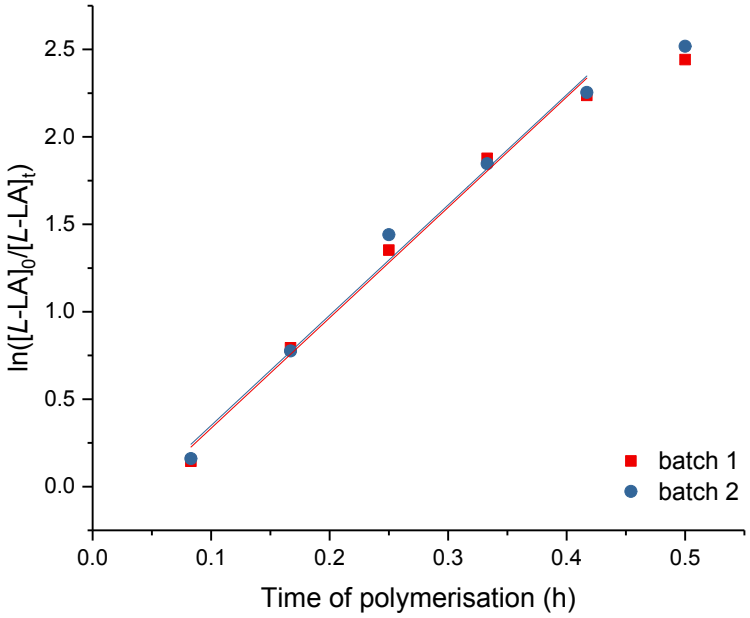

Fig. S78 Plots of $\ln([L\text{-LA}]_0/[L\text{-LA}]_t)$ *vs.* time. Red squares: batch 1 (k_{obs} = 6.32 ± 0.37 h^{-1}. R^2 = 0.987), Blue circles: batch 2 (k_{obs} = 6.30 ± 0.42 h^{-1}. R^2 = 0.982). Conditions: $[L\text{-LA}]_0$:$[\mathbf{5}]_0$ = 1000:1, $[L\text{-LA}]_0$ = 0.5 M, $[\mathbf{5}]_0$ = 0.0005 M, 7.0 mL toluene at 70 °C.

Table S21 ROP of *rac*-LA using ^{Me_2}SB(^{iPr}N,I*)Sc(O-2,4-^{t}Bu-C_6H_3)(THF) (**5**) with $[rac\text{-LA}]_0$:$[\mathbf{5}]_0$ = 1000:1 at 70 °C.[a]

Time (h)	Conversion 1 (%)[b]	Time (h)	Conversion 2 (%)[b]
0.083	7	0.083	7
0.167	45	0.167	40
0.250	74	0.250	71
0.333	86	0.333	85
0.417	88	0.417	86
0.500	91	0.500	91
k_{obs} = 7.69 ± 0.37 h^{-1}. R^2 = 0.993 P_r (integration) = 0.74 ± 0.13 P_r (deconvolution) = 0.68 ± 0.06		k_{obs} = 7.40 ± 0.50 h^{-1}. R^2 = 0.986 M_n = 64 540 g mol^{-1} M_w/M_n = 1.23 P_r (integration) = 0.64 ± 0.04 P_r (deconvolution) = 0.68 ± 0.07	

[a]Conditions: $[rac\text{-LA}]_0$:$[\mathbf{5}]_0$ = 1000:1, $[rac\text{-LA}]_0$ = 0.5 M, 7 mL toluene at 70 °C. Aliquots were taken at given intervals. [b]Measured by ^{1}H NMR spectroscopic analyses.

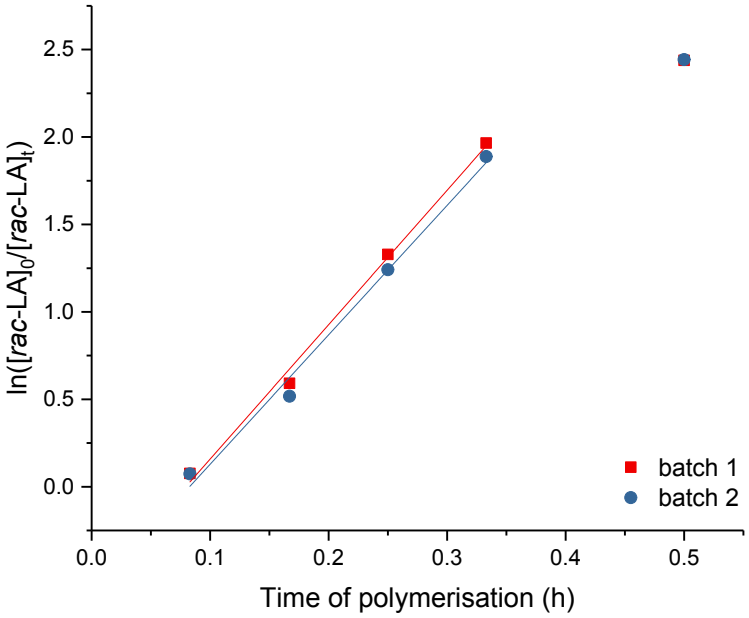

Fig. S79 Plots of $\ln([rac\text{-LA}]_0/[rac\text{-LA}]_t)$ *vs.* time. Red squares: batch 1 (k_{obs} = 7.69 ± 0.37 h^{-1}. R^2 = 0.993), Blue circles: batch 2 (k_{obs} = 7.40 ± 0.50 h^{-1}. R^2 = 0.986). Conditions: $[rac\text{-LA}]_0$:$[\mathbf{5}]_0$ = 1000:1, $[rac\text{-LA}]_0$ = 0.5 M, $[\mathbf{5}]_0$ = 0.0005 M, 7.0 mL toluene at 70 °C.

Table S22 ROP of *L*-LA using ^{Me_2}SB(^{iPr}N,I*)Sc(O-2,4-^{t}Bu-C_6H_3)(THF) (**5**) with $[L\text{-LA}]_0$:$[\mathbf{5}]_0$ = 1000:1 at 100 °C.[a]

Time (h)	Conversion 1 (%)[b]	Time (h)	Conversion 2 (%)[b]
0.05	22	0.05	20
0.10	62	0.10	63
0.15	80	0.15	79
0.20	85	0.20	84
0.25	88	0.25	87
0.30	89	0.30	88
0.35	89	0.35	89
0.40	91	0.40	89
k_{obs} = 11.12 ± 1.34 h^{-1}. R^2 = 0.957		k_{obs} = 10.84 ± 1.64 h^{-1}. R^2 = 0.934 M_n = 60 790 g mol^{-1} M_w/M_n = 1.21	

[a]Conditions: $[L\text{-LA}]_0$:$[\mathbf{5}]_0$ = 1000:1, $[L\text{-LA}]_0$ = 0.5 M, 7 mL toluene at 100 °C. Aliquots were taken at given intervals.
[b]Measured by ^{1}H NMR spectroscopic analyses.

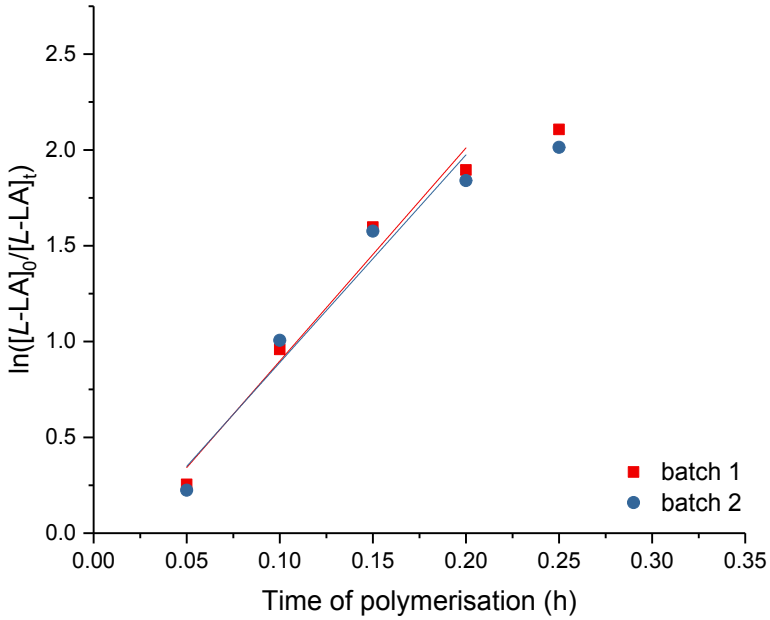

Fig. S80 Plots of $\ln([L\text{-LA}]_0/[L\text{-LA}]_t)$ *vs.* time. Red squares: batch 1 (k_{obs} = 11.12 ± 1.34 h^{-1}. R^2 = 0.957), Blue circles: batch 2 (k_{obs} = 10.84 ± 1.64 h^{-1}. R^2 = 0.934). Conditions: $[L\text{-LA}]_0$:$[\mathbf{5}]_0$ = 1000:1, $[L\text{-LA}]_0$ = 0.5 M, $[\mathbf{5}]_0$ = 0.0005 M, 7.0 mL toluene at 100 °C.

Table S23 ROP of *L*-LA using ^{Me_2}SB(^{Ph}N,I*)Sc(O-2,6-^{i}Pr-C_6H_3)(THF) (**7**) with $[L\text{-LA}]_0$:$[\mathbf{7}]_0$ = 1000:1 at 70 °C.[a]

Time (h)	Conversion 1 (%)[b]	Time (h)	Conversion 2 (%)[b]
0.25	9	0.25	8
0.50	13	0.50	13
0.75	21	0.75	20
1.00	28	1.00	27
1.25	36	1.25	34
1.50	43	1.50	42
1.75	49	1.75	49
2.00	55	2.00	55
2.25	62	2.25	61
2.50	67	2.50	65
2.75	70	2.75	70
3.00	71	3.00	73
3.25	75	3.25	77
3.5	80	3.5	80
		3.75	82
		4.00	84
k_{obs} = 0.47 ± 0.01 h^{-1}. R^2 = 0.993		k_{obs} = 0.48 ± 0.01 h^{-1}. R^2 = 0.992	

[a]Conditions: $[L\text{-LA}]_0$:$[\mathbf{7}]_0$ = 1000:1, $[L\text{-LA}]_0$ = 0.5 M, 7 mL toluene at 70 °C. Aliquots were taken at given intervals.
[b]Measured by ^{1}H NMR spectroscopic analyses.

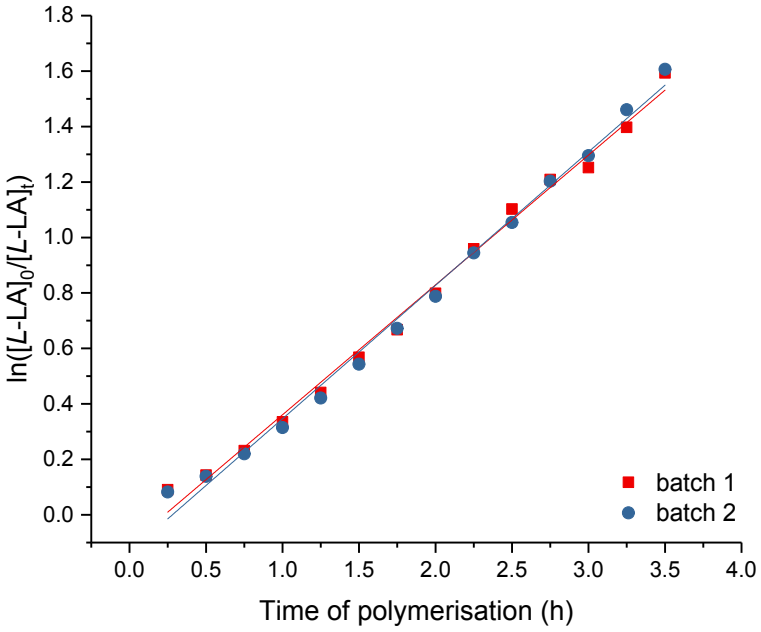

Fig. S81 Plots of $\ln([L\text{-LA}]_0/[L\text{-LA}]_t)$ *vs.* time. Red squares: batch 1 (k_{obs} = 0.47 ± 0.01 h^{-1}. R^2 = 0.993), Blue circles: batch 2 (k_{obs} = 0.48 ± 0.01 h^{-1}. R^2 = 0.992). Conditions: $[L\text{-LA}]_0$:$[\mathbf{7}]_0$ = 1000:1, $[L\text{-LA}]_0$ = 0.5 M, $[\mathbf{7}]_0$ = 0.0005 M, 7.0 mL toluene at 70 °C.

Table S24 ROP of *rac*-LA using ^{Me_2}SB(^{Ph}N,I*)Sc(O-2,6-^{i}Pr-C_6H_3)(THF) (**7**) with $[rac\text{-LA}]_0$:$[\mathbf{7}]_0$ = 1000:1 at 70 °C.[a]

Time (h)	Conversion 1 (%)[b]	Time (h)	Conversion 2 (%)[b]
0.25	14	0.25	16
0.50	22	0.50	25
0.75	30	0.75	35
1.00	40	1.00	44
1.25	46	1.25	53
1.50	56	1.50	59
1.75	62	1.75	64
2.00	68	2.00	66
2.25	67	2.25	75
2.50	76	2.50	78
2.75	79	2.75	81
3.00	82	3.00	82
3.25	84	3.25	85
3.5	85	3.5	86
k_{obs} = 0.57 ± 0.01 h^{-1}. R^2 = 0.992 P_r (integration) = 0.75 ± 0.12 P_r (deconvolution) = 0.66 ± 0.02		k_{obs} = 0.58 ± 0.01 h^{-1}. R^2 = 0.992 M_n = 64 820 g mol^{-1} M_w/M_n = 1.17 P_r (integration) = 0.76 ± 0.13 P_r (deconvolution) = 0.63 ± 0.03	

[a]Conditions: $[rac\text{-LA}]_0$:$[\mathbf{7}]_0$ = 1000:1, $[rac\text{-LA}]_0$ = 0.5 M, 7 mL toluene at 70 °C. Aliquots were taken at given intervals. [b]Measured by ^{1}H NMR spectroscopic analyses.

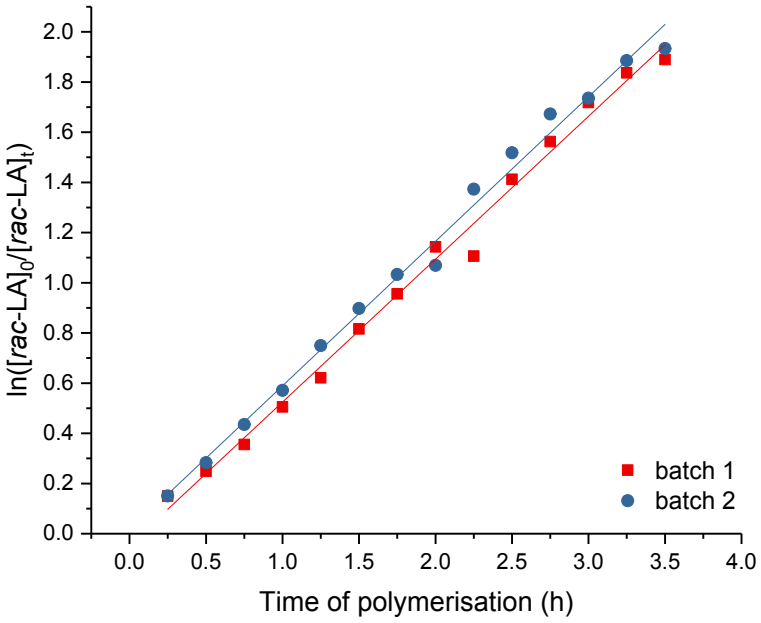

Fig. S82 Plots of $\ln([rac\text{-LA}]_0/[rac\text{-LA}]_t)$ *vs.* time. Red squares: batch 1 (k_{obs} = 0.57 ± 0.01 h^{-1}. R^2 = 0.992), Blue circles: batch 2 (k_{obs} = 0.58 ± 0.01 h^{-1}. R^2 = 0.992). Conditions: $[rac\text{-LA}]_0$:$[\mathbf{7}]_0$ = 1000:1, $[rac\text{-LA}]_0$ = 0.5 M, $[\mathbf{7}]_0$ = 0.0005 M, 7.0 mL toluene at 70 °C.

Table S25 ROP of *L*-LA using ^{Me_2}SB(^{Ph}N,I*)Sc(O-2,6-^{i}Pr-C_6H_3)(THF) (**7**) with $[L\text{-LA}]_0$:$[\mathbf{7}]_0$ = 1000:1 at 100 °C.[a]

Time (h)	Conversion 1 (%)[b]	Time (h)	Conversion 2 (%)[b]
0.167	16	0.167	16
0.333	30	0.333	32
0.500	45	0.500	44
0.667	55	0.667	55
0.830	61	0.830	64
1.000	70	1.000	71
1.167	74	1.167	69
1.333	79	1.333	75
1.500	81	1.500	76
1.667	84	1.667	82
1.833	83	1.833	84
2.000	86	2.000	86
k_{obs} = 1.10 ± 0.03 h^{-1}. R^2 = 0.994		k_{obs} = 0.98 ± 0.06 h^{-1}. R^2 = 0.970	

[a]Conditions: $[L\text{-LA}]_0$:$[\mathbf{7}]_0$ = 1000:1, $[L\text{-LA}]_0$ = 0.5 M, 7 mL toluene at 100 °C. Aliquots were taken at given intervals.
[b]Measured by ^{1}H NMR spectroscopic analyses.

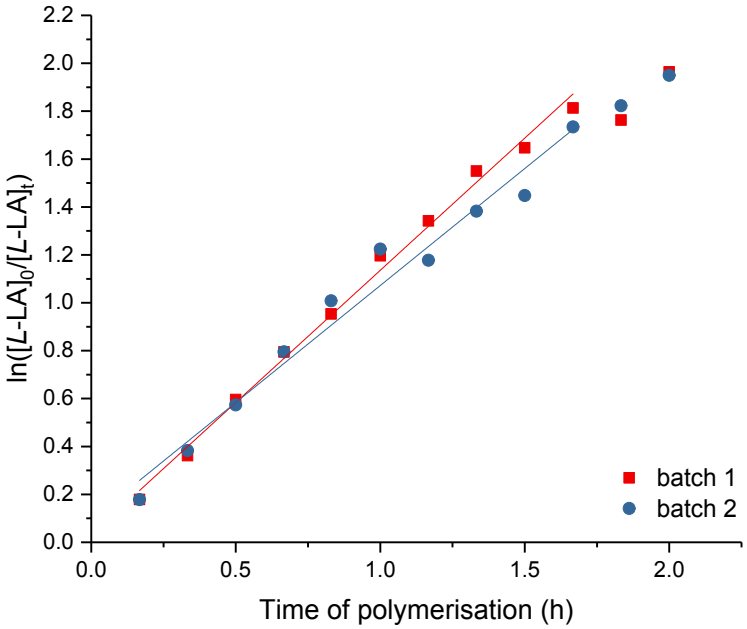

Fig. S83 Plots of $\ln([L\text{-LA}]_0/[L\text{-LA}]_t)$ *vs.* time. Red squares: batch 1 (k_{obs} = 1.10 ± 0.03 h^{-1}. R^2 = 0.994), Blue circles: batch 2 (k_{obs} = 0.98 ± 0.06 h^{-1}. R^2 = 0.970). Conditions: $[L\text{-LA}]_0$:$[\mathbf{7}]_0$ = 1000:1, $[L\text{-LA}]_0$ = 0.5 M, $[\mathbf{7}]_0$ = 0.0005 M, 7.0 mL toluene at 100 °C.

Table S26 ROP of *L*-LA using ^{Me_2}SB(^{tBu}N,I*)Al(Cl)(THF) (**8**) and benzyl alcohol with $[L\text{-LA}]_0$:$[\mathbf{8}]_0$:$[\text{BnOH}]_0$ = 100:1:1 at 100 °C.[a]

Time (h)	Conversion 1 (%)[b]	Time (h)	Conversion 2 (%)[b]
1	12	1	12
2	21	2	19
3	26	3	28
4	36	4	35
5	43	5	42
6.5	51	6.5	53
7.5	55	7.5	56
23	80	23	77
k_{obs} = 0.11 ± 0.01 h^{-1}. R^2 = 0.994 M_n = 17 600 g mol^{-1} M_w/M_n = 1.37		k_{obs} = 0.11 ± 0.01 h^{-1}. R^2 = 0.994 M_n = 16 250 g mol^{-1} M_w/M_n = 1.47	

[a]Conditions: $[L\text{-LA}]_0$:$[\mathbf{8}]_0$:$[\text{BnOH}]_0$ = 100:1:1, $[L\text{-LA}]_0$ = 0.5 M, $[\mathbf{8}]_0$ = 0.05 M, 4.0 mL toluene at 100 °C. Aliquots were taken at given intervals. [b]Measured by ^{1}H NMR spectroscopic analyses.

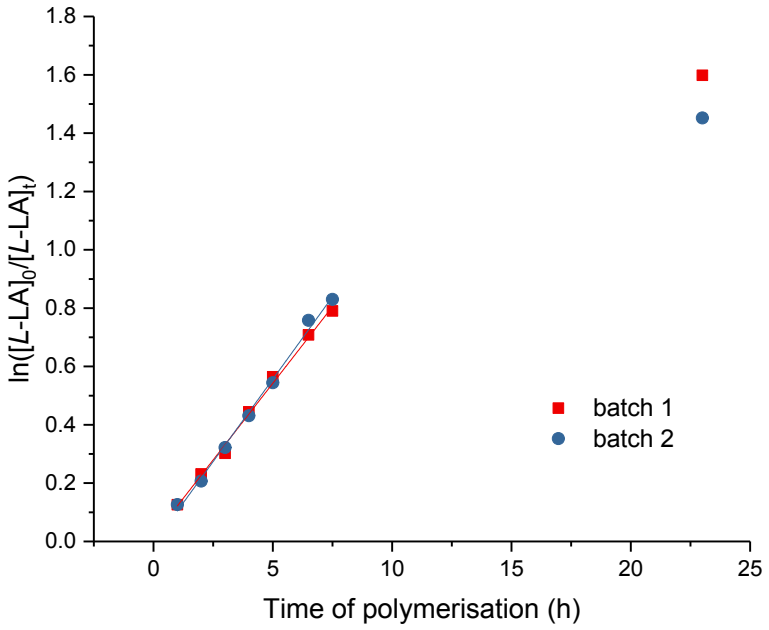

Fig. S84 Plots of $\ln([L\text{-LA}]_0/[L\text{-LA}]_t)$ *vs.* time. Red squares: batch 1 (k_{obs} = 0.11 ± 0.01. h^{-1}. R^2 = 0.994), Blue circles: batch 2 (k_{obs} = 0.11 ± 0.01 h^{-1}. R^2 = 0.994). Conditions: $[L\text{-LA}]_0$:$[\mathbf{8}]_0$:$[\text{BnOH}]_0$ = 100:1:1, $[L\text{-LA}]_0$ = 0.5 M, $[\mathbf{8}]_0$ = 0.05 M, 4.0 mL toluene at 100 °C.

Table S27 ROP of *L*-LA using ^{Me_2}SB(^{tBu}N,I*)Al(O-2,6-Me-C_6H_3)(THF) (**9**) with [*L*-LA]$_0$:[**9**]$_0$ = 100:1 at 100 °C.[a]

Time (h)	Conversion 1 (%)[b]	Time (h)	Conversion 2 (%)[b]
1	11	1	9
2	24	2	22
3	43	3	39
4	54	4	53
5	64	5	64
6	72	6	74
7	78	7	77
8	82	8	82
9	85	9	86
k_{obs} = 0.23 ± 0.01 h^{-1}. R^2 = 0.998		k_{obs} = 0.24 ± 0.01 h^{-1}. R^2 = 0.995	
M_n = 12 310 g mol^{-1}		M_n = 12 420 g mol^{-1}	
M_w/M_n = 1.33		M_w/M_n = 1.35	

[a]Conditions: [*L*-LA]$_0$:[**9**]$_0$ = 100:1, [*L*-LA]$_0$ = 0.5 M, [**9**]$_0$ = 0.05 M, 4.0 mL toluene at 100 °C. Aliquots were taken at given intervals. [b]Measured by ^{1}H NMR spectroscopic analyses.

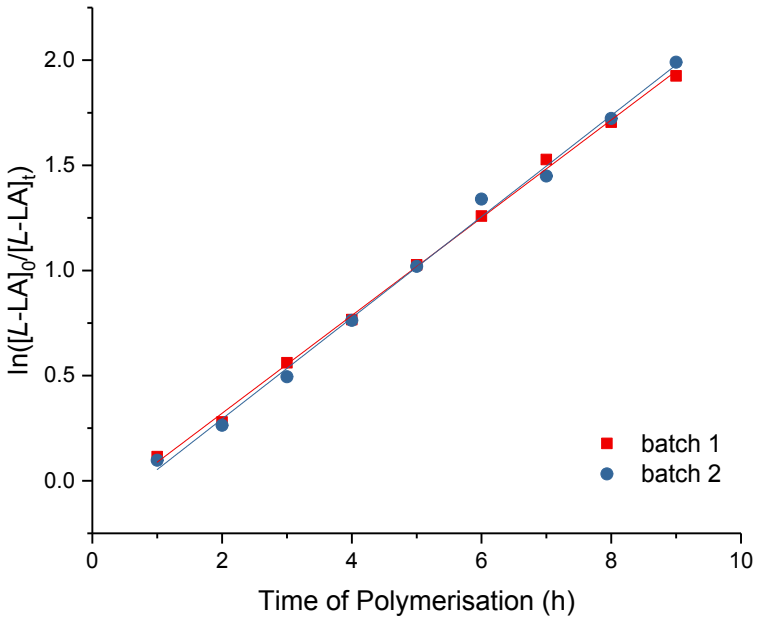

Fig. S85 Plots of ln([*L*-LA]$_0$/[*L*-LA]$_t$) *vs.* time. Red squares: batch 1 (k_{obs} = 0.23 ± 0.01 h^{-1}. R^2 = 0.998), Blue circles: batch 2 (k_{obs} = 0.24 ± 0.01 h^{-1}. R^2 = 0.995). Conditions: [*L*-LA]$_0$:[**9**]$_0$ = 100:1, [*L*-LA]$_0$ = 0.5 M, [**9**]$_0$ = 0.05 M, 4.0 mL toluene at 100 °C.

Table S28 ROP of *L*-LA using ^{Me_2}SB(^{tBu}N,I*)Al(O-2,6-Me-C_6H_3)(THF) (**9**) with [*L*-LA]$_0$:[**9**]$_0$ = 100:1 at 90 °C.[a]

Time (h)	Conversion 1 (%)[b]	Time (h)	Conversion 2 (%)[b]
2	9	2	10
4	25	4	28
6	41	6	45
8	56	8	59
10	67	10	68
23	90	23	91
k_{obs} = 0.11 ± 0.01 h^{-1}. R^2 = 0.988		k_{obs} = 0.11 ± 0.01 h^{-1}. R^2 = 0.988	
M_n = 15 320 g mol^{-1}		M_n = 14 520 g mol^{-1}	
M_w/M_n = 1.45		M_w/M_n = 1.37	

[a]Conditions: [*L*-LA]$_0$:[**9**]$_0$ = 100:1, [*L*-LA]$_0$ = 0.5 M, [**9**]$_0$ = 0.05 M, 4.0 mL toluene at 90 °C. Aliquots were taken at given intervals. [b]Measured by ^{1}H NMR spectroscopic analyses.

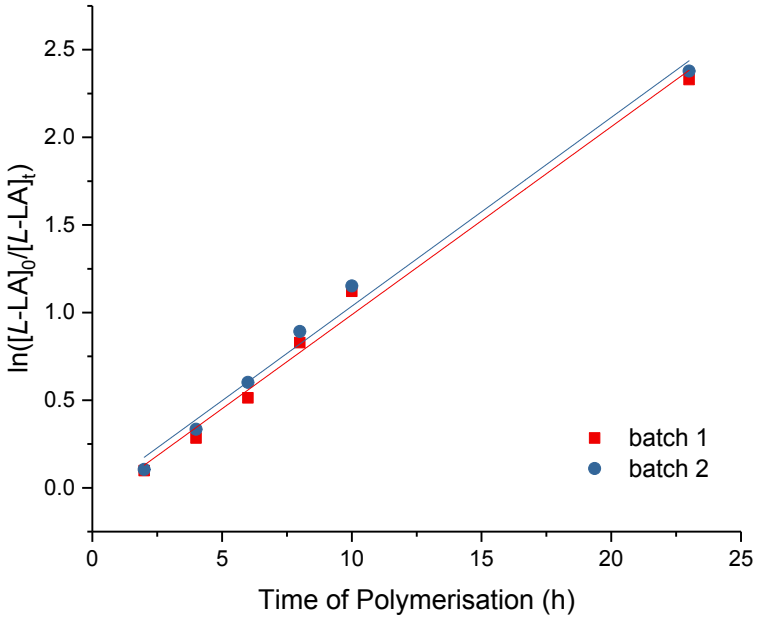

Fig. S86 Plots of ln([*L*-LA]$_0$/[*L*-LA]$_t$) *vs.* time. Red squares: batch 1 (k_{obs} = 0.11 ± 0.01 h^{-1}. R^2 = 0.990), Blue circles: batch 2 (k_{obs} = 0.11 ± 0.01 h^{-1}. R^2 = 0.990). Conditions: [*L*-LA]$_0$:[**9**]$_0$ = 100:1, [*L*-LA]$_0$ = 0.5 M, [**9**]$_0$ = 0.05 M, 4.0 mL toluene at 90 °C.

Table S29 ROP of *L*-LA using ^{Me_2}SB(^{tBu}N,I*)Al(O-2,6-Me-C_6H_3)(THF) (**9**) with [*L*-LA]$_0$:[**9**]$_0$ = 100:1 at 80 °C.[a]

Time (h)	Conversion 1 (%)[b]	Time (h)	Conversion 2 (%)[b]
2	8	2	6
4	10	4	12
6	14	6	15
24	62	24	59
27	68	27	66
30	74	30	70
47	89	47	88
k_{obs} = 0.05 ± 0.01 h^{-1}. R^2 = 0.996 M_n = 15 290 g mol^{-1} M_w/M_n = 1.41		k_{obs} = 0.04 ± 0.01 h^{-1}. R^2 = 0.993 M_n = 16 460 g mol^{-1} M_w/M_n = 1.36	

[a]Conditions: [*L*-LA]$_0$:[**9**]$_0$ = 100:1, [*L*-LA]$_0$ = 0.5 M, [**9**]$_0$ = 0.05 M, 4.0 mL toluene at 80 °C. Aliquots were taken at given intervals. [b]Measured by ^{1}H NMR spectroscopic analyses.

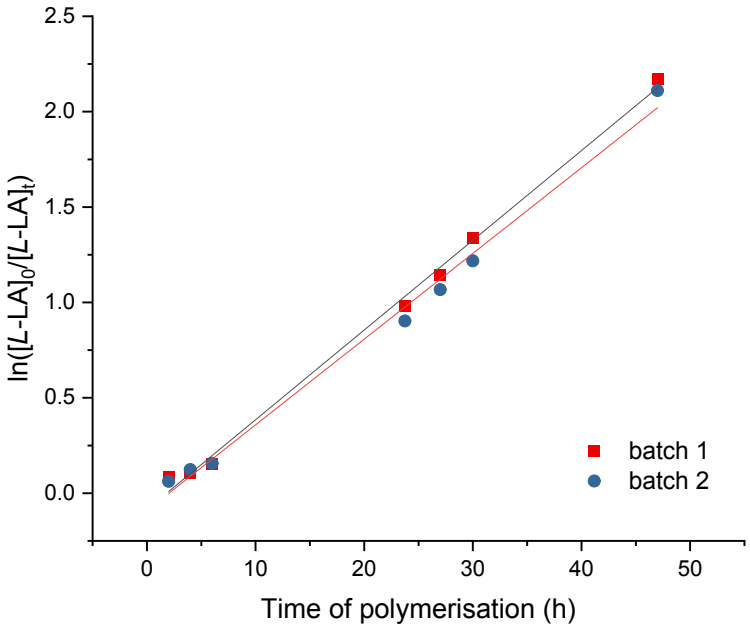

Fig. S87 Plots of ln([*L*-LA]$_0$/[*L*-LA]$_t$) *vs.* time. Red squares: batch 1 (k_{obs} = 0.05 ± 0.01 h^{-1}. R^2 = 0.996), Blue circles: batch 2 (k_{obs} = 0.04 ± 0.01 h^{-1}. R^2 = 0.993). Conditions: [*L*-LA]$_0$:[**9**]$_0$ = 100:1, [*L*-LA]$_0$ = 0.5 M, [**9**]$_0$ = 0.05 M, 4.0 mL toluene at 80 °C.

Table S30 ROP of *L*-LA using ^{Me_2}SB(^{tBu}N,I*)Al(O-2,6-Me-C_6H_3)(THF) (**9**) with $[L\text{-LA}]_0$:$[\mathbf{9}]_0$ = 100:1 at 70 °C.[a]

Time (h)	Conversion 1 (%)[b]	Time (h)	Conversion 2 (%)[b]
8	10	8	10
24	42	24	44
27	48	27	49
30	56	30	55
48	77	48	74
51	80	51	76
55	82	55	79
k_{obs} = 0.04 ± 0.01 h^{-1}. R^2 = 0.994 M_n = 11 600 g mol^{-1} M_w/M_n = 1.44		k_{obs} = 0.03 ± 0.01 h^{-1}. R^2 = 0.999 M_n = 13 170 g mol^{-1} M_w/M_n = 1.43	

[a]Conditions: $[L\text{-LA}]_0$:$[\mathbf{2}]_0$ = 100:1, $[L\text{-LA}]_0$ = 0.5 M, $[\mathbf{2}]_0$ = 0.05 M, 4.0 mL toluene at 70 °C. Aliquots were taken at given intervals. [b]Measured by ^{1}H NMR spectroscopic analyses.

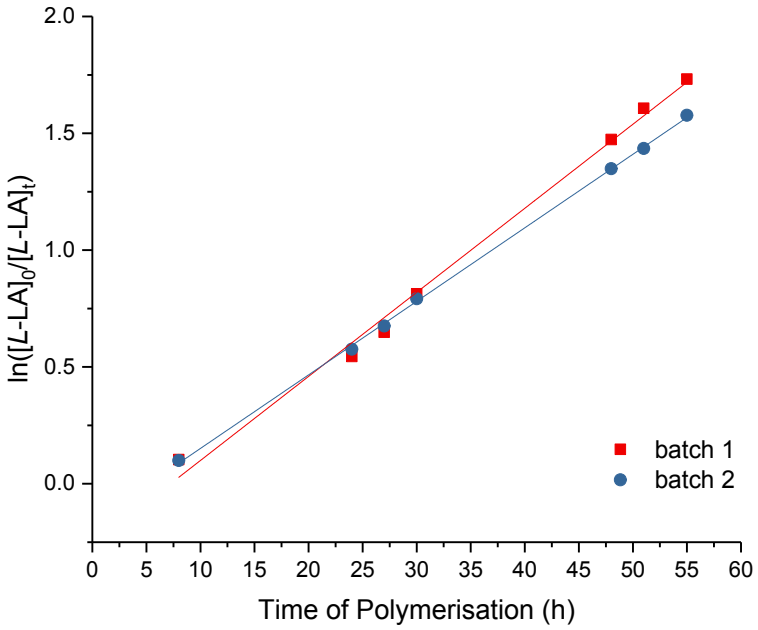

Fig. S88 Plots of $\ln([L\text{-LA}]_0/[L\text{-LA}]_t)$ *vs.* time. Red squares: batch 1 (k_{obs} = 0.04 ± 0.01 h^{-1}. R^2 = 0.994), Blue circles: batch 2 (k_{obs} = 0.03 ± 0.01 h^{-1}. R^2 = 0.999). Conditions: $[L\text{-LA}]_0$:$[\mathbf{9}]_0$ = 100:1, $[L\text{-LA}]_0$ = 0.5 M, $[\mathbf{9}]_0$ = 0.05 M, 4.0 mL toluene at 70 °C.

Table S31 ROP of *L*-LA using ^{Me_2}SB(^{iPr}N,I*)Al(O-2,6-^{i}Pr-C_6H_3)(THF) (**9**) with various temperatures.[a]

Entry	T (°C)	Time (h)	Conv. (%)[b]	k_{obs} (h^{-1})[c]	R^{2c}	M_n (GPC)[d]	M_n (calcd)[e]	M_w/M_n
1	70	55	82	0.04 ± 0.01	0.994	11 600	11 938	1.44
2	70	55	79	0.03 ± 0.01	0.999	13 170	11 506	1.43
3	80	47	89	0.05 ± 0.01	0.996	15 290	12 947	1.41
4	80	47	88	0.04 ± 0.01	0.993	16 460	12 803	1.36
5	90	23	90	0.11 ± 0.01	0.988	15 320	13 091	1.45
6	90	23	91	0.11 ± 0.01	0.988	14 520	13 235	1.37
7	100	9	85	0.23 ± 0.01	0.998	12 310	12 371	1.33
8	100	9	86	0.24 ± 0.01	0.995	12 420	12 515	1.35

[a]Conditions: $[L\text{-LA}]_0$:$[\mathbf{9}]_0$ = 100:1, $[L\text{-LA}]_0$ = 0.5 M, 4.0 mL toluene at stated temperature. Polymerisations were quenched by THF. [b]Measured by ^{1}H NMR spectroscopic analyses. [c]First order rate constant (k_{obs}) with standard error and R^2 were obtained from plots of $\ln([L\text{-LA}]_0/[L\text{-LA}]_t)$ *vs.* time. [d]Determined by GPC in THF against PS standards using the appropriate Mark-Houwink corrections.[7] [e]Calculated M_n for PLA synthesised with **9** = conv. (%) × $[L\text{-LA}]_0/[\mathbf{9}]_0$ × 144.1 + 122.2.

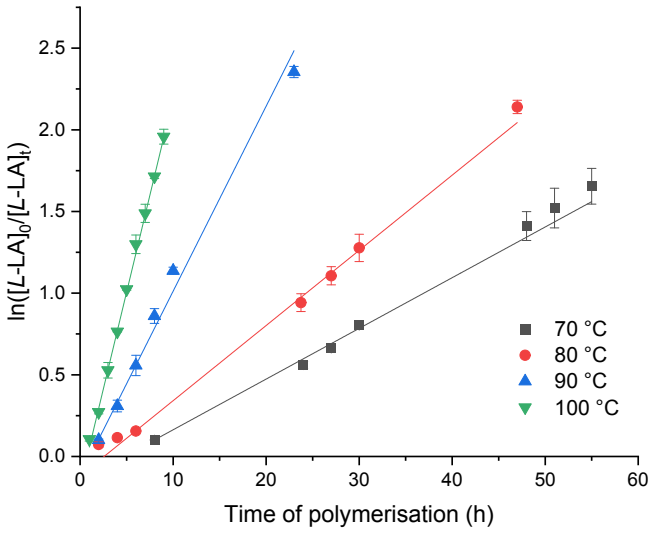

Fig. S89 Plots of $\ln([L\text{-LA}]_0/[L\text{-LA}]_t)$ *vs.* time. 70 °C, black square: k_{obs} = 0.03 ± 0.01 h^{-1}, R^2 = 0.993. 80 °C, red circle: k_{obs} = 0.04 ± 0.01 h^{-1}, R^2 = 0.994. 90 °C, blue triangle: k_{obs} = 0.11 ± 0.01 h^{-1}, R^2 = 0.989. 100 °C, green down triangle: k_{obs} = 0.24 ± 0.01 h^{-1}, R^2 = 0.995. Conditions: $[L\text{-LA}]_0$:$[\mathbf{9}]_0$ = 100:1, $[L\text{-LA}]_0$ = 0.5 M, $[\mathbf{9}]_0$ = 0.005 M, 4.0 mL toluene. Values of $\ln([L\text{-LA}]_0/[L\text{-LA}]_t)$ with standard error were determined from duplicate experiments.

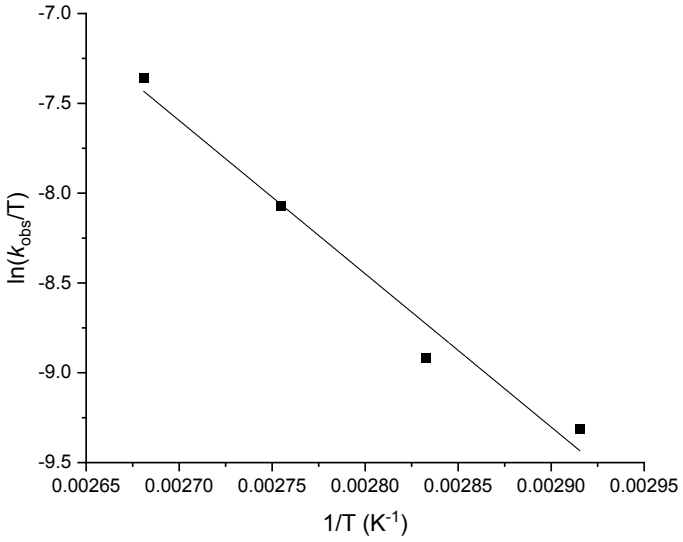

Figure S90 Eyring plot of ln(k_{obs}/T) *vs.* 1/T. Slope = −8533 ± 951, Intercept = 15.4 ± 2.7 with R^2 = 0.976. $\Delta H^{\ddagger}$ = 71 ± 8 kJ mol^{-1}, $\Delta S^{\ddagger}$ = −69 ± 22 J mol^{-1} K^{-1} for ROP of *L*-LA with ^{Me}$_2$SB(^{tBu}N,I*)Al(O-2,6-Me-C_6H_3)(THF) (**9**).

Table S32 ROP of *rac*-LA using ^{Me_2}SB(^{tBu}N,I*)Al(O-2,6-Me-C_6H_3)(THF) (**9**) with [*L*-LA]$_0$:[**9**]$_0$ = 200:1 at 100 °C.[a]

Time (h)	Conversion 1 (%)[b]	Time (h)	Conversion 2 (%)[b]
2	12	2	12
3	23	3	21
4	36	4	30
5	48	5	43
6	60	6	54
7	67	7	61
8	72	8	74
9	77	9	76
10	80	10	81
k_{obs} = 0.20 ± 0.01 h^{-1}. R^2 = 0.994 M_n = 23 940 g mol^{-1} M_w/M_n = 1.13		k_{obs} = 0.20 ± 0.01 h^{-1}. R^2 = 0.980 M_n = 21 230 g mol^{-1} M_w/M_n = 1.27	

[a]Conditions: [*L*-LA]$_0$:[**9**]$_0$ = 200:1, [*L*-LA]$_0$ = 0.5 M, [**9**]$_0$ = 0.0025 M, 4.0 mL toluene at 100 °C. Aliquots were taken at given intervals. [b]Measured by ^{1}H NMR spectroscopic analyses.

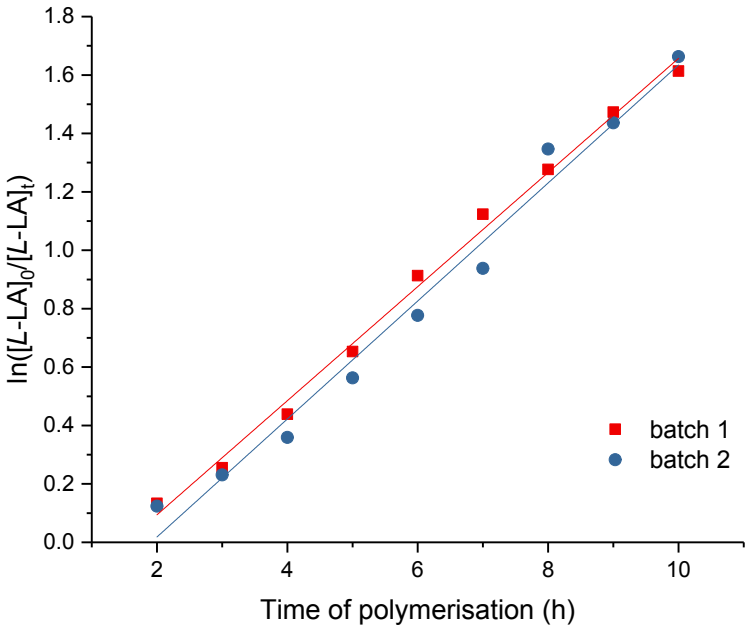

Fig. S91 Plots of ln([*L*-LA]$_0$/[*L*-LA]$_t$) *vs.* time. Red squares: batch 1 (k_{obs} = 0.20 ± 0.01 h^{-1}. R^2 = 0.994), Blue circles: batch 2 (k_{obs} = 0.20 ± 0.01 h^{-1}. R^2 = 0.980). Conditions: [*L*-LA]$_0$:[**9**]$_0$ = 200:1, [*L*-LA]$_0$ = 0.5 M, [**9**]$_0$ = 0.0025 M, 4.0 mL toluene at 100 °C.

Table S33 ROP of *rac*-LA using ^{Me_2}SB(^{tBu}N,I*)Al(O-2,6-Me-C_6H_3)(THF) (**9**) with [*L*-LA]$_0$:[**9**]$_0$ = 300:1 at 100 °C.[a]

Time (h)	Conversion 1 (%)[b]	Time (h)	Conversion 2 (%)[b]
3	20	3	20
4	32	4	31
5	40	5	41
6	50	6	51
7	57	7	59
8	65	8	66
9	71	9	71
10	77	10	75
11	79	11	79
k_{obs} = 0.17 ± 0.01 h^{-1}. R^2 = 0.995		k_{obs} = 0.17 ± 0.01 h^{-1}. R^2 = 0.998 M_n = 25 310 g mol^{-1} M_w/M_n = 1.33	

[a]Conditions: [*L*-LA]$_0$:[**9**]$_0$ = 300:1, [*L*-LA]$_0$ = 0.5 M, [**9**]$_0$ = 0.0016 M, 4.0 mL toluene at 100 °C. Aliquots were taken at given intervals. [b]Measured by ^{1}H NMR spectroscopic analyses.

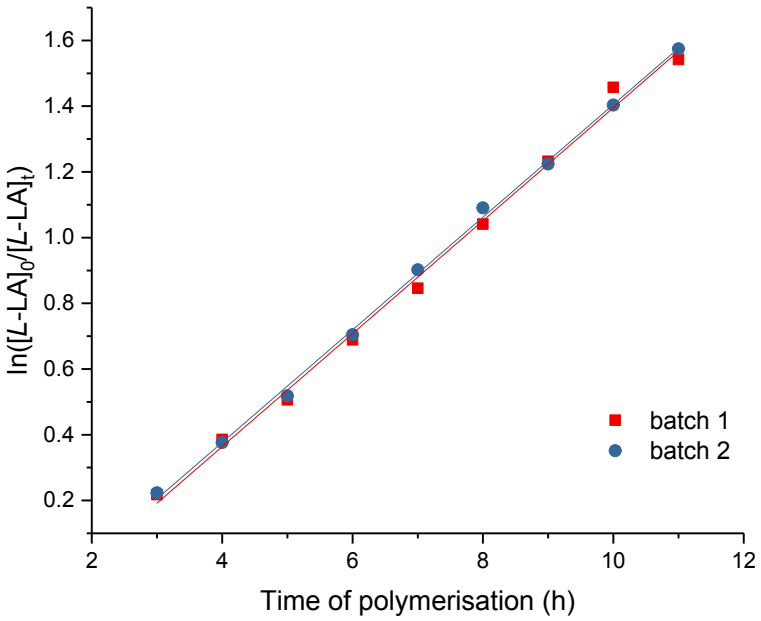

Fig. S92 Plots of ln([*L*-LA]$_0$/[*L*-LA]$_t$) *vs.* time. Red squares: batch 1 (k_{obs} = 0.17 ± 0.01 h^{-1}. R^2 = 0.995), Blue circles: batch 2 (k_{obs} = 0.17 ± 0.01 h^{-1}. R^2 = 0.998). Conditions: [*L*-LA]$_0$:[**9**]$_0$ = 300:1, [*L*-LA]$_0$ = 0.5 M, [**9**]$_0$ = 0.0016 M, 4.0 mL toluene at 100 °C.

Table S34 ROP of *rac*-LA using $^{Me}_2$SB($^{t Bu}$N,I*)Al(O-2,6-Me-C_6H_3)(THF) (**9**) with [*L*-LA]$_0$:[**9**]$_0$ = 500:1 at 100 °C.[a]

Time (h)	Conversion 1 (%)[b]	Time (h)	Conversion 2 (%)[b]
3	15	3	13
4	23	4	21
5	33	5	30
6	38	6	36
7	44	7	42
8	46	8	46
24	85	24	83
k_{obs} = 0.08 ± 0.01 h^{-1}. R^2 = 0.997		k_{obs} = 0.08 ± 0.01 h^{-1}. R^2 = 0.994	
M_n = 46 040 g mol^{-1}		M_n = 40 430 g mol^{-1}	
M_w/M_n = 1.33		M_w/M_n = 1.25	

[a]Conditions: [*L*-LA]$_0$:[**9**]$_0$ = 500:1, [*L*-LA]$_0$ = 0.5 M, [**9**]$_0$ = 0.001 M, 4.0 mL toluene at 100 °C. Aliquots were taken at given intervals. [b]Measured by ^{1}H NMR spectroscopic analyses.

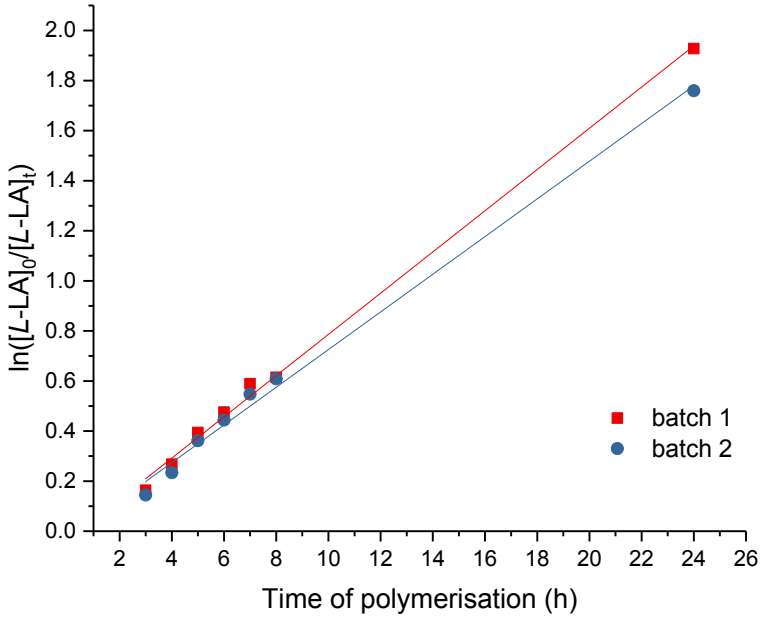

Fig. S93 Plots of ln([*L*-LA]$_0$/[*L*-LA]$_t$) *vs.* time. Red squares: batch 1 (k_{obs} = 0.08 ± 0.01 h^{-1}. R^2 = 0.997), Blue circles: batch 2 (k_{obs} = 0.08 ± 0.01 h^{-1}. R^2 = 0.994). Conditions: [*L*-LA]$_0$:[**9**]$_0$ = 500:1, [*L*-LA]$_0$ = 0.5 M, [**9**]$_0$ = 0.001 M, 4.0 mL toluene at 100 °C.

Table S35 ROP of *rac*-LA using $^{Me}_2$SB($^{t Bu}$N,I*)Al(O-2,6-Me-C_6H_3)(THF) (**9**) with [*L*-LA]$_0$:[**9**]$_0$ = 700:1 at 100 °C.[a]

Time (h)	Conversion 1 (%)[b]	Time (h)	Conversion 2 (%)[b]
3	14	3	10
4	20	4	15
5	28	5	23
6	36	6	29
7	41	7	34
8	47	8	41
24	84	24	77
k_{obs} = 0.08 ± 0.01 h^{-1}. R^2 = 0.996 M_n = 55 870 g mol^{-1} M_w/M_n = 1.22		k_{obs} = 0.06 ± 0.01 h^{-1}. R^2 = 0.993 M_n = 53 110 g mol^{-1} M_w/M_n = 1.31	

[a]Conditions: [*L*-LA]$_0$:[**9**]$_0$ = 700:1, [*L*-LA]$_0$ = 0.5 M, [**9**]$_0$ = 0.0007 M, 4.0 mL toluene at 100 °C. Aliquots were taken at given intervals. [b]Measured by ^{1}H NMR spectroscopic analyses.

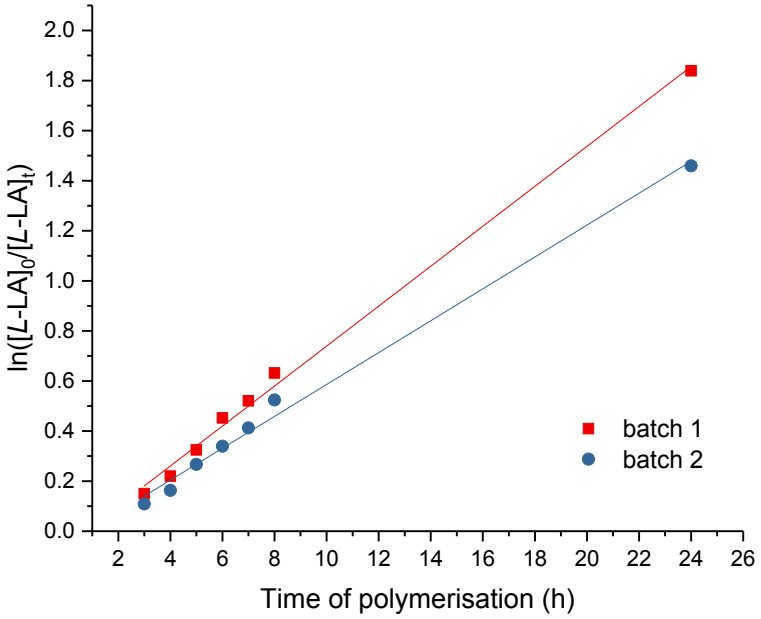

Fig. S94 Plots of ln([*L*-LA]$_0$/[*L*-LA]$_t$) *vs.* time. Red squares: batch 1 (k_{obs} = 0.08 ± 0.01 h^{-1}. R^2 = 0.996), Blue circles: batch 2 (k_{obs} = 0.06 ± 0.01 h^{-1}. R^2 = 0.993). Conditions: [*L*-LA]$_0$:[**9**]$_0$ = 700:1, [*L*-LA]$_0$ = 0.5 M, [**9**]$_0$ = 0.0007 M, 4.0 mL toluene at 100 °C.

Table S36 ROP of *rac*-LA using $^{Me}_2$SB(^{t}BuN,I*)Al(O-2,6-Me-C_6H_3)(THF) (**9**) with [*L*-LA]$_0$:[**9**]$_0$ = 1000:1 at 100 °C.[a]

Time (h)	Conversion 1 (%)[b]	Time (h)	Conversion 2 (%)[b]
3	13	3	13
4	20	4	18
5	24	5	22
6	30	6	26
7	34	7	30
8	37	8	35
23.5	70	23.5	65
27	76	27	68
k_{obs} = 0.05 ± 0.01 h^{-1}. R^2 = 0.996		k_{obs} = 0.04 ± 0.01 h^{-1}. R^2 = 0.994	
M_n = 74 390 g mol^{-1}		M_n = 58 670 g mol^{-1}	
M_w/M_n = 1.16		M_w/M_n = 1.23	

[a]Conditions: [*L*-LA]$_0$:[**9**]$_0$ = 1000:1, [*L*-LA]$_0$ = 0.5 M, [**9**]$_0$ = 0.0005 M, 4.0 mL toluene at 100 °C. Aliquots were taken at given intervals. [b]Measured by ^{1}H NMR spectroscopic analyses.

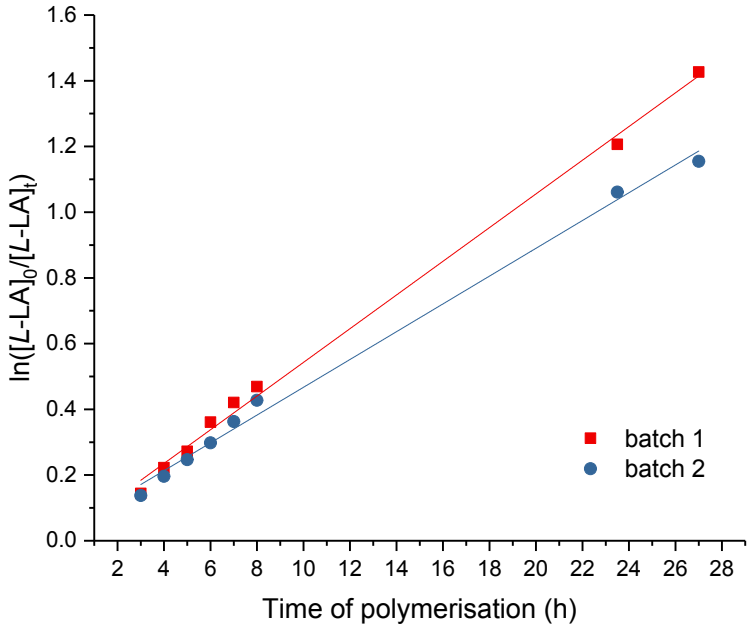

Fig. S95 Plots of ln([*L*-LA]$_0$/[*L*-LA]$_t$) *vs.* time. Red squares: batch 1 (k_{obs} = 0.05 ± 0.01 h^{-1}. R^2 = 0.996), Blue circles: batch 2 (k_{obs} = 0.04 ± 0.01 h^{-1}. R^2 = 0.994). Conditions: [*L*-LA]$_0$:[**9**]$_0$ = 1000:1, [*L*-LA]$_0$ = 0.5 M, [**9**]$_0$ = 0.0005 M, 4.0 mL toluene at 100 °C.

Table S37 ROP of *L*-LA using ^{Me_2}SB(^{iPr}N,I*)Al(O-2,6-Me-C_6H_3)(THF) (**9**) with various ratios of [*L*-LA]$_0$:[**9**]$_0$.[a]

[*L*-LA]$_0$:[**9**]$_0$	Time (h)	Conv. (%)[b]	k_{obs} (h^{-1})[c]	R^{2c}	M_n (GPC)[d]	M_n (calcd)[e]	M_w/M_n
200	10	80	0.20 ± 0.01	0.994	23 940	23 178	1.13
200	10	81	0.20 ± 0.01	0.980	21 230	23 466	1.27
300	11	79	0.17 ± 0.01	0.995	N/A	34 274	N/A
300	11	79	0.17 ± 0.01	0.998	25 310	34 274	1.33
500	24	85	0.08 ± 0.01	0.997	46 040	61 364	1.33
500	24	83	0.08 ± 0.01	0.994	40 430	59 924	1.25
700	24	84	0.08 ± 0.01	0.996	55 870	84 853	1.22
700	24	77	0.06 ± 0.01	0.993	53 110	77 792	1.31
1000	27	76	0.05 ± 0.01	0.996	74 390	109 638	1.16
1000	27	68	0.04 ± 0.01	0.994	58 670	98 110	1.23

[a]Conditions: [*L*-LA]$_0$:[**9**]$_0$ as stated, [*L*-LA]$_0$ = 0.5 M, 4.0 mL toluene at 100 °C. Polymerisations were quenched by THF. [b]Measured by ^{1}H NMR spectroscopic analyses. [c]First order rate constant (k_{obs}) with standard error and R^2 were obtained from plots of ln([*L*-LA]$_0$/[*L*-LA]$_t$) *vs.* time. [d]Determined by GPC in THF against PS standards using the appropriate Mark-Houwink corrections.[7] [e]Calculated M_n for PLA synthesised with **9** = conv. (%) × [*L*-LA]$_0$:[**9**]$_0$ × 144.1 + 122.2.

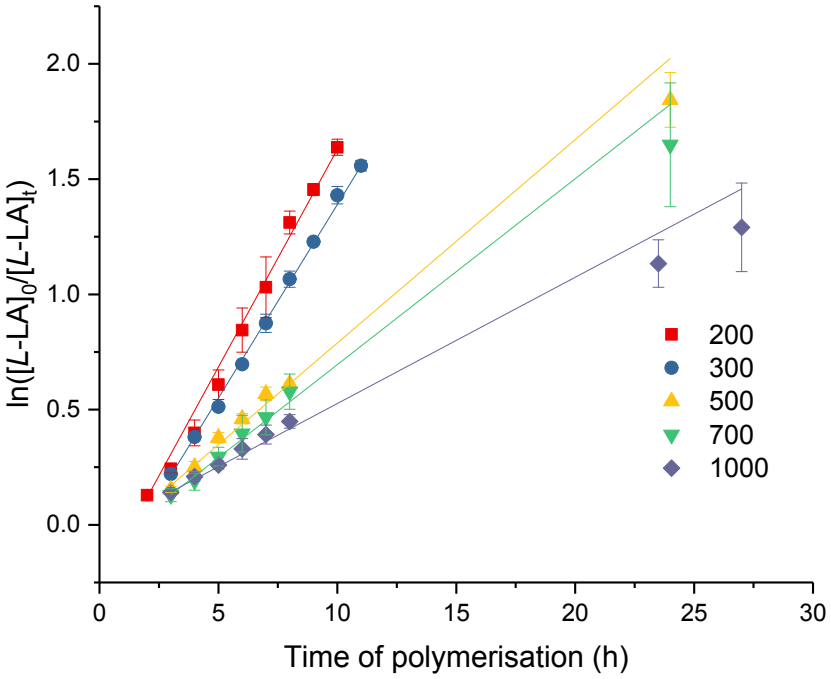

Fig. S96 Plots of ln([*L*-LA]$_0$/[*L*-LA]$_t$) *vs.* time of polymerisation. ROP of *L*-lactide using **9**. [*L*-LA]$_0$/[**9**]$_0$ = 200, red square: k_{obs} = 0.19 ± 0.01 h^{-1}, R^2 = 0.994. [*L*-LA]$_0$/[**9**]$_0$ = 300, blue circle: k_{obs} = 0.17 ± 0.01 h^{-1}, R^2 = 0.999. [*L*-LA]$_0$/[**9**]$_0$ = 500, yellow triangle: k_{obs} = 0.09 ± 0.01 h^{-1}, R^2 = 0.992. [*L*-LA]$_0$/[**9**]$_0$ = 700, green down triangle: k_{obs} = 0.08 ± 0.01 h^{-1}, R^2 = 0.982. [*L*-LA]$_0$/[**9**]$_0$ = 1000, purple diamond: k_{obs} = 0.06 ± 0.01 h^{-1}, R^2 = 0.982. Conditions: [*L*-LA]$_0$ = 0.5 M, 4.0 mL toluene at 100 °C. Values of ln([*L*-LA]$_0$/[*L*-LA]$_t$) with standard error were determined from duplicate experiments.

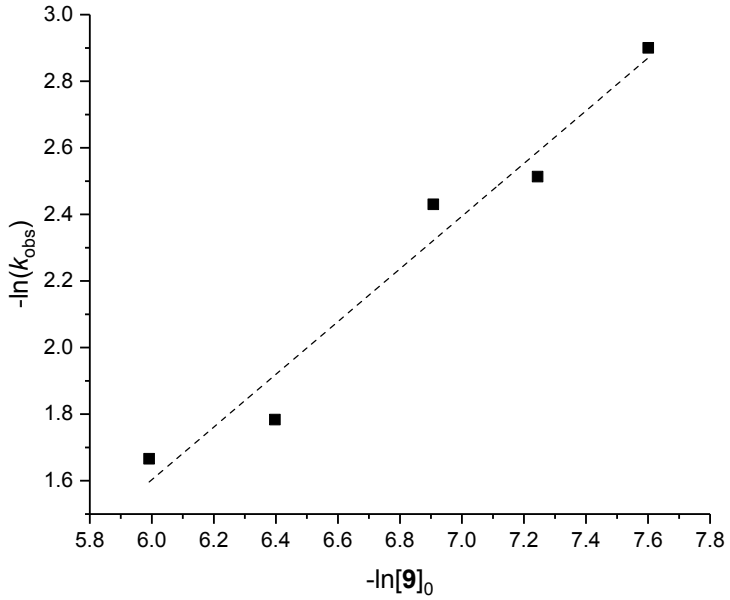

Fig. S97 Plot of $-\ln(k_{obs})$ *vs.* $-\ln[\mathbf{9}]_0$. ROP of *L*-lactide using **9**. Slope = 0.79 ± 0.09 with R^2 = 0.951. Conditions: $[L\text{-LA}]_0$ = 0.5 M, 4.0 mL toluene at 100 °C.

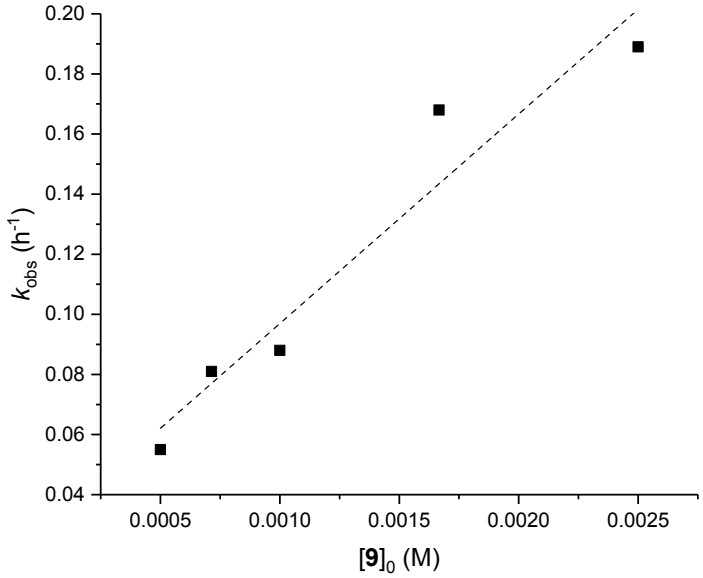

Fig. S98 Plot of k_{obs} *vs.* $[\mathbf{9}]_0$. ROP of *L*-lactide using **9**. Slope = 70 ± 11 with R^2 = 0.912. Conditions: $[L\text{-LA}]_0$ = 0.5 M, 4.0 mL toluene at 100 °C.

Table S38 ROP of *rac*-LA using ^{Me_2}SB($^{t Bu}$N,I*)Al(O-2,6-Me-C_6H_3)(THF) (**9**) with [*rac*-LA]$_0$:[**9**]$_0$ = 100:1 at 100 °C.[a]

Time (h)	Conversion 1 (%)[b]	Time (h)	Conversion 2 (%)[b]
1	10	1	9
2	20	2	20
3	38	3	36
4	57	4	55
5	72	5	70
6	79	6	78
7	83	7	83
8	87	8	87
k_{obs} = 0.30 ± 0.01 h^{-1}. R^2 = 0.987		k_{obs} = 0.30 ± 0.01 h^{-1}. R^2 = 0.988	
M_n = 12 070 g mol^{-1}		M_n = 10 970 g mol^{-1}	
M_w/M_n = 1.29		M_w/M_n = 1.33	
P_r (integration) = 0. ± 0.		P_r (integration) = 0. ± 0.	
P_r (deconvolution) = 0. ± 0.0		P_r (deconvolution) = 0. ± 0.	

[a]Conditions: [*rac*-LA]$_0$:[**9**]$_0$ = 100:1, [*rac*-LA]$_0$ = 0.5 M, [**9**]$_0$ = 0.05 M, 4.0 mL toluene at 100 °C. Aliquots were taken at given intervals. [b]Measured by ^{1}H NMR spectroscopic analyses.

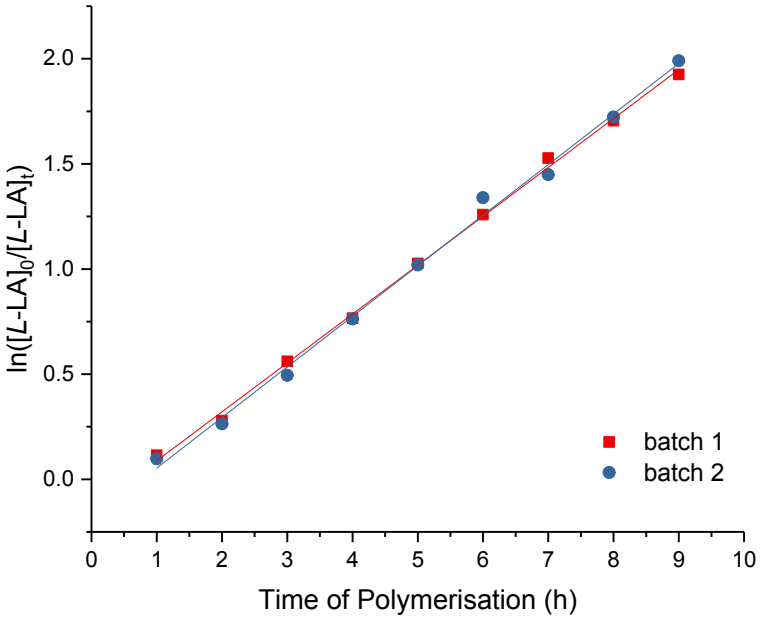

Fig. S99 Plots of ln([*rac*-LA]$_0$/[*rac*-LA]$_t$) *vs.* time. Red squares: batch 1 (k_{obs} = 0.30 ± 0.01 h^{-1}. R^2 = 0.987), Blue circles: batch 2 (k_{obs} = 0.30 ± 0.01 h^{-1}. R^2 = 0.988). Conditions: [*rac*-LA]$_0$:[**9**]$_0$ = 100:1, [*rac*-LA]$_0$ = 0.5 M, [**9**]$_0$ = 0.005 M, 4.0 mL toluene at 100 °C.

Table S39 ROP of *L*-LA using ^{Me_2}SB(^{tBu}N,I*)Al(O-2,4-^{t}Bu-C_6H_3)(THF) (**10**) with [*L*-LA]$_0$:[**10**]$_0$ = 100:1 at 100 °C.[a]

Time (h)	Conversion 1 (%)[b]	Time (h)	Conversion 2 (%)[b]
1	7	1	7
2	16	2	14
3	30	3	24
4	43	4	34
5	53	5	45
6	62	6	54
7	70	7	61
8	74	8	66
9	79	9	71
10	82	10	76
k_{obs} = 0.19 ± 0.01 h^{-1}. R^2 = 0.998 M_n = 13 310 g mol^{-1} M_w/M_n = 1.37		k_{obs} = 0.16 ± 0.01 h^{-1}. R^2 = 0.995 M_n = 11 910 g mol^{-1} M_w/M_n = 1.26	

[a]Conditions: [*L*-LA]$_0$:[**10**]$_0$ = 100:1, [*L*-LA]$_0$ = 0.5 M, [**10**]$_0$ = 0.05 M, 4.0 mL toluene at 100 °C. Aliquots were taken at given intervals. [b]Measured by ^{1}H NMR spectroscopic analyses.

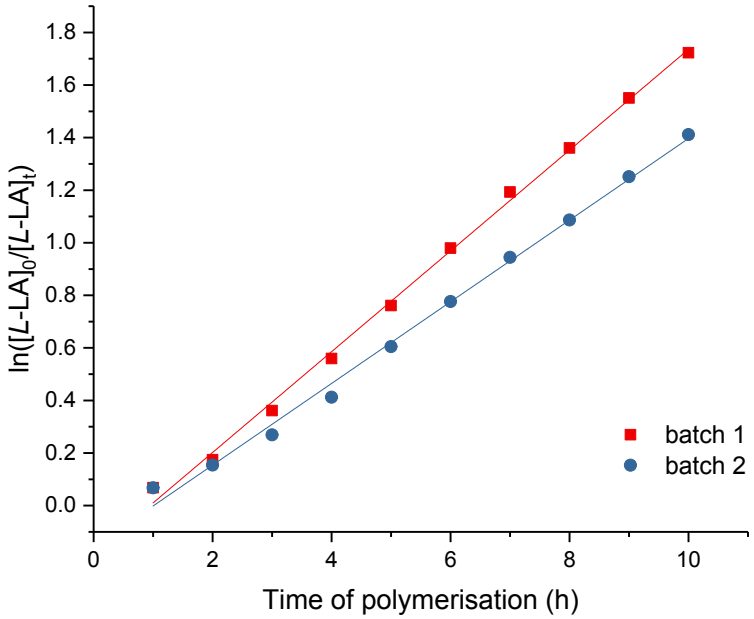

Fig. S100 Plots of ln([*L*-LA]$_0$/[*L*-LA]$_t$) *vs.* time. Red squares: batch 1 (k_{obs} = 0.19 ± 0.01 h^{-1}. R^2 = 0.998), Blue circles: batch 2 (k_{obs} = 0.16 ± 0.01 h^{-1}. R^2 = 0.995). Conditions: [*L*-LA]$_0$:[**10**]$_0$ = 100:1, [*L*-LA]$_0$ = 0.5 M, [**10**]$_0$ = 0.005 M, 4.0 mL toluene at 100 °C.

Table S40 ROP of *L*-LA using ^{Me_2}SB(^{tBu}N,I*)Al(O-2,4-^{t}Bu-C_6H_3)(THF) (**10**) with [*L*-LA]$_0$:[**10**]$_0$ = 1000:1 at 100 °C.[a]

Time (h)	Conversion 1 (%)[b]	Time (h)	Conversion 2 (%)[b]
1	4	1	4
2	6	2	6
3	10	3	10
4	13	4	11
5	19	5	15
6	25	6	21
7	62	7	58
8	63	8	63
23	66	23	67
30	67	30	68
k_{obs} = 0.04 ± 0.01 h^{-1}. R^2 = 0.992 M_n = 70 510 g mol^{-1} M_w/M_n = 1.11		k_{obs} = 0.04 ± 0.01 h^{-1}. R^2 = 0.995 M_n = 65 640 g mol^{-1} M_w/M_n = 1.17	

[a]Conditions: [*L*-LA]$_0$:[**10**]$_0$ = 1000:1, [*L*-LA]$_0$ = 0.5 M, [**10**]$_0$ = 0.005 M, 4.0 mL toluene at 100 °C. Aliquots were taken at given intervals. [b]Measured by ^{1}H NMR spectroscopic analyses.

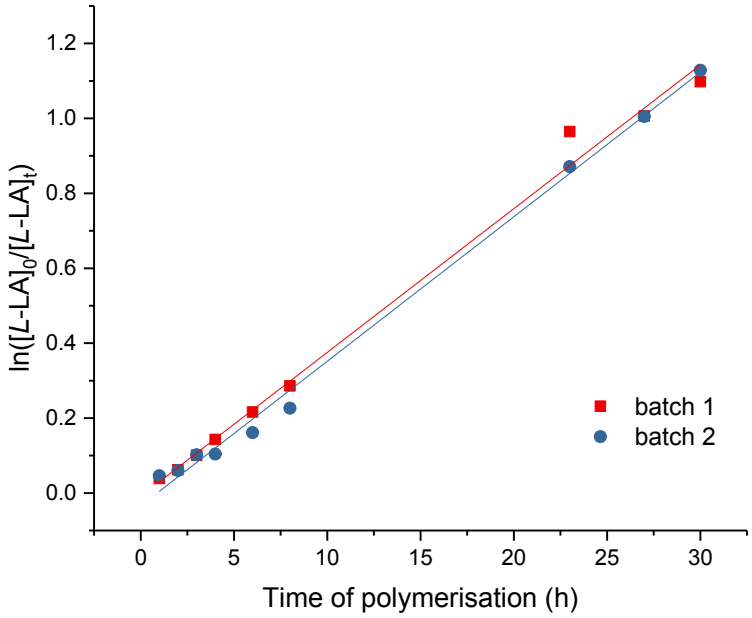

Fig. S101 Plots of ln([*L*-LA]$_0$/[*L*-LA]$_t$) *vs.* time. Red squares: batch 1 (k_{obs} = 0.04 ± 0.01 h^{-1}. R^2 = 0.992), Blue circles: batch 2 (k_{obs} = 0.04 ± 0.01 h^{-1}. R^2 = 0.995). Conditions: [*L*-LA]$_0$:[**10**]$_0$ = 1000:1, [*L*-LA]$_0$ = 0.5 M, [**10**]$_0$ = 0.0005 M, 4.0 mL toluene at 100 °C.

Additional GPC Data

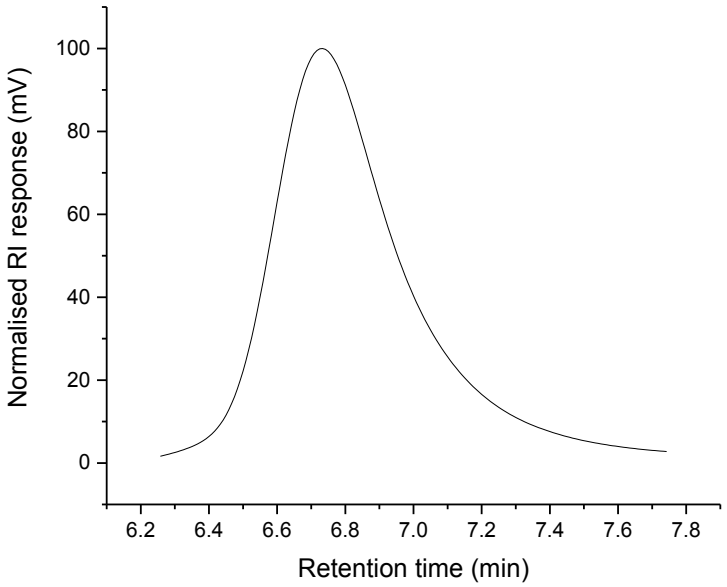

Fig. S102 GPC trace of PLA synthesised from the ROP of *L*-LA using ^{Me_2}SB(^{iPr}N,I*)Sc(Cl)(THF) (**1**) and benzyl alcohol. M_n = 42 290 g mol^{-1}, M_w/M_n = 1.17. Conditions: [*L*-LA]$_0$:[**1**]$_0$:[BnOH]$_0$ = 400:1:1, [*L*-LA] = 0.5 M, 5.0 mL toluene at 70 °C.

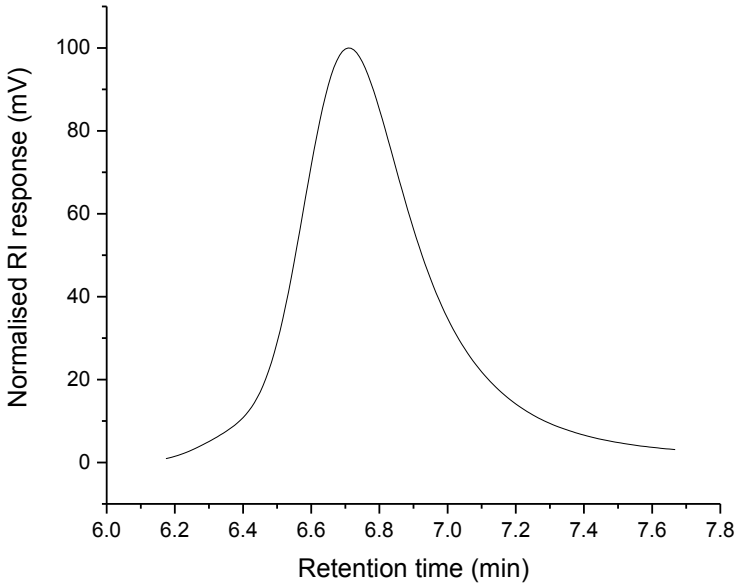

Fig. S103 GPC trace of PLA synthesised from the ROP of *L*-LA using ^{Me_2}SB(^{nBu}N,I*)Sc(Cl)(THF) (**3**) and benzyl alcohol. M_n = 44 920 g mol^{-1}, M_w/M_n = 1.17. Conditions: [*L*-LA]$_0$:[**3**]$_0$:[BnOH]$_0$ = 400:1:1, [*L*-LA] = 0.5 M, 5.0 mL toluene at 70 °C.

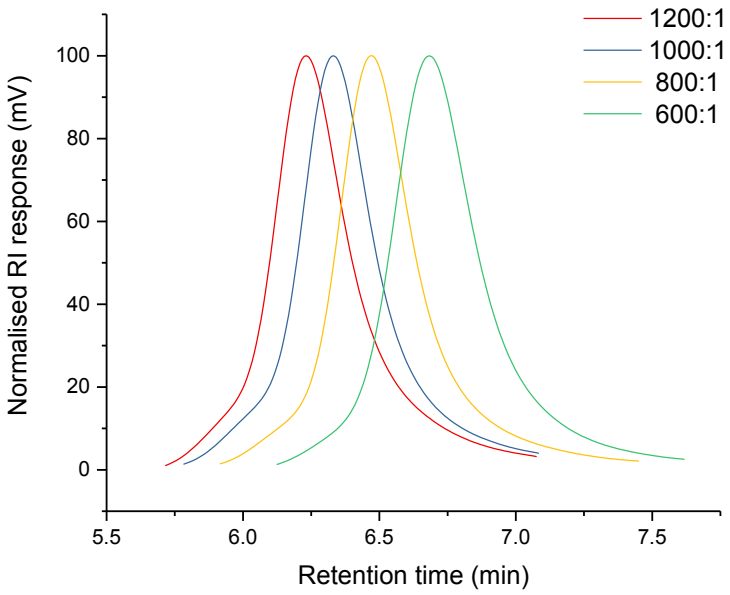

Fig. S104 Stacked GPC traces of PLAs synthesised from the ROP of *L*-LA using $^{Me}_2$SB(^{iPr}N,I*)Sc(O-2,6-^{i}Pr-C_6H_3)(THF) (**4**). Red: $[L\text{-LA}]_0$:[**4**]$_0$ = 1200:1, M_n = 103 670 g mol^{-1} , M_w/M_n = 1.14, Blue: $[L\text{-LA}]_0$:[**4**]$_0$ = 1000:1, M_n = 91 500 g mol^{-1}, M_w/M_n = 1.13, Yellow: $[L\text{-LA}]_0$:[**4**]$_0$ = 800:1, M_n = 69 700 g mol^{-1}, M_w/M_n = 1.16, Green: $[L\text{-LA}]_0$:[**4**]$_0$ = 600:1, M_n = 49 150 g mol^{-1}, M_w/M_n = 1.16, Conditions: $[L\text{-LA}]_0$:[**4**]$_0$ as stated, $[L\text{-LA}]_0$ = 0.5 M, 7.0 mL toluene at 70 °C.

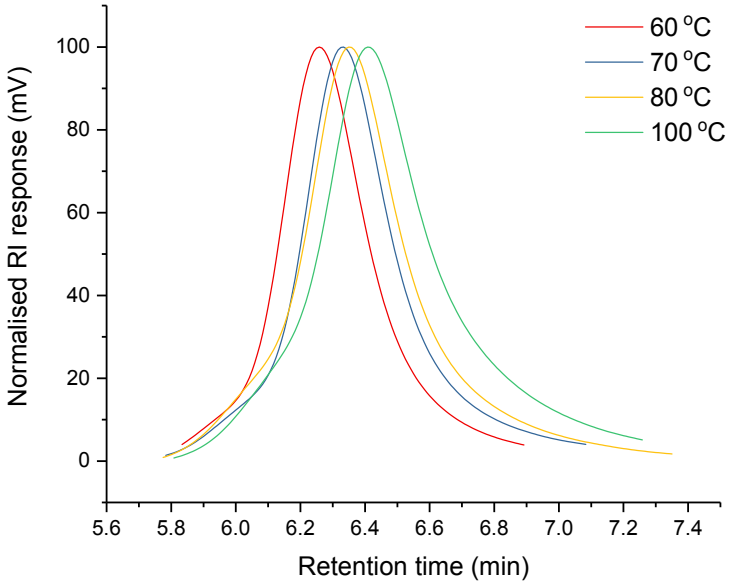

Fig. S105 Stacked GPC traces of PLAs synthesised from the ROP of *L*-LA using $^{Me}_2$SB(^{iPr}N,I*)Sc(O-2,6-^{i}Pr-C_6H_3)(THF) (**4**). Red: 60 °C, M_n = 105 980 g mol^{-1}, M_w/M_n = 1.09, Blue: 70 °C, M_n = 91 500 g mol^{-1}, M_w/M_n = 1.13, Yellow: 80 °C, M_n = 85 090 g mol^{-1}, M_w/M_n = 1.18, Green: 100 °C, M_n = 75 280 g mol^{-1}, M_w/M_n = 1.19, Conditions: $[L\text{-LA}]_0$:[**4**]$_0$ = 1000:1, $[L\text{-LA}]_0$ = 0.5 M, 7.0 mL toluene at stated temperature.

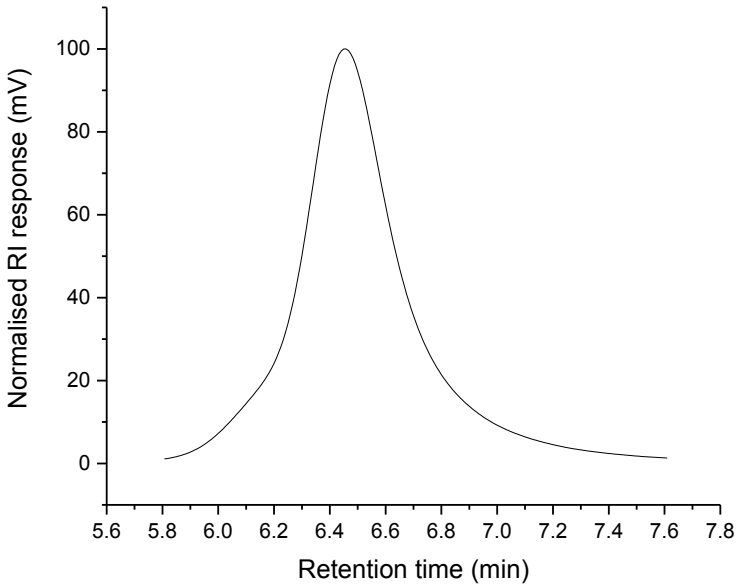

Fig. S106 GPC trace of PLA synthesised from the ROP of *rac*-LA using ^{Me_2}SB(^{iPr}N,I*)Sc(O-2,6-^{i}Pr-C_6H_3)(THF) (**4**). M_n = 70 280 g mol^{-1}, M_w/M_n = 1.21. Conditions: [*rac*-LA]$_0$:[**4**]$_0$ = 1000:1, [*rac*-LA] = 0.5 M, 7.0 mL toluene at 70 °C.

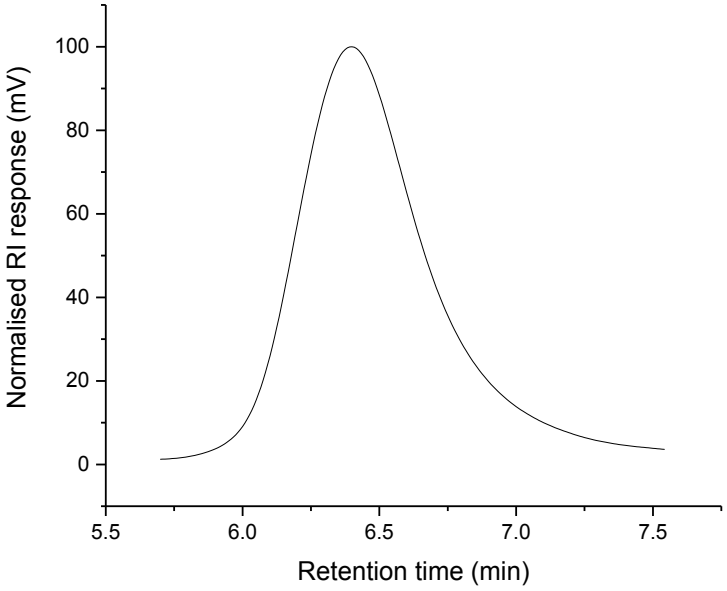

Fig. S107 GPC trace of PLA synthesised from the ROP of *L*-LA using ^{Me_2}SB(^{iPr}N,I*)Sc(O-2,4-^{t}Bu-C_6H_3)(THF) (**5**). M_n = 72 180 g mol^{-1}, M_w/M_n = 1.23. Conditions: [*L*-LA]$_0$:[**5**]$_0$ = 1000:1, [*L*-LA] = 0.5 M, 7.0 mL toluene at 70 °C.

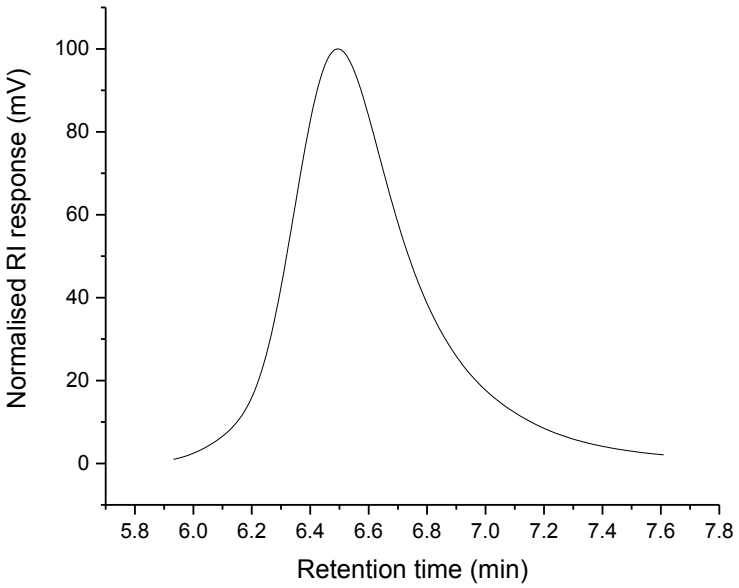

Fig. S108 GPC trace of PLA synthesised from the ROP of *L*-LA using ^{Me_2}SB(^{iPr}N,I*)Sc(O-2,4-^{t}Bu-C_6H_3)(THF) (**5**). M_n = 60 790 g mol^{-1}, M_w/M_n = 1.21. Conditions: [*L*-LA]$_0$:[**5**]$_0$ = 1000:1, [*L*-LA] = 0.5 M, 7.0 mL toluene at 100 °C.

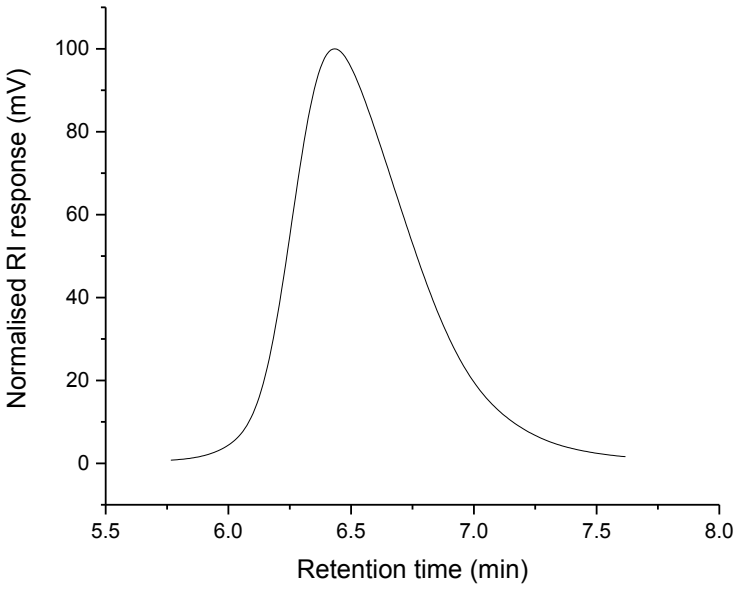

Fig. S109 GPC trace of PLA synthesised from the ROP of *rac*-LA using ^{Me_2}SB(^{iPr}N,I*)Sc(O-2,4-^{t}Bu-C_6H_3)(THF) (**5**). M_n = 64 540 g mol^{-1}, M_w/M_n = 1.23. Conditions: [*rac*-LA]$_0$:[**5**]$_0$ = 1000:1, [*rac*-LA] = 0.5 M, 7.0 mL toluene at 70 °C.

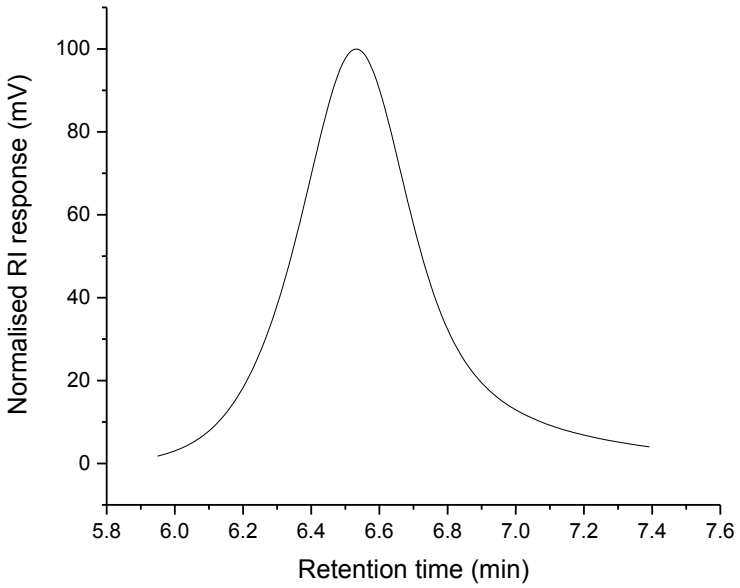

Fig. S110 GPC trace of PLA synthesised from the ROP of *rac*-LA using ^{Me_2}SB(^{Ph}N,I*)Sc(O-2,6-^{i}Pr-C_6H_3)(THF) (**7**). M_n = 64 820 g mol^{-1}, M_w/M_n = 1.17. Conditions: [*rac*-LA]$_0$:[**7**]$_0$ = 1000:1, [*rac*-LA] = 0.5 M, 7.0 mL toluene at 70 °C.

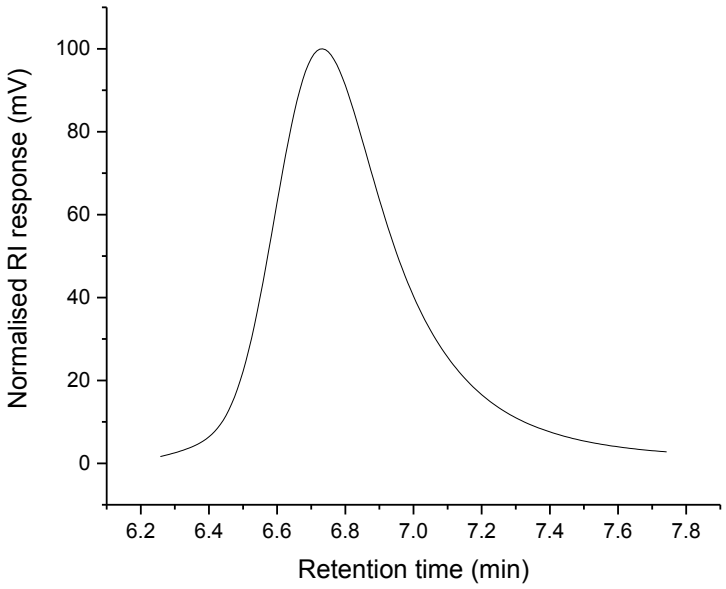

Fig. S111 GPC trace of PLA synthesised from the ROP of *L*-LA using ^{Me_2}SB(^{iPr}N,I*)Al(Cl)(THF) (**8**) and benzyl alcohol. M_n = 17 600 g mol^{-1} M_w/M_n = 1.37. Conditions: [*L*-LA]$_0$:[**8**]$_0$:[BnOH]$_0$ = 100:1:1, [*L*-LA] = 0.5 M, 4.0 mL toluene at 100 °C.

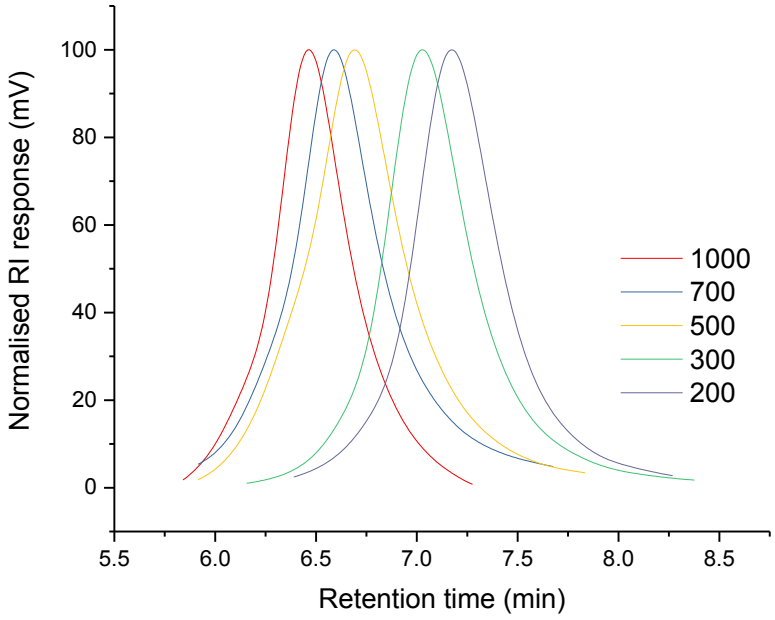

Fig. S112 Stacked GPC traces of PLAs synthesised from the ROP of *L*-LA using ^{Me2}SB(^{tBu}N,I*)Al(O-2,6-Me-C_6H_3)(THF) (**9**). Red: $[L\text{-LA}]_0$:$[\mathbf{9}]_0$ = 1000, M_n = 74 390 g mol^{-1}, M_w/M_n = 1.16, Blue: $[L\text{-LA}]_0$:$[\mathbf{9}]_0$ = 700, M_n = 53 110 g mol^{-1}, M_w/M_n = 1.31, Yellow: $[L\text{-LA}]_0$:$[\mathbf{9}]_0$ = 500, M_n = 46 040 g mol^{-1}, M_w/M_n = 1.33, Green: $[L\text{-LA}]_0$:$[\mathbf{9}]_0$ = 300, M_n = 25 310 g mol^{-1}, M_w/M_n = 1.33, Purple: $[L\text{-LA}]_0$:$[\mathbf{9}]_0$ = 200, M_n = 21 230 g mol^{-1}, M_w/M_n = 1.27, Conditions: $[L\text{-LA}]_0$:$[\mathbf{9}]_0$ as stated, $[L\text{-LA}]_0$ = 0.5 M, 4.0 mL toluene at 100 °C.

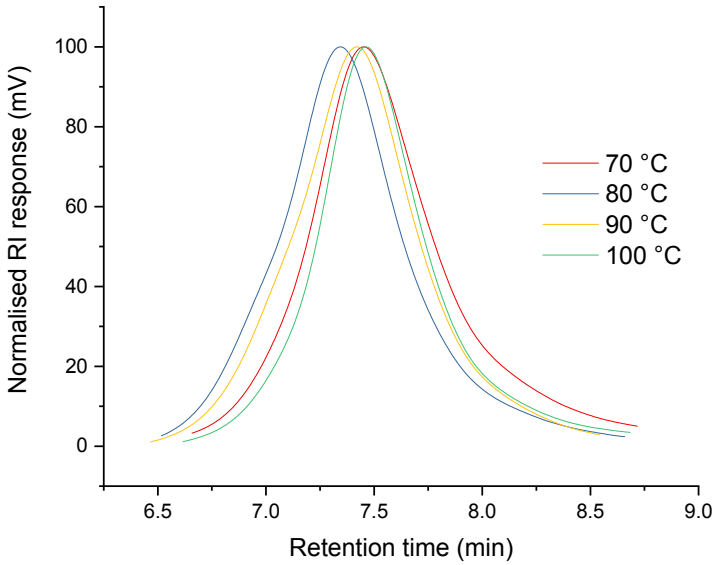

Fig. S113 Stacked GPC traces of PLAs synthesised from the ROP of *L*-LA using ^{Me2}SB(^{tBu}N,I*)Al(O-2,6-Me-C_6H_3)(THF) (**9**). Red: 70 °C, M_n = 11 600 g mol^{-1}, M_w/M_n = 1.44, Blue: 80 °C, M_n = 15 290 g mol^{-1}, M_w/M_n = 1.41, Yellow: 90 °C, M_n = 14 520 g mol^{-1}, M_w/M_n = 1.37, Green: 100 °C, M_n = 12 420 g mol^{-1}, M_w/M_n = 1.35, Conditions: $[L\text{-LA}]_0$:$[\mathbf{9}]_0$ = 100:1, $[L\text{-LA}]_0$ = 0.5 M, 4.0 mL toluene at stated temperature.

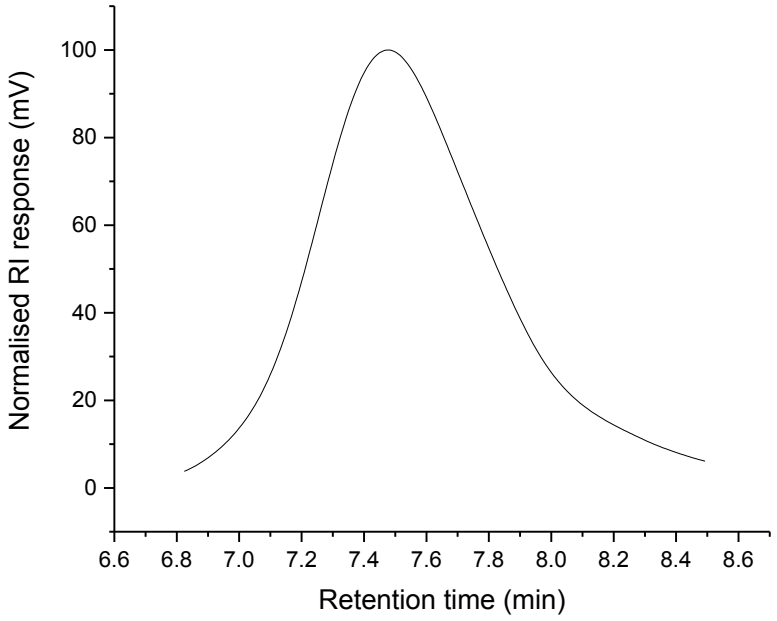

Fig. S114 GPC trace of PLA synthesised from the ROP of *rac*-LA using ^{Me_2}SB(^{tBu}N,I*)Al(O-2,6-Me-C_6H_3)(THF) (**9**). M_n = 12 070 g mol^{-1} M_w/M_n = 1.29. Conditions: [*rac*-LA]$_0$:[**9**]$_0$ = 100:1:1, [*rac*-LA] = 0.5 M, 4.0 mL toluene at 100 °C.

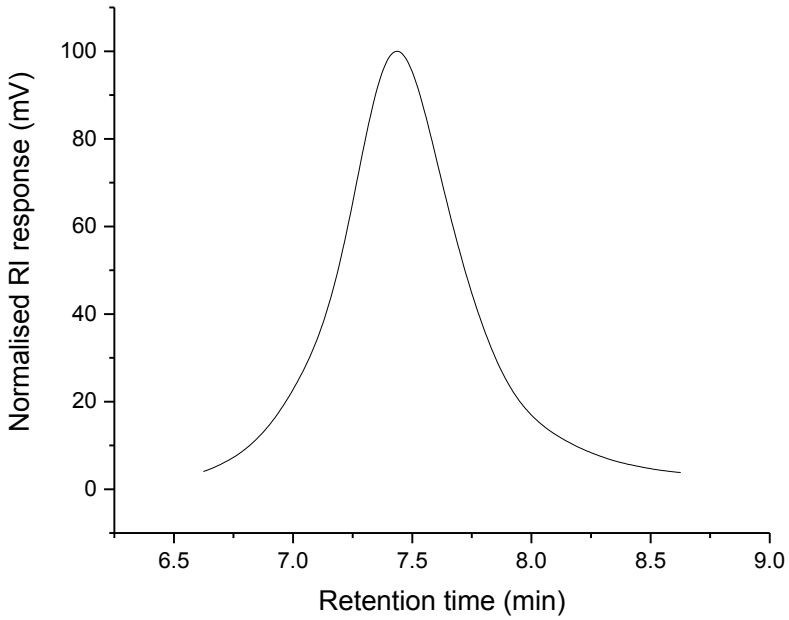

Fig. S115 GPC trace of PLA synthesised from the ROP of *L*-LA using ^{Me_2}SB(^{tBu}N,I*)Al(O-2,4-^{t}Bu-C_6H_3)(THF) (**10**). M_n = 13 310 g mol^{-1} M_w/M_n = 1.37. Conditions: [*L*-LA]$_0$:[**10**]$_0$ = 100:1:1, [*L*-LA] = 0.5 M, 4.0 mL toluene at 100 °C.

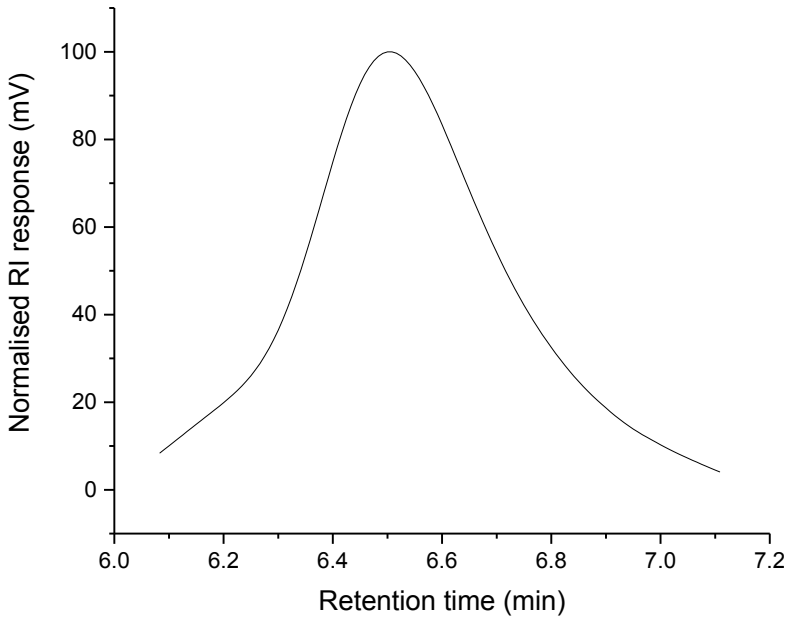

Fig. S116 GPC trace of PLA synthesised from the ROP of *L*-LA using $^{Me}{}_2$SB($^{t\text{Bu}}$N,I*)Al(O-2,4-^{t}Bu-C_6H_3)(THF) (**10**). M_n = 70 510 g mol^{-1} M_w/M_n = 1.11. Conditions: [*L*-LA]$_0$:[**10**]$_0$ = 1000:1:1, [*L*-LA] = 0.5 M, 4.0 mL toluene at 100 °C.

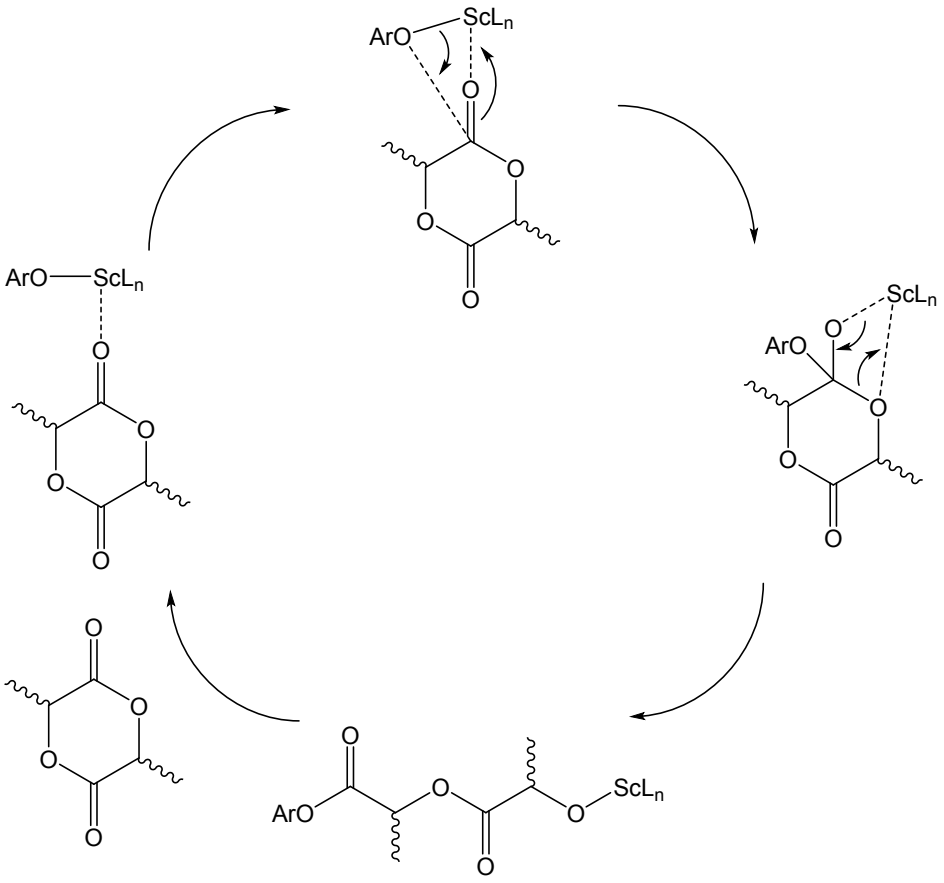

Scheme S1 Coordination-insertion mechanism for ring-opening polymerisation (ROP) of lactide catalysed by $^{Me}{}_2$SB($^{i\text{Pr}}$N,I*)Sc(O-2,6-^{i}Pr-C_6H_3)(THF) (**4**). L_n = $^{Me}{}_2$SB($^{t\text{Bu}}$N,I*) and OAr = O-2,6-^{i}Pr-C_6H_3.

References

1. D. F. Shriver and M. A. Drezdzon, *The Manipulation of Air-Sensitive Compounds, 2nd Edition*, 1986.
2. J. Cosier and A. M. Glazer, *J. Appl. Crystallogr.*, 1986, **19**, 105-107.
3. CrysAlisPRO, Oxford Diffraction /Agilent Technologies UK Ltd, Yarnton, England.
4. A. Altomare, G. Cascarano, C. Giacovazzo and A. Guagliardi, *J. Appl. Crystallogr.*, 1994, **27**, 435-435.
5. L. Palatinus and G. Chapuis, *J. Appl. Crystallogr.*, 2007, **40**, 786-790.
6. L. J. Farrugia, *J. Appl. Crystallogr.*, 1999, **32**, 837-838.
7. J. R. Dorgan, J. Janzen, D. M. Knauss, S. B. Hait, B. R. Limoges and M. H. Hutchinson, *J. Polym. Sci. B Polym. Phys.*, 2005, **43**, 3100-3111.
8. P. McKeown, M. G. Davidson, G. Kociok-Köhn and M. D. Jones, *Chem. Commun.*, 2016, **52**, 10431-10434.
9. J. Coudane, C. Ustariz-Peyret, G. Schwach and M. Vert, *J. Polym. Sci. A Polym. Chem.*, 1997, **35**, 1651-1658.
10. P. G. Hayes and W. E. Piers, *Inorganic Synthesis*, 2010, 1-55.
11. F. M. Alías, S. Barlow, J. S. Tudor, D. O'Hare, R. T. Perry, J. M. Nelson and I. Manners, *J. Organomet. Chem.*, 1997, **528**, 47.
12. J. Tudor, S. Barlow, B. R. Payne, D. O'Hare, P. Nguyen, C. E. B. Evans and I. Manners, *Organometallics*, 1999, **18**, 2281-2284.
13. T. J. Williams, J.-C. Buffet, Z. R. Turner and D. O'Hare, *Catal. Sci. Technol.*, 2018, **8**, 5454-5461.